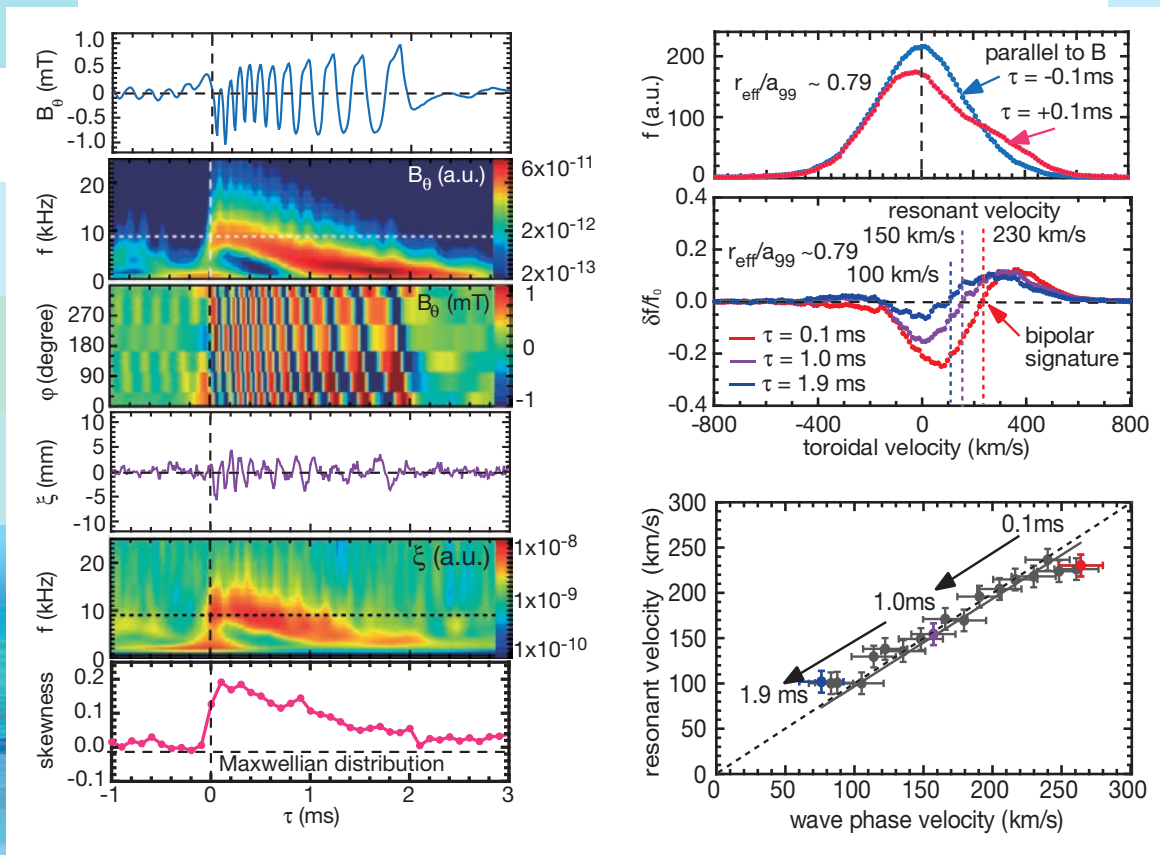


ANNUAL REPORT OF NATIONAL INSTITUTE FOR FUSION SCIENCE

April 2022 – March 2023



Front Cover Caption:

Direct observation of mass-dependent collisionless energy transfer via Landau and transit-time damping.

Communications Physics 5, 228, (2022)

Editorial Board

NAGAOKA, Kenichi

NUNAMI, Masanori

GOTO, Motoshi

YAMAGUCHI, Hiroyuki

KATO, Daiji

HOSHI, Takeo

SEKI, Ryosuke

HORI, Kumiko

MUKAI, Keisuke

HIRANO, Naoki

Inquiries about copyright should be addressed to the NIFS Library,
National Institute for Fusion Science, Oroshi-cho, Toki-shi, Gifu-ken 509-5292 Japan.
E-mail: tosho@nifs.ac.jp

<Notice about copyright>

NIFS authorized Japan Academic Association For Copyright Clearance (JAC) to license our reproduction rights and reuse rights of copyrighted works. If you wish to obtain permissions of these rights, please refer to the homepage of JAC (<http://jaacc.org/eng/>) and confirm appropriate organizations to request permission.

Printer: Arakawa Printing Co., Ltd.

2-16-38 Chiyoa, Naka-ku, Nagoya-shi 460-0012, JAPAN

Phone: +81-52-262-1006, Facsimile: +81-52-262-2296



ANNUAL REPORT OF NATIONAL INSTITUTE FOR FUSION SCIENCE

April 2022 – March 2023



December 2023

Inter-University Research Institute Corporation
National Institutes of Natural Sciences

NATIONAL INSTITUTE FOR FUSION SCIENCE

Address : Oroshi-cho, Toki-shi, Gifu-ken 509-5292, JAPAN

Phone : +81-572-58-2222

Facsimile : +81-572-58-2601

Homepage on internet : URL = <http://www.nifs.ac.jp/>



Contents

National Institute for Fusion Science April 2022 – March 2023	iv
1. Large Helical Device (LHD) Project	1
2. Fusion Engineering Research Project	23
3. Numerical Simulation Reactor Research Project	31
4. Network-Type Collaboration Research	43
5. Basic, Applied, and Innovative Research	45
6. Fusion Science Archives (FSA)	47
7. Bilateral Collaboration Research	49
8. Activities of Rokkasho Research Center (RRC)	61
9. Research Enhancement Strategy Office	63
10. Division of Health and Safety Promotion	65
11. Division of Deuterium Experiments Management	67
12. Division of Information and Communication Systems	69
13. International Collaboraiton	71
14. Division of External Affairs	83
15. Department of Engineering and Technical Services	85

16. Department of Administration	95
APPENDIX 1 Organization of the Institute	97
APPENDIX 2 Members of Committees	98
APPENDIX 3 Advisors, Fellows, and Professors Emeritus	99
APPENDIX 4 List of Staff	100
APPENDIX 5 List of Publications I (NIFS Reports)	104
APPENDIX 6 List of Publications II (Journals, etc.)	105



National Institute for Fusion Science

April 2022 – March 2023





Towards a new era of fusion science

Fusion science is a comprehensive area encompassing various disciplines with extremely high potential. Not only the immense merit of fusion energy, but also the possibilities of new discoveries give us the motivation to climb a high mountain — the history of overcoming every challenge has brought academic depth and breadth to fusion science. While the physics of fusion reactions is already well known, we have yet to understand how a “system”, called high-temperature plasma, can maintain a stable condition. It is a macroscopic system producing an internal energy by which autonomous dynamics sustains. The aim of fusion science is to elucidate the mechanism of such a spontaneous process; the fundamental principle must be common to the dynamics of the universe, society, or life. Recognizing the problem in a wide context, we pave the way in a zone of fundamental studies. On the way to fusion, the ultimate energy source, we will encounter many crossroads leading to future science and technology.

As we know, there are three different states of matter, i.e., solid, liquid, and gas. Even if the same molecules constitute matter, its “state” varies as the temperature is changed. At a high temperature, all matter becomes gas, in which molecules are disconnected and distribute sparsely, moving freely. When the temperature is raised further, molecules are broken into ions (positively charged heavy particles) and electrons (negatively charged light particles) by disconnecting the electrical bonding of ions and electrons; we call such a high temperature state “plasma”. While plasma is not common on Earth, it is the most typical state of matter in the universe. Our sun is a huge mass of plasma, consisting mainly of hydrogen. Inside it fusion reactions produce enormous energy. A star is a naturally made sustainable system of high temperature plasma, energized by fusion reactions.

Although the fusion energy is often likened to a “sun on Earth”, we need to think of a system that is completely different from stars. The challenge of fusion science is, indeed, to build a sustainable fusion system, based on a thoroughly new mechanism that we cannot find an example of in nature. A star confines plasma by gravity, but it is a very weak force, only effective against huge masses such as celestial bodies. We have to invoke a much stronger force to create a compact confinement system; magnetic force is the recourse. However, magnetic force acts like a “vortex” and its role in creating macroscopic structures is an interesting subject of contemporary physics and mathematics. We also need a much higher temperature than that at the center of the sun. In a typical star like our sun (the main sequence star), the reaction of synthesizing a helium atom from a hydrogen atom proceeds slowly. This reaction (a so-called p-p chain reaction) is too slow for producing sufficient fusion power in a compact system. We need to apply a faster reaction than that of the sun; the easiest is the deuterium-tritium fusion reaction, which produces helium and neutrons, but occurs at temperatures of around 100 million degrees Celsius. On the other hand, several meters away from the plasma, we have to place super-conducting magnets to generate the magnetic field, which are operated at ultra-low temperature. Therefore, fusion on Earth requires an extreme technology, dealing with ultra-high and ultra-low temperatures, separated only by several meters.

The road to fusion power is purgatorial and much harder than the prediction made at the beginning (the mid-20th century). However, it is not necessarily unfortunate that we encounter unexpected challenges. As many great researchers say that discovery is born from failure, unknown truths exist outside the range that one can predict. Fusion energy is a steep peak for development researchers to climb, but it is also a treasure trove for academic researchers. The task of the academic researcher is to generate new knowledge from the input of difficult problems.

All members of the National Institute for Fusion Science (NIFS) are working on the construction of a lighthouse that illuminates the direction of fusion science in choppy academic waters ahead. NIFS is a broad avenue for many researchers, through which the scope of “fusion science” will extend in the world of science. We hope that many people will pay attention to our endeavor and participate in these activities.

YOSHIDA Zensho
Director General of National Institute for Fusion Science

1. Large Helical Device (LHD) Project

The Large Helical Device (LHD) is a sizeable superconducting plasma confinement device employing a heliotron magnetic configuration. The objectives are to conduct academic research on the confinement of steady-state/high-temperature plasma for a comprehensive understanding of torus plasma. In the deuterium plasma experiment that started in 2017, we succeeded in generating plasma with both electron and ion temperatures reaching 100 million degrees. With this success, LHD research has entered a new phase, shifting to interdisciplinary research in 2021 and advanced study in 2022. We conducted the 24th experiment campaign for 14 weeks from the end of September to the end of December 2022.

The following four topical groups lead the LHD experiment by receiving support from domestic and international advisers, (1) Multi-ion plasma TG, (2) Turbulence TG, (3) Spectroscopy TG, and (4) Instability TG.

- The Multi-ion plasma TG deals with multi-ion transport, which is one of the crucial issues in a magnetically confined fusion reactor. The key research phrases are (i) mock test of sustainable burning and (ii) multi-ion transport (circulation) in terms of core-edge-wall coupling.
- The Turbulence TG emphasizes being aware of the intervention of turbulence in various physical phenomena occurring in LHD plasmas and actively investigates the relationships among them, particularly focusing on the turbulence interaction in PHASE and REAL space.
- The Spectroscopy TG addresses the following topics by employing various spectrometers with ranges from visible to X-ray. (i) Collisional-radiative properties of heavy ions, (ii) neutral particle transport in divertor and plasma boundary regions, and (iii) the non-Maxwell and anisotropic velocity distribution function of particles.
- The Instability TG deals with topics on (i) wave-particle interaction, (ii) abrupt events, (iii) transition phenomena, and (iv) topological effects. Also, the TG will cover the basic topic related to high-beta, MHD, and energetic-particle physics.

In 2022, 397 domestic and international researchers were registered in the LHD experiment groups, and 209 experiment proposals were submitted to each topical group, as shown in Figure. Many research results were achieved during the 24th experiment campaign in 2022, as described in the following URL.

https://www-lhd.nifs.ac.jp/pub/Science_en.html

Significant results were made public through press releases and introduced on the NIFS web page at the following URL.

https://www.nifs.ac.jp/en/news/index_list.html

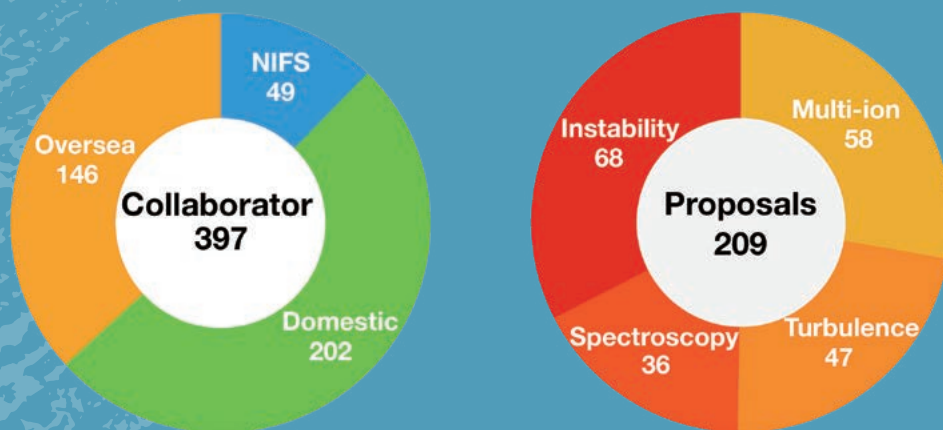


Figure: (left) number of domestic and international researchers, and (right) number of Proposals

The 24th experiment campaign is the final one of a ten year venture as the Project to Promote Large Scientific Frontiers of MEXT. In the coming years, the LHD will be born again in the framework of the Academic Research Platform of MEXT as a three year project from 2023 to 2025. The Academic Research Platform, utilizes the LHD, which can stably produce high-temperature plasma, as an interdisciplinary research platform, conduct international joint research to explore the principles of various complex phenomena common not only to fusion but also to space and astronomical plasmas.

(R. Sakamoto)

Multi-ion Plasma

Highlight

Data-Driven Control for Radiative Collapse Avoidance [1]

A data-driven predictor of radiative collapse, which is the major cause of sudden plasma termination in stellarator-heliotron devices, has been developed by means of a machine-learning technique. The control system with this predictor has successfully demonstrated the avoidance of radiative collapse and a secure high-density operation in the LHD.

A support vector machine (SVM), which is one of the machine-learning models, has been trained to distinguish whether the plasma is “close-to-collapse” or “stable” based on high-density experiment data in the LHD. The predictor has been designed to calculate the “collapse likelihood”, which is 0 when the plasma is stable and close to unity when the plasma approaches collapse, from plasma parameters featured by the trained SVM [2].

The schematic diagram of the collapse-avoidance control system is shown in Fig. 1. The control system receives signals of plasma density, temperature, and impurity line emission intensities, and calculates the collapse likelihood in real-time. When the likelihood approaches unity, a control signal is sent to the EC heating system to inject additional heating power and to the gas-puff controller to stop fueling. When the likelihood decreases, the control signal is turned off.

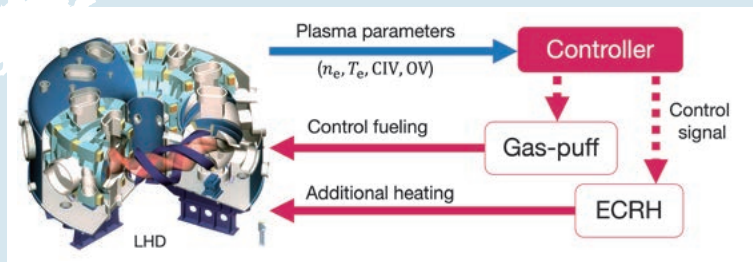


Fig. 1 Schematic diagram of the collapse avoidance control system.

Figure 2 shows the discharges with and without the collapse-avoidance control in LHD experiments. When the density increased, the radiative collapse occurred at the initial phase in the discharge without the control. In the discharge with the control, the collapse in the initial phase was avoided by regulating gas-puff and ECH. Consequently, the discharge evolved to a high density of $1.2 \times 10^{20} \text{ m}^{-3}$ successfully while avoiding radiative collapse. This is the first reported work to control stellarator-heliotron plasma with avoidance of radiative collapse by means of a machine-learning model.

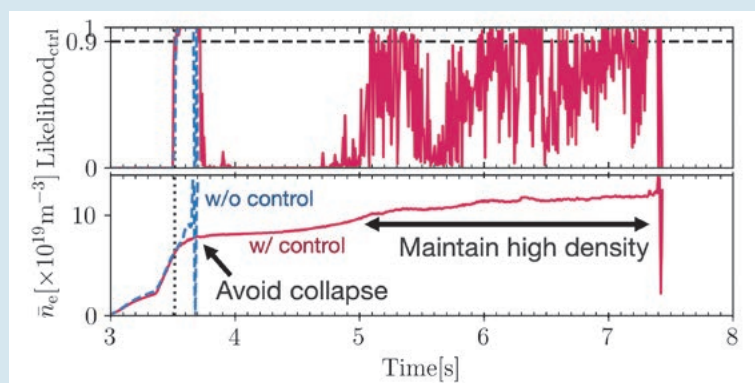


Fig. 2 The collapse likelihood (upper) and line-averaged electron density (bottom) in the discharges with (red) and without (blue) the collapse avoidance control system. The dashed horizontal line in the top panel and the dotted vertical line show the threshold value and the time when the likelihood initially exceeded the threshold.

[1] T. Yokoyama *et al.*, “Data-Driven Control for Radiative Collapse Avoidance in Large Helical Device,” *Plasma and Fusion Research* **17**, 2402042 (2022).

[2] T. Yokoyama *et al.*, “Data-Driven Approach on the Mechanism of Radiative Collapse in the Large Helical Device,” *Plasma and Fusion Research* **16**, 2402010 (2021).

Non-contact thermometer to measure the temperature of ultra-high temperature plasma –Successful observation of multi-temperature anisotropic energetic ions [1]

In fusion plasmas, α -particles generated by the fusion reaction between deuterium and tritium in the plasma sustain the burning of the plasma and generate energy. Therefore, to realize nuclear fusion, it is necessary to know and control the state of the energetic α -particles generated in the high-temperature plasma. Although it is challenging to measure α -particles in the high-temperature plasma, we considered non-contact measurement and started the development of collective Thomson scattering (CTS) measurement using electromagnetic waves.

The research team has reported on a method for evaluating ion temperature and velocity distribution using the scattering phenomena of millimeter electromagnetic waves [2]. This study developed a high-precision in-situ calibration method for CTS measurements and applied it to temperature measurements in the Large Helical Device (LHD) plasmas. Conventionally, a radiation of electromagnetic waves in plasma is used to calibrate the receiver for CTS measurements. However, the local position of the emitted radiation was inaccurate due to the refraction, and it was necessary to determine the location. To solve this problem, we combined a ray tracing calculation of electromagnetic waves with the calibration of receiver sensitivity by electron radiation. As a result, we succeeded in dramatically improving the reproducibility of the scattering spectrum. Furthermore, we have demonstrated that in-situ calibration is possible using this method simultaneously with actual temperature measurements.

Using this method, we observed the scattering spectrum at the center of the LHD plasma by the CTS measurement. As expected from the model calculation of the scattering spectrum, the observed spectrum has an asymmetric shape (asymmetric when there is a population of ions with different velocities in the positive and negative directions of v_{\parallel} in the figure). This asymmetry indicated complex confinement of anisotropic ions with parallel and perpendicular velocities to the magnetic field lines and was found to be due to plasma heating.

These results are essential for the study of confinement physics of alpha particles to maintain a self-burning state in fusion plasmas. Furthermore, since in-situ calibration is also possible, it is expected to be widely used as a calibration and analysis method for electromagnetic heating devices and millimeter-wave measurement devices used in fusion power generation.

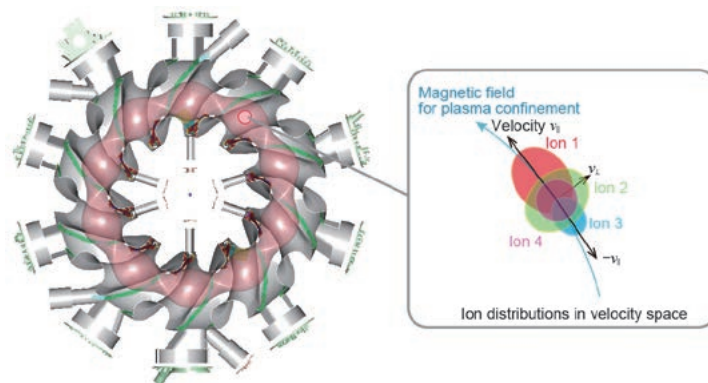


Fig. 1 LHD and high temperature plasma

Plasma confined in the magnetic field of the LHD has the shape of a twisted donut. Using a non-contact thermometer, we measured the temperature of the high-temperature plasma core by injecting millimeter waves and measuring their scattered light. The results show that the velocity spread of the ion population, which corresponds to the ion temperature, has a variety of directions: along the confinement magnetic field (ion 1), in the opposite direction (ion 3), perpendicularly (ion 2), and a thermalized isotropic component (ion 4). This complex state can be attributed to plasma heating to generate and maintain the high-temperature plasma.

[1] M. Nishiura, S. Adachi, K. Tanaka, N. Kenmochi, T. Shimozuma, R. Yanai, T. Saito, H. Nuga, R. Seki, "Collective Thomson scattering diagnostic with *in situ* calibration system for velocity space analysis in large helical device" Rev. Sci. Instrum. **93**, 053501 (2022). <https://doi.org/10.1063/5.0079296>

[2] M. Nishiura *et al.*, Nucl. Fusion **54**, 023006 (2014).

(M. Nishiura)

Validation of plasma-wall interaction simulation code ERO2.0 by analysis of tungsten migration in the open divertor configuration

Tungsten migration in an open divertor configuration in the LHD was analyzed for validating the three-dimensional plasma-wall interaction simulation code ERO2.0 [1]. In the experimental campaign in Fiscal Year 2008, a tungsten-coated divertor plate was installed on the right-divertor plate array in the inboard side of the torus. Figure 1 (a) shows a three-dimensional grid model for analyzing the tungsten migration in an open divertor configuration for the ERO2.0 code. The simulation reproduced a measured localization of tungsten migration near a tungsten-coated divertor plate along the divertor plate array. Figure 1 (b) indicates the simulation of the integrated net tungsten areal density profile on the carbon divertor plates. The simulation qualitatively reproduced the experimental results of high tungsten areal density in the private side on a carbon divertor plate (“R18”) installed next to the tungsten-coated divertor plate (shown by a gray arrow). It showed that it was mainly caused by tungsten prompt redeposition in plasma discharges for low magnetic fields in a counterclockwise toroidal direction. Figure 1 (c) presents the integrated net tungsten areal density profile along the black lines on four selected carbon divertor plates (“R20”, “R18”, “R16”, and “R8” shown in Figure 1 (b)). The measured tungsten areal densities at three positions (“a”, “b”, and “c”) on the four divertor plates are shown as red circles. While the simulation reproduced the above two experimental results, it disagreed with the measurement of low tungsten areal density on the plasma-wetted areas on the divertor plates. It demonstrated that the actual erosion rate of the redeposited tungsten in the plasma-wetted areas on the divertor plates should be much higher than that adopted in the ERO2.0 simulation code [2].

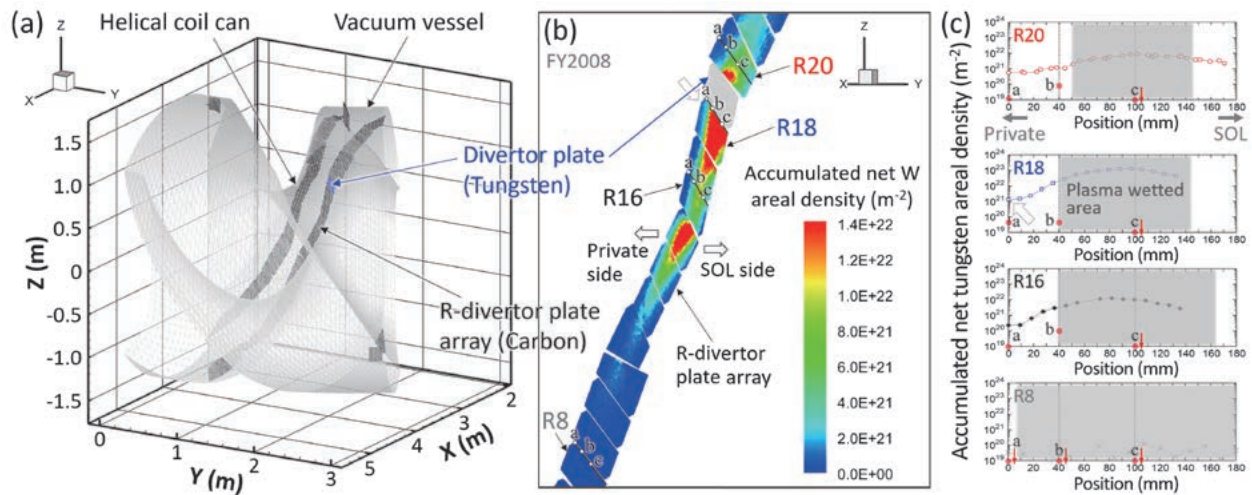


Fig. 1 (a) A three-dimensional grid model for analyzing the tungsten migration in the open divertor configuration in the LHD for one helical pitch angle (36° in toroidal direction) for the ERO2.0 code. (b) The simulation of the integrated net tungsten areal density profile on the carbon divertor plates installed along the right divertor plate array in the experimental campaign (FY2008). (c) The integrated net tungsten areal density profiles along the black lines on the four carbon divertor plates shown in Figure (b). The measured tungsten areal densities at the three positions (“a”, “b”, and “c”) on the four selected divertor plates (“R20”, “R18”, “R16”, and “R8”) indicated as red circles. Gray-shaded regions show the plasma-wetted areas on the divertor plates.

[1] J. Romazanov *et al.*, Nucl. Mater. Energy **18**, 331 (2019).

[2] M. Shoji *et al.*, Nucl. Mater. Energy **33**, 101294 (2022).

Extraction of three-dimensional structure of radiative cooling from two-dimensional radiation images in Large Helical Device [1]

Three-dimensional localization of radiative cooling due to nitrogen (N_2) seeding for divertor heat load reduction has been detected experimentally. A fusion reaction occurs by confining high-temperature plasma exceeding 100 million Celsius degrees in fusion reactors. Since the flow from the core plasma with a high temperature to a place called the “divertor” on the wall of the device is huge, it is necessary to mitigate the local heat load of the divertor. Therefore, an operational method called “divertor detachment” is being studied, in which impurities are injected from outside the plasma and the heat load is dispersed as radiation. In the LHD, we performed experiments on the divertor detachment.

Although toroidally-symmetric divertor heat load reduction is preferable for fusion reactors, toroidally asymmetric reduction is observed in various torus devices. The localization of radiative cooling along some magnetic field lines is implied as the reason for the asymmetry, however, the localization has not been measured in previous works. In this research, a three-dimensionally localized structure was extracted using principal component analysis (PCA) from two-dimensional radiation images measured with an InfraRed imaging Video Bolometer (IRVB). By applying PCA to 34 images each in N_2 seeded plasmas with toroidally-asymmetric reduction (Fig. 1 (a)) and in neon (Ne) seeded plasmas with toroidally-symmetric reduction (Fig. 1 (b)), a radiation feature in N_2 seeded plasmas was found as one of the principal components (Fig. 1 (c)). The three-dimensional transport code EMC3-EIRENE indicated that the ionization in one of the divertor legs was enhanced in nitrogen seeding compared with Ne seeding due to the difference in the first ionization energy. The magnetic field lines from the divertor leg were along the extracted radiation structure and were terminated by the divertor where the heat load decreased due to the N_2 seeding (Fig. 2). These results indicate that the three-dimensionally localized structure of radiative cooling was detected experimentally.

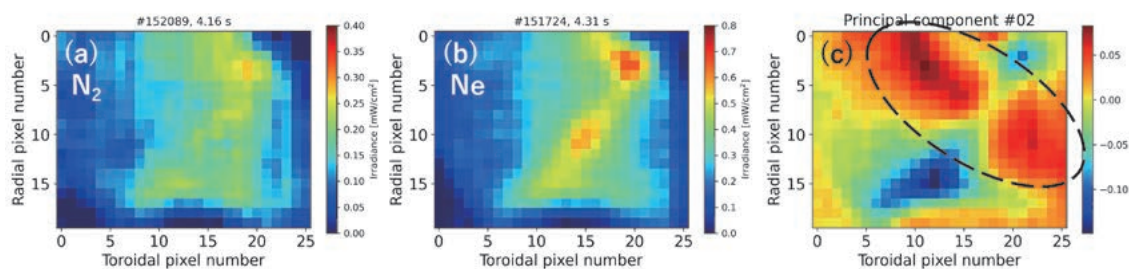
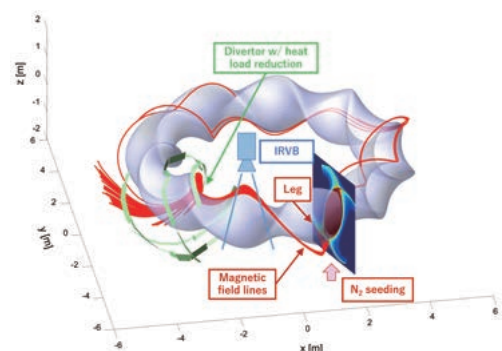


Fig. 1 Typical radiation images of IRVB in (a) N_2 and (b) Ne seeded plasmas. (c) Principal component extracted from 68 images of N_2 and Ne seeded plasmas. A dashed ellipse indicates the localized structure in N_2 seeded plasmas.

Fig. 2 Magnetic field lines traced from the divertor leg of the N_2 seeding port with the field of view of IRVB and divertor plates.



[1] K. Mukai *et al.*, Nucl. Mater. Energy **33**, 101294 (2022).

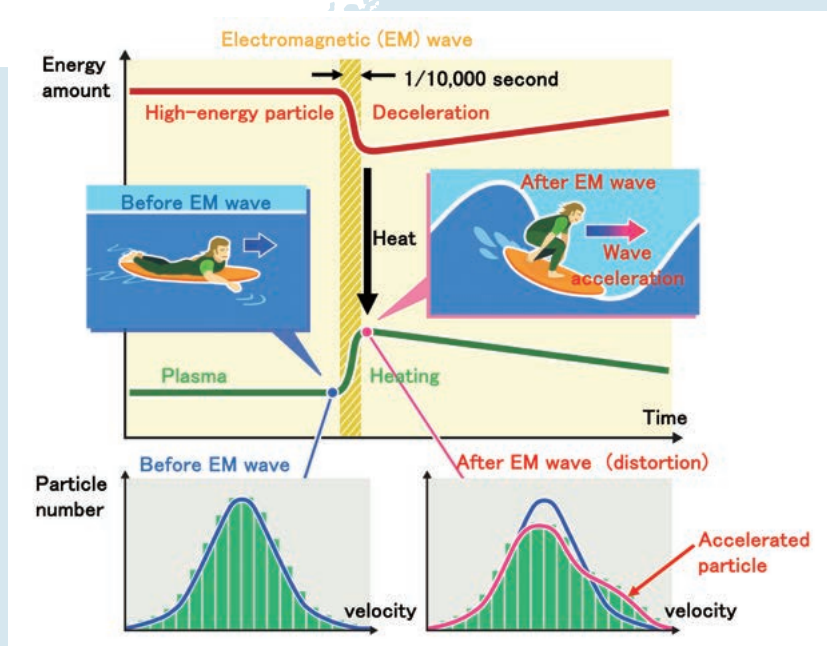
TG2: Turbulence Topical Group

Highlight

Direct observation of mass-dependent collisionless energy transfer via Landau and transit-time damping

There has been no method to directly measure the collisionless energy transfer from high-energy ions to bulk ions through the electromagnetic waves generated inside plasma. Therefore, it is not known whether this process exists. To directly measure the heating process, it is necessary to determine the time variation of the velocity distribution, which indicates which velocity ions are present and in what proportion. A high-speed charge exchange spectroscopy system has been developed to measure the time variation of the velocity distribution of plasma ions at an ultrahigh-speed of 10 kHz.

In the LHD, experiments are being conducted to investigate plasma self-heating using a high-speed neutral beam that simulates high-energy Helium from nuclear fusion reactions. In this experiment, to simulate self-heating, a newly developed measurement system was used to measure in detail the time variation of the velocity distribution of plasma ions. As a result, it was discovered for the first time in the world that the plasma was heated due to the slowing down of the high-speed beam and the distortion of the velocity profile of the plasma ions caused by the generation of electromagnetic waves inside the plasma (see Figure). The reason for this distortion of the velocity profile was found to be that the energy of the high-speed beam was transferred to the electromagnetic wave through a process called Landau/transit-time damping, and the energy of the electromagnetic wave was transferred to the plasma ions. In other words, the electromagnetic waves carried the energy of the high-speed beam to the plasma and heated it, which is basically the same process as so-called alpha-channeling in fusion plasma. [1]



Heat is carried by electromagnetic waves, which simultaneously slow down the high-speed particle beam (red line) and heat up the plasma particles (green line). Distortion of the velocity distribution is observed due to the acceleration of the particles as a result of the electromagnetic waves.

[1] K. Ida *et al.*, *Communications Physics* **5**, 228 (2022).

Isotope effect in the internal transport barrier threshold condition

As a long-standing mystery in the magnetically confined plasma community, the background physics of the hydrogen isotope effect has been intensively studied. The isotope effect in the threshold power necessary for triggering H-mode transitions is experimentally demonstrated, which is favorable to plasmas with larger isotope mass [1]. Such an observation is routinely obtained in different tokamak devices, but the knowledge concerning stellarators is scarcely accumulated in literature due to the lack of experimental cases. In the Large Helical Device (LHD), the hydrogen isotope effect on the transition threshold for the electron internal transport barrier (electron-ITB) is discovered.

In the LHD, the electron-ITB is produced typically in plasmas with low density and high electron cyclotron resonance heating (ECH) power. The hydrogen isotope effect in the electron-ITB is assessed based on a perturbative experiment. In a steady state plasma discharge, the ECH heating power is modulated and the response in the electron temperature gradient is observed. When the base electron density is sufficiently high, the modulation amplitude in the electron temperature gradient is maintained to be small and does not depend on line-averaged density. However, it monotonically increases as the line averaged density is decreased in a lower density range,

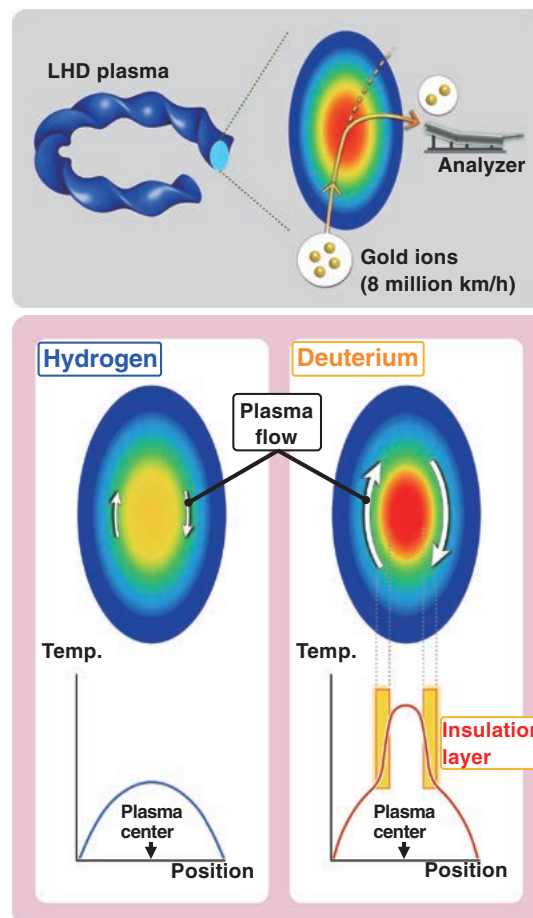


Fig. 1 Top: Plasma measurement using a heavy ion beam probe. A high-speed beam of gold ions is injected into the plasma to measure the flow generated inside it. Bottom left: Hydrogen plasma has weak flow and no insulation layer. Bottom right: Deuterium plasma has strong flow and a high-performance insulation layer.

which is considered to be due to the transient electron-ITB formation/deformation synchronizing the modulation ECH. The threshold density for the electron-ITB transition is higher in the deuterium case, i.e., the electron-ITB is easily formed in the heavier hydrogen isotope fuel. This isotope effect is found to be predominantly caused by a branch transition in local electron thermal diffusivity. In a higher density range, the local electron thermal diffusivity follows the $\bar{n}_e^{-1.2}$ trend, likely due to the density stabilization effect in global confinement scaling. Once the density crosses the electron-ITB threshold, the local electron thermal diffusivity drops off from the $\bar{n}_e^{-1.2}$ trend [2]. Unlike the local transport property, the nonlocal contribution scarcely has any meaningful difference in deuterium and hydrogen plasmas [2,3]. According to the heavy ion beam probe (HIBP) data, it is found that a central radial electric field transition occurs at a higher density level in deuterium plasmas [4], as shown in Fig. 1, which is likely responsible for the isotope effect in the electron-ITB formation. The fact that self-organized radial electric field criticality has a susceptibility to plasma ion mass is systematically pointed out for the first time.

[1] C. F. Maggi *et al.*, Plasma Phys. Control. Fusion **60**, 014045 (2017).

[2] T. Kobayashi *et al.*, Nucl. Fusion **60**, 076015 (2020).

[3] T. Kobayashi *et al.*, Plasma Fusion Res. **15**, 1402072 (2020).

[4] T. Kobayashi *et al.*, Sci. Rep. **12**, 5507 (2022).

(T. Kobayashi)

Discovery of fast moving plasma turbulence: New insights into the understanding of fusion plasma turbulence

To achieve a fusion power plant, a plasma of more than 100 million degrees Celsius must be stably confined in a magnetic field and maintained for a long time. In the Large Helical Device (LHD), it has been discovered for the first time that when heat escapes from the plasma, turbulence moves faster than heat [1]. The characteristic of this turbulence makes it possible to predict changes in plasma temperature, and it is expected that the observation of turbulence will lead to the development of a method for real-time control of plasma temperature in the future.

In a high-temperature plasma confined by a magnetic field, “turbulence” – a flow with vortexes of varying sizes – is generated. This turbulence disturbs the plasma and the heat from the confined plasma flows outwards, causing the plasma temperature to drop. To solve this problem, it is necessary to understand the characteristics of heat and turbulence in plasma. However, turbulence in plasmas is so complex that we still do not fully understand it. In particular, how the generated turbulence moves in the plasma is not well understood because it requires instruments that can measure the time evolution of minute turbulence with high sensitivity and extremely high spatial and temporal resolution.

A “barrier” can form in the plasma that blocks the transport of heat from the center outwards. The barrier creates a strong pressure gradient in the plasma and generates turbulence. We have developed a method to break this barrier by designing a magnetic field structure (Fig. 1). This method allows us to focus on the heat and turbulence that flow strongly when the barrier is broken, and to study their relationship in detail. We then use electromagnetic waves of different wavelengths to measure the changing temperature and heat flow of electrons and millimeter-sized fine turbulence with the world’s highest accuracy. Heat and turbulence were previously known to move almost simultaneously at a speed of 5,000 kilometers per hour, about the speed of an airplane, but this experiment

led to the world's first discovery of turbulence moving ahead of heat at a speed of 40,000 kilometers per hour. The speed of this turbulence is close to that of a rocket.

This research has advanced our understanding of turbulence in fusion plasmas. The new property of turbulence, that it moves much faster than heat in a plasma, suggests that we may be able to predict plasma temperature changes by observing predictive turbulence. In the future, we expect to develop methods to control plasma temperatures in real time.

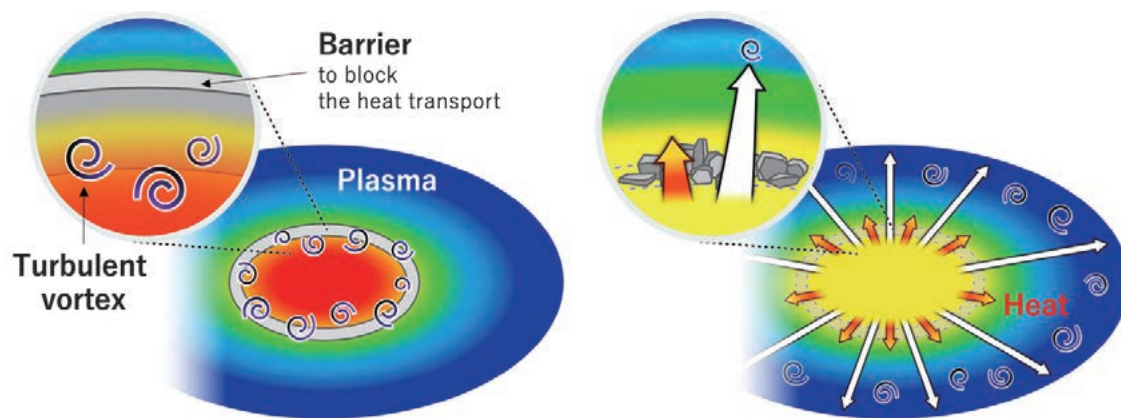


Fig. 1 Figure (left): Creating a barrier in the plasma to confirm the heat inside. (Right): Breaking the barrier revealed turbulence moving faster than the heat escaping from inside the plasma.

[1] N. Kenmochi *et al.*, *Scientific Reports* **12**, 6979 (2022).

(N. Kenmochi)

Plasma Spectroscopy

Highlight

Electron temperature and density measurement by Thomson scattering with a high repetition rate laser of 20 kHz on LHD [1]

In order to measure the electron temperature (T_e) and density (n_e) during fast phenomena in plasmas, a high-repetition frequency Nd:YAG laser and fast digitizers are installed in the Thomson scattering system in the LHD. This laser has been newly developed under the collaboration of NIFS and the University of Wisconsin-Madison, based on a pulse-burst technique and can be operated with two repetition frequencies, one of which is 1 kHz with 30 laser pulses and the other is 20 kHz with 100 laser pulses.

The temporal development of the scattered light signals is acquired by the fast digitizers of the switched-capacitor type with 1 GS/s. The minimum read-out time of these digitizers is shorter than 50 μ s in order that the signals in the 20 kHz operation of the laser can be acquired. Since the data which are obtained by the switched-capacitor type digitizers require some kinds of corrections, the cell-size and peak corrections, are made. Some methods of the evaluation of the background level and the time integration are developed. After these data processing procedures, the T_e profiles are derived by the χ^2 -method. n_e is evaluated with the results of the Raman scattering calibration.

Figure 1 shows temporal development of the spatial profiles of T_e (red), n_e (blue) and electron pressure (yellow) after a pellet injection in the LHD plasma. n_e started to increase at $t = 8.00275$ s (Fig. 1b) from the outside of the torus. The low T_e region where $T_e < 0.3$ keV penetrated the core region of the plasma. In Fig. 1c, quite high n_e was observed in the torus outer region. The temporal development of T_e and n_e within 1 ms was observed in detail by this diagnostic.

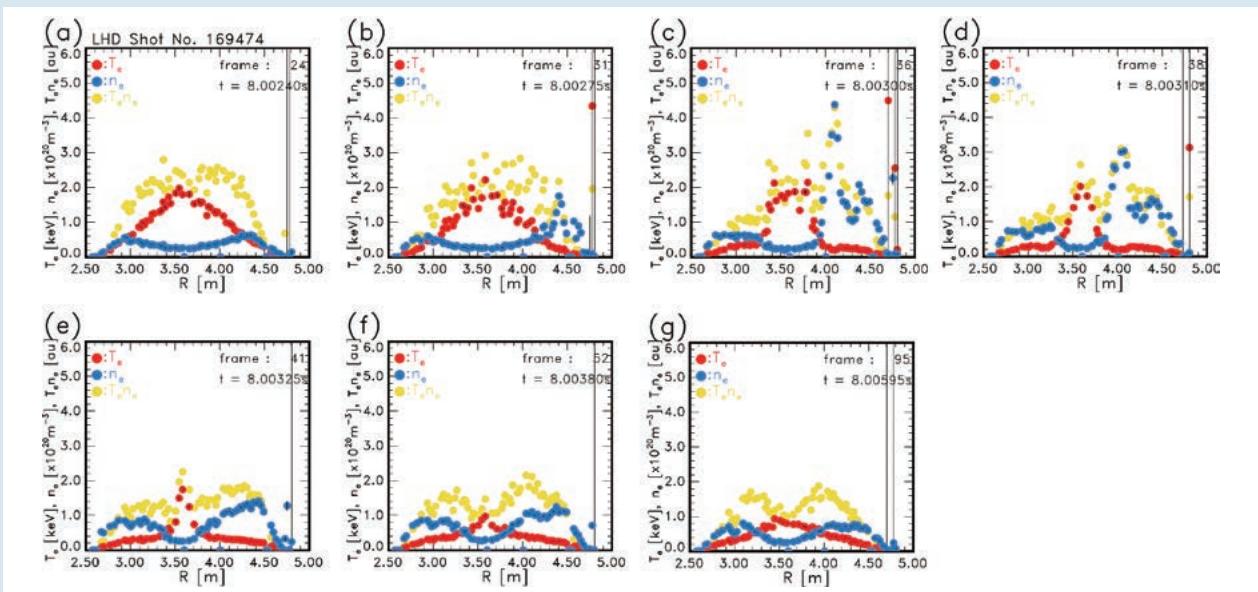


Fig. 1 Spatial profiles of electron temperature (red), electron density (blue) and electron pressure (yellow) of a pellet injected plasma in the LHD. They are measured by the Thomson scattering system with a high-repetition rate Nd:YAG laser of 20 kHz.

[1] H. Funaba *et al.*, Sci. Rep. **62**, 15112 (2022).

(H. Funaba and R. Yasuhara)

Experimental Study on Boron Distribution and Transport at Plasma-Facing Components during Impurity Powder Dropping in the Large Helical Device [1]

We performed spatially-resolved spectroscopic measurements of emissions by boron ions and BH molecules (Fig. 1). As a result, a concentration of BH and B⁺ was confirmed in the diverter region during impurity powder dropping experiments with boron powder (Fig. 2), which suggest successful observation of boron deposition and desorption processes on the diverter plate. By comparing H γ emissions with and without boron injection, neutral hydrogen shows uniform reduction in the SOL region, whereas less reduction of neutral hydrogen is confirmed in the divertor region. Although emissions from BH and B⁺ increased linearly, those by B⁰ and B⁴⁺ became constant after the middle of the discharge (Fig. 3). Continuous reduction of carbon density in the core plasma was confirmed even after B⁰ and B⁴⁺ became constant. The results may show reduction of hydrogen recycling and facilitation of impurity gettering by boron in the divertor region and thus effective real-time wall conditioning.

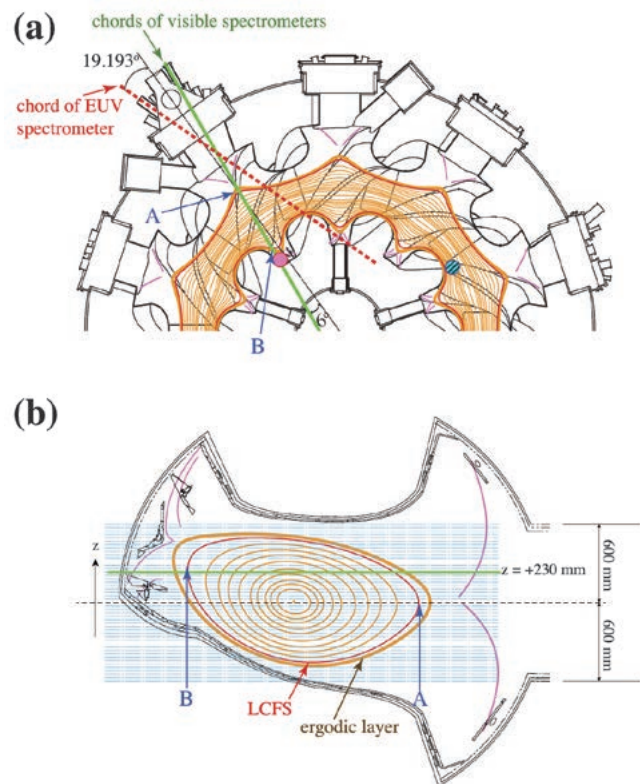


Fig. 1 Line of sight of visible and EUV spectrometers. (a) Half equatorial cross section of LHD. Positions of powder dropper (blue circle, hatched) and Langmuir probe array examined in this study (pink circle) also shown. (b) Plane of chords of visible spectrometers. In (a) and (b), A and B indicate outer and inner edges of LCFS in plane of chords of spectrometers.

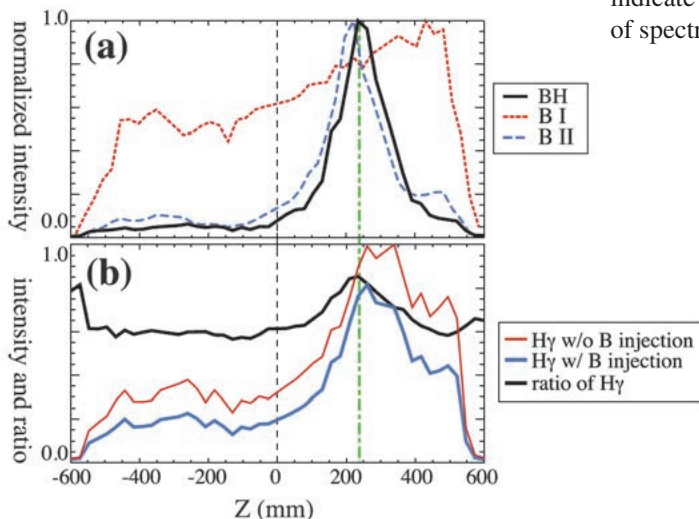


Fig. 2 (a) Observed emission distributions of BH, B I, and B II at $t = 6.0$ s. (b) Observed emission distributions of H γ during shot without and with boron injection at $t = 6.0$ s. Ratio of H γ intensities between two discharges with and without boron injection at $t = 6.0$ s shown as black curve. Vertical green dot-dashed line indicate position of divertor viewing chord.

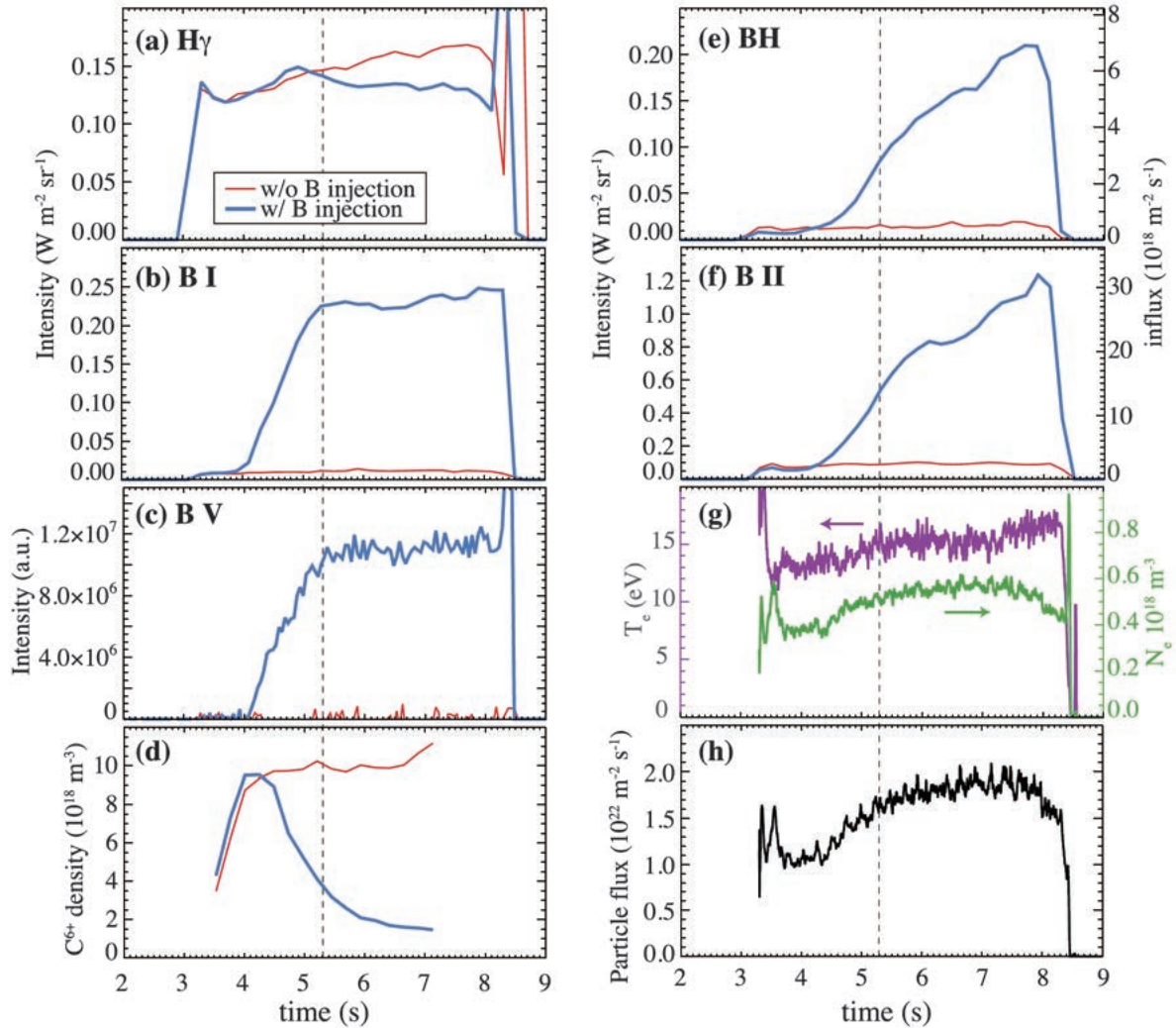


Fig. 3 Temporal evolutions of intensities of (a) $H\gamma$, (b) B I, (c) B V, (d) C^{6+} density on magnetic axis measured by CXS, (e) BH, (f) and B II in discharges without and with boron injection (thick blue), (g) Te and Ne on divertor, and (h) particle flux onto divertor. (a), (b), (e) and (f) are data in divertor viewing chords. Vertical dashed lines show $t = 5.3$ s, after which flattening structure appeared in evolutions of B I and B V.

[1] T. Kawate *et al.*, Nuclear Fusion **62**, 126052 (2022).

(T. Kawate)

Detailed Analysis of Spectra from Ga-like Ions of Heavy Elements Observed in High-Temperature Plasmas [1]

Extreme ultraviolet (EUV) and soft X-ray emission spectra from highly charged heavy ions are of great interest in various research fields, including nuclear fusion and industrial light source applications, as well as basic atomic physics. Among a wide range of ion stages, gallium-like (Ga-like) ions give rise to relatively simple spectral features because of their simple electron configuration of the ground state: $[\text{Ar}]3d^{10}4s^24p$. However, experimental and theoretical investigations of them are still incomplete.

This study focuses on the atomic number (Z) dependence of spectra from Ga-like ions of heavy elements based on the spectral data which have systematically been recorded in high-temperature plasmas produced in the Large Helical Device (LHD). A small amount of heavy elements are injected into LHD plasmas, mainly by a tracer-encapsulated solid pellet (TESPEL), and the temporal evolutions of EUV/soft X-ray emission spectra are recorded by multiple grazing incidence spectrometers. The measured wavelengths are compared with theoretical values calculated with a multi-configuration Dirac Fock code: GRASP92. Consequently, Z dependent wavelengths of several prominent transitions of Ga-like ions have successfully been obtained. Some of them have been experimentally identified for the first time in the LHD.

It has already been reported that the energy level crossing of $[\text{Ar}]3d^{10}4s^24d$ and $[\text{Ar}]3d^{10}4s4p^2$ configurations takes place between $Z=62$ and 63 because of a strong configuration interaction [2]. The present study gives additional results of Z dependence analysis for the other transitions. In particular, the present study has successfully identified the lines due to magnetic dipole (M1) transitions between doublets of the ground configuration (Fig. 1). The Z dependence of the measured wavelengths for Z from 63 onward is lined up along a single smooth curve and is in very good agreement with the calculation. The wavelengths of these M1 lines correspond to the energy splitting due to spin-orbit interaction. In this respect, the present results provide some fundamental data to study atomic physics specific to highly charged heavy ions: Z -dependent configuration interaction and spin-orbit interaction.

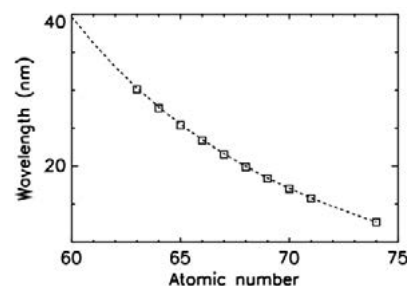


Fig. 1 Z dependence of the wavelength of the magnetic dipole (M1) transition from $(4p_+)_{3/2}$ to the ground state $(4p_-)_{1/2}$ of Ga-like ions. The measured and calculated wavelengths are shown by squares and a broken line, respectively.

[1] C. Suzuki *et al.*, *Atoms* **11**, 33 (2023).

[2] F. Koike *et al.*, *Phys. Rev. A* **105**, 032802 (2022).

(C. Suzuki)

EUV/VUV Spectroscopy for the Study of Carbon Impurity Transport in Hydrogen and Deuterium Plasmas in the Edge Stochastic Magnetic Field Layer of the Large Helical Device [1]

The ergodic layer in the Large Helical Device (LHD) consists of stochastic magnetic fields exhibiting a three-dimensional structure that is intrinsically formed by helical coils. Spectroscopic diagnostics were employed in the extreme ultraviolet (EUV) and vacuum ultraviolet (VUV) wavelength ranges to investigate emission lines of carbon impurities in both hydrogen (H) and deuterium (D) plasmas, aiming to elucidate the impact of distinct bulk ions on impurity generation and transport in the edge plasmas of the LHD. Figure 1 exhibits the dependence of carbon line intensity on the line-averaged electron density for different charge states: (a) CIII (977.03 Å, 2s²-2s2p), (b) CIV (1548.02 Å, 2s-2p), (c) CV (40.27 Å, 1s²-1s2p), and (d) CVI (33.73 Å, 1s-2p), normalized by the line-averaged electron density. The emission intensity of carbon ions in all charge states is enhanced in deuterium discharges. This enhancement can be attributed to the higher sputtering rate of carbon materials by deuterium plasma compared to hydrogen plasma, resulting in an increased generation of carbon impurities from the divertor plates. Figure 1(e) presents a line ratio of CV/CIV as an indicator of the impurity screening effect, where smaller values indicate a stronger impurity screening effect. A comparison between deuterium and hydrogen plasmas in Figure 1(e) reveals that the impurity screening effect is more pronounced in deuterium plasmas. A Doppler profile measurement of the second order of CIV line emission (1548.20 × 2 Å) was attempted using a 3 m normal-incidence VUV spectrometer in the edge plasma at a horizontally elongated plasma position. The flow velocity reaches its maximum value close to the outermost region of the ergodic layer, and the observed flow direction

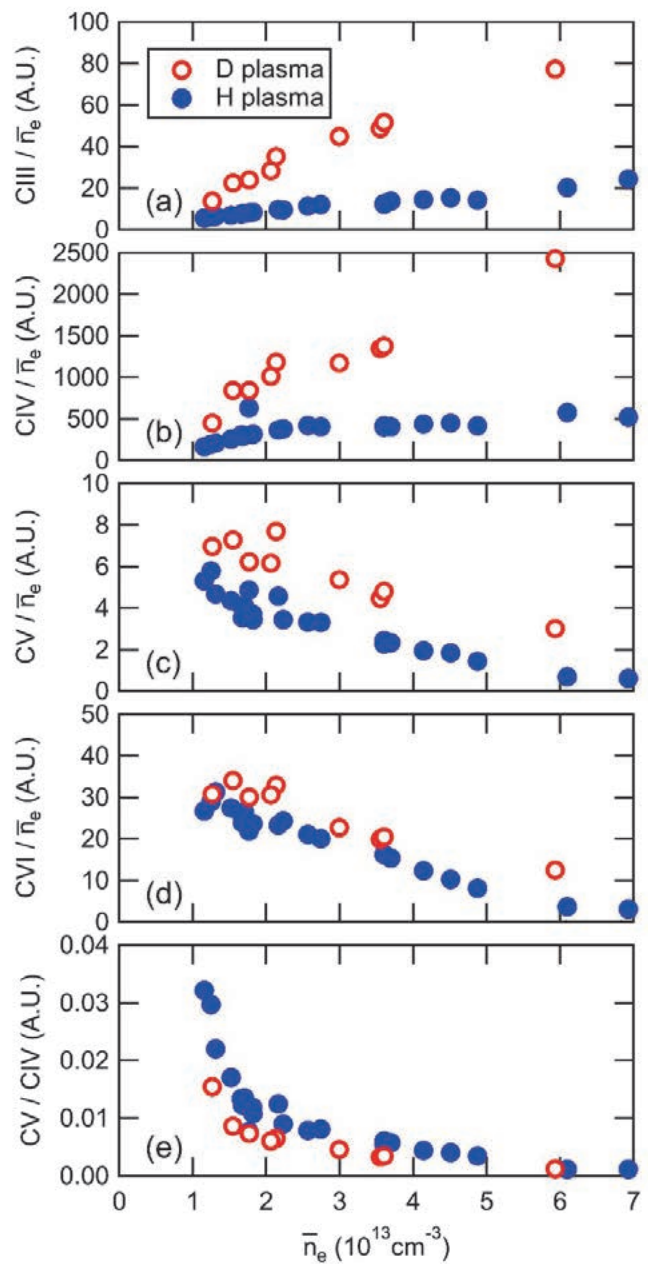


Fig. 1 Line-averaged electron density dependence of line intensity of (a) CIII, (b) CIV, (c) CV, (d) CVI normalized by the electron density and (e) line ratio CV/CIV for deuterium and hydrogen discharges.

aligns with the friction force in the parallel momentum balance. The flow velocity increases with the electron density in H plasmas, suggesting that the friction force becomes more dominant in the force balance at higher density regimes. This leads to an increase in the impurity flow, which can contribute to the impurity screening. In contrast, the flow velocity in the D plasma is smaller than that in the H plasma. The difference in flow values between D and H plasmas, when the friction force term dominates in the momentum balance, could be attributed to the mass dependence of the thermal velocity of the bulk ions (Fig. 2).

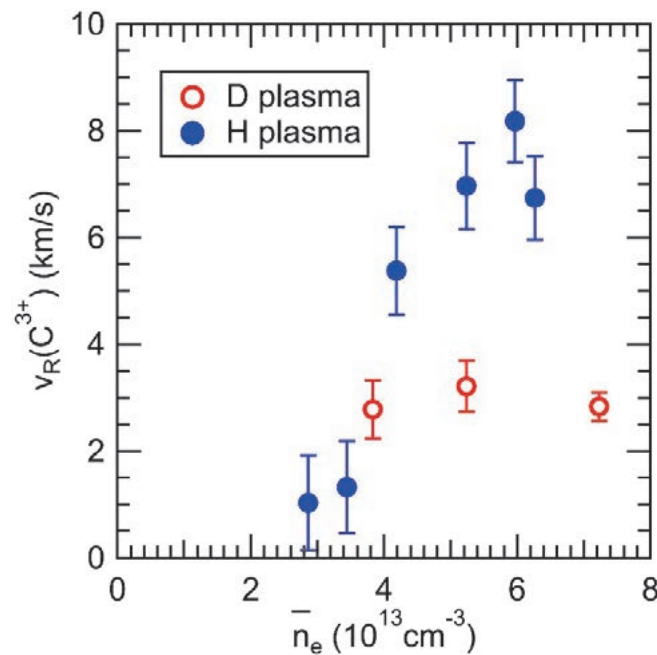


Fig. 2 Observed C^{3+} flow at the bottom edge of the ergodic layer in the D and H plasmas as a function of line-averaged electron density for $R_{ax} = 3.6$ m.

[1] T. Oishi *et al.*, Plasma **6**, 308–321 (2023).

(T. Oishi)

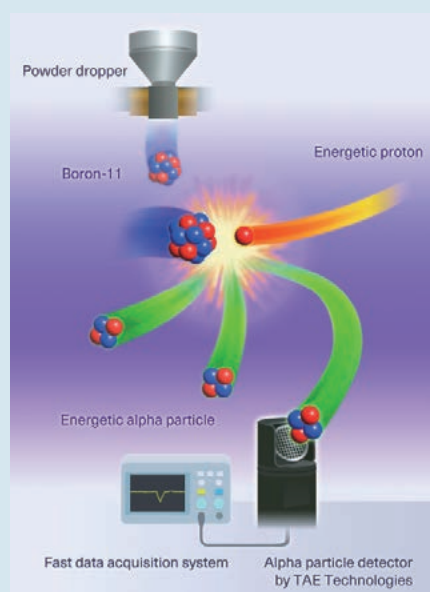
Instability

Highlight

Demonstration of fusion reactions using advanced fusion fuels

In recent years, research toward cleaner fusion reactors has been active, especially among venture companies from around the world. Cleaner fusion reactors will use advanced fusion fuels, which are more difficult to fuse than deuterium and tritium ones, but do not produce neutrons. A hydrogen and boron-11 reactor is possible using energetic hydrogen beams, and the research for this has been led by TAE Technologies. To efficiently cause a fusion reaction, protons must collide with boron-11 at a speed of more than 15,000,000 km/h. The LHD is equipped with the world's only operational hydrogen beam injectors that can shoot the hydrogen into plasma at speeds exceeding 15,000,000 km/h and a powder dropper that can inject boron into plasma. These enable fusion reactions between protons and boron-11 in a magnetically confined plasma.

The fusion reaction between protons and boron-11 produces energetic helium. To demonstrate the reaction, the energetic helium must be detected. The amount of helium produced, and its trajectories are predicted based on numerical simulations, validated in LHD experiments. An alpha particle detector based on a large area semiconductor detector was placed near the surface of the plasma where the energetic helium was predicted to appear. As a result of an experiment in which an energetic hydrogen beam was injected into the boron-sprinkled plasma, energetic helium produced by the fusion reaction between protons and boron-11 was successfully detected, as predicted. This was the world's first demonstration of a fusion reaction between protons and boron-11 in a magnetic confinement fusion plasma. The results of this research are a major first step toward the realization of a cleaner magnetic confinement fusion reactor.



Proton and boron-11 experiment in LHD

(R. M. Magee)

First Observation of Ion Cyclotron Emission from fusion-born protons in a heliotron-stellarator plasma [1]

Ion cyclotron emission (ICE) from fusion-born protons has been observed for the first time in a heliotron-stellarator. During perpendicular deuterium beam injection in the LHD, intense bursty emissions were detected just after the onset of the tongue event that caused a magnetic reconnection and resulted in the exhausting of high energy ions (Fig. 1). We found successive ICE spectral peaks have a typical frequency spacing of 26.6 MHz, comparable to the proton cyclotron frequency in the plasma peripheral region. We stress that these peaks are not located close to the integer multiples of cyclotron frequency but shift from the 8th to 12th. cyclotron harmonics by approximately half the proton cyclotron frequency.

Based on the assumptions that a bursting ICE signal originates from fusion-born ions, at a single location to be identified with the magnetic field strength, under a single collective plasma physics process of the magnetoacoustic cyclotron instability, fusion-born protons which have a perpendicular velocity (v_{\perp}) approximately equal to Alfvén velocity (V_A) and a parallel velocity (v_{\parallel}) approximately 2.4 times V_A might be responsible for the measured frequency shift of the ICE, propagating almost perpendicular to the magnetic field. First principle computations of the collective relaxation of a proton subpopulation near its birth energy $E_H=3.02$ MeV, within a majority thermal deuterium plasma, were carried out using a particle-in-cell approach. We found substantial frequency shifts in the peaks of the simulated ICE spectra, which corresponded closely to the measurement.

This first probable detection of collective electromagnetic radiation from fusion-born ions in a stellarator-type plasma is an encouraging development for magnetically confined (MCF) plasma physics, and shows the flexibility of the LHD heliotron-stellarator and its diagnostic systems. The foregoing is also an example of the reconstruction of the zeroth-order features of the velocity space distribution function of an energetic ion population, based solely on ICE measurements, which reinforces the case for the adoption of ICE as a fast ion diagnostic in ITER.

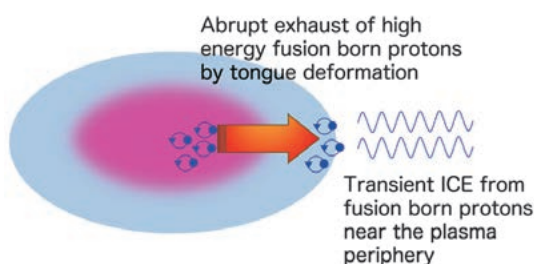


Fig. 1 By abrupt tongue deformation of the confinement magnetic field, transient ICE from fusion born protons which are exhausted from the plasma central region.

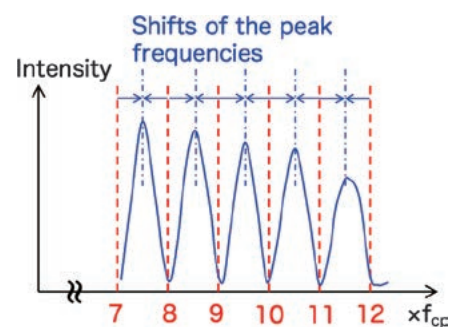


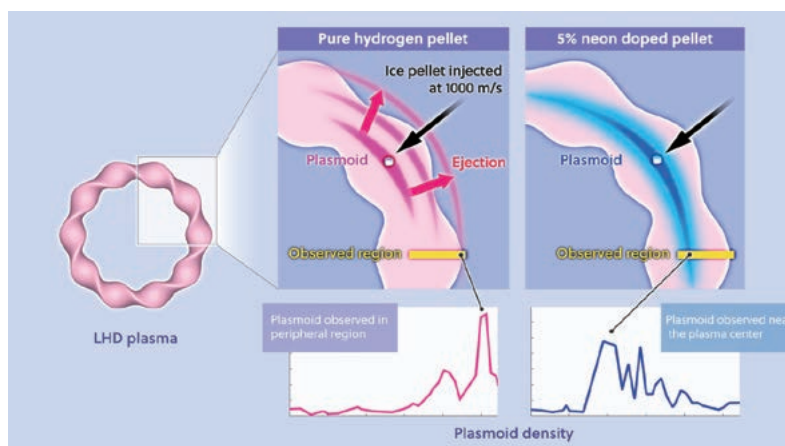
Fig. 2 Successive ICE spectral peaks shift from the integer multiples of proton cyclotron frequency at the likely emitting region.

[1] B C G Reman, R O Dendy, H Igami, T Akiyama, M Salewski, S C Chapman, J W S Cook, S Inagaki, K Saito, R Seki, M Toida, M H Kim, S G Thatipamula and G S Yun, "First observation and interpretation of spontaneous collective radiation from fusion-born ions in a stellarator plasma" *Plasma Phys. Control. Fusion* **64**, 085008 (2022). <https://doi.org/10.1088/1361-6587/ac7892>

Cooling 100 million degree plasma with hydrogen–neon mixture ice pellet injection

At ITER – the world’s largest experimental fusion reactor, currently under construction in France – a so-called “disruption” poses a major open issue. Disruptions are the abrupt termination of magnetic confinement, which causes high-temperature plasma to flow into the inner surface of the containing vessel. Therefore, a dedicated machine-protection strategy is required as a safeguard. As a baseline strategy, researchers are developing a method using ice pellets and injecting them into a high-temperature plasma. The injected ice melts from the surface and evaporates and ionizes owing to heating by the ambient high-temperature plasma, forming a layer of low-temperature high-density plasma (hereafter referred to as a “plasmoid”) around the ice. Such a low-temperature, high-density plasmoid mixes with the main plasma, the temperature of which is reduced during the process, thereby mitigating the heat load to the plasma-facing material components.

However, in recent experiments, it has been observed that when pure hydrogen ice is used, the plasmoid is ejected before it can mix with the target plasma, making it ineffective for cooling the high-temperature plasma deeper below the surface. A solution to this problem was proposed based on an LHD experiment [1]. In the LHD, we discovered that by adding approximately 5% neon to a hydrogen ice pellet, it is possible to cool the plasma more deeply below its surface, and hence, more effectively than when pure hydrogen ice pellets are injected. This result is consistent with model calculations [2], which predict that by mixing a small amount of neon into hydrogen, the internal energy of the plasmoid can be emitted as photon energy, resulting in a suppression of the outward drift motion experienced by the plasmoid. This effect of neon doping is not only interesting as a new experimental phenomenon, but will also contribute to the establishment of plasma control technologies for future fusion reactors.



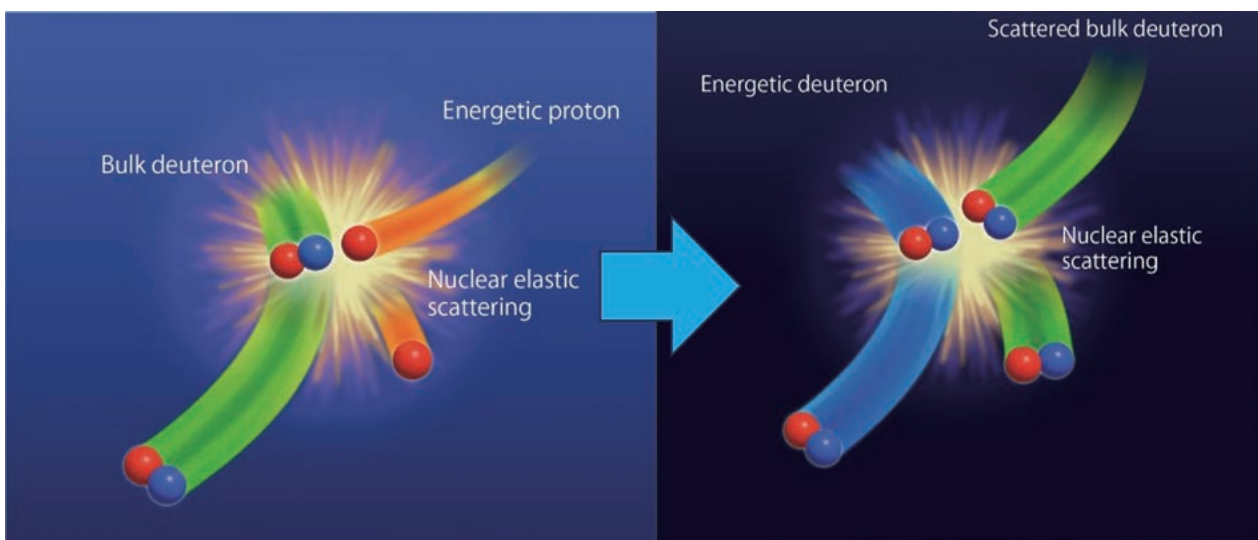
Plasmoid behavior of pure hydrogen and hydrogen mixed with 5 % neon. In this experiment, a new Thomson Scattering (TS) diagnostic system operating at (an unprecedented rate of) 20 kHz was used to (i) measure the density of the plasmoid at the moment it passed through the observation region and (ii) identify its position, which verified the theoretical predictions.

[1] A. Matsuyama, R. Sakamoto, R. Yasuhara *et al.*, Phys. Rev. Lett. **129**, 255001 (2022).

[2] A. Matsuyama, Phys. Plasmas **29**, 042501 (2022).

Observation of energy transfer due to nuclear elastic scattering

Coulomb scattering is usually regarded as the dominant process in the ion collisions in a fusion plasma. However, as the energy of the ions increases, the nuclear elastic scattering due to the ‘nuclear force’, the force becomes non-negligible. Coulomb scattering has a small scattering angle and a small energy transfer per collision, whereas nuclear elastic scattering has a large scattering angle and a large energy transfer per collision. Nuclear elastic scattering has the effect of enhancing ion heating and changing the distribution function of ions, which is expected to improve fusion reactivity in future fusion reactors. In the LHD deuterium plasma experiments, the research group injected deuterium and hydrogen beams simultaneously into the deuterium plasma and analyzed the neutron emission rate and decay time. The neutrons are mainly due to the reaction between bulk deuterons and energetic deuterons. The decay time of the neutron emission rate reflects the change in the velocity distribution of the energetic deuterons. The decay time of the neutron emission rate obtained in the experiment is longer than that predicted by the numerical simulation considering only Coulomb scattering. Energy transfer between energetic ions cannot be explained only by the Coulomb scattering process. To understand the energy transfer between energetic ions, a numerical analysis was carried out using a Boltzmann-Fokker-Planck simulation, in which a Boltzmann collision term describing nucleoplasmic scattering was added to the Fokker-Planck analysis model, which analyses the distribution function of the plasma. The results show that energy is transferred from the energetic protons to the energetic deuterons via the bulk deuterons. Since nuclear elastic scattering has a large energy transfer per collision, the energy transfer by nuclear elastic scattering becomes equivalent to the energy transfer by Coulomb scattering. This result might provide an important insight into the efficiency of power generation in future fusion reactors.



Energy transfer from energetic proton to energetic deuteron via bulk deuteron by nuclear elastic scattering

(H. Matsuura)

Research and Development Collaboration Program for LHD-Project

Highlight

Reduction of co-extracted electron current owing to expansion of deuterium negative-ion plasma region

Negative-ion source-based neutral beam injection (NBI) has the problem that the electron current co-extracted from deuterium plasma is higher than that from hydrogen plasma. A deflection magnetic field is applied near the plasma grid (PG), and an ionic plasma composed of positive and negative ions is maintained near the PG surface. Here, negative ions are produced by irradiating a PG made of aluminum (Al-PG) with hydrogen/deuterium plasma without caesiation. The irradiation surface is set to the axial position of -1.3 cm. Plasma axial distributions are measured by a Langmuir probe when deflecting magnets are embedded inside the Al-PG (the magnet center at -0.8 cm). Figure 1 (a) shows the axial distributions of the probe negative/positive saturation-current ratio, depending on the DC voltage biased to the Al-PG. The current ratio is about 30 or more in the discharge plasma and around one in the ionic plasma. The boundary region of the ionic plasma has a current ratio of 2–3, and the boundary position changes depending on the Al-PG voltage. For Al-PG voltage higher than $+2$ V, the ionic plasma is maintained at -2.3 cm. For Al-PG voltage lower than $+2$ V, the electron-rich region (the current ratio higher than 3) is in the discharge plasma and downstream from the Al-PG aperture. It has been clarified that these electrons downstream are not the co-extracted electrons derived from the discharge plasma but detached electrons that appear after precursor ions decay. The axial distributions of the current ratio at the Al-PG voltage of $+2$ V are shown in Fig. 1 (b). When the deflection magnet center is at -4.9 cm, the ionic plasma is maintained downstream from -6.5 cm, and the volume of the ionic plasma significantly increases. The current ratio is higher than 18 without the magnets, and no ionic plasma region is formed. Regardless of the position of the magnet center, the deflection magnetic-flux density is 22 mT at the boundary position. The co-extracted electron current is suppressed when the meniscus near the Al-PG aperture is far from the boundary region.

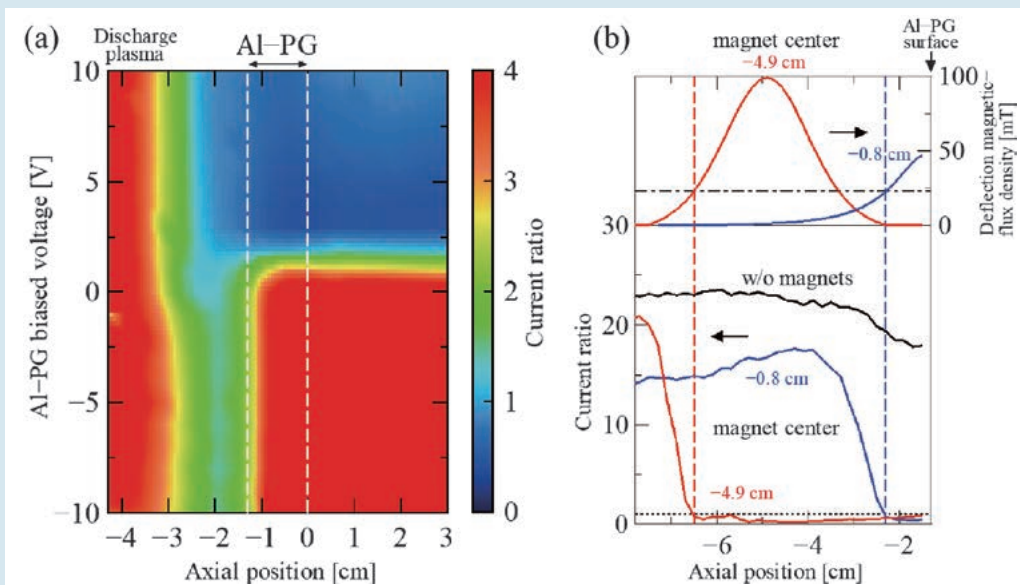


Fig. 1 (a) Axial distributions of probe negative/positive saturation-current ratio depending on DC voltage biased to Al-PG, (b) axial distributions of current ratio and deflection magnetic-flux density at Al-PG voltage of $+2$ V.

(W. Oohara)

Development of ghost imaging absorption spectroscopy and observation of 3-D structure of detached plasma

We are developing a ghost imaging absorption spectroscopy method by integrating computational ghost imaging (CGI) with plasma absorption spectroscopy. Ghost imaging is a method that employs a single-pixel detector such as a photodiode to capture an image of an object [1]. Figure 1 shows schematics of a CGI absorption spectroscopy system. A random intensity pattern, $I_r(x,y)$, is computationally generated by a personal computer, and the structure is transcribed to an illumination laser using a digital micromirror device (DMD). As depicted in Fig. 1, the structured light is absorbed by plasma with a transmittance distribution $T(x,y)$. A lens focuses the transmitted light onto a photodiode, and its total intensity b_r is measured. The value of $T(x,y)$ is subsequently computed as follows:

$$T(x,y) = \frac{\langle b_r I_r(x,y) \rangle - \langle I_r(x,y) \rangle \langle b_r \rangle}{|\langle I_r(x,y) \rangle|^2}, \quad (1)$$

where $\langle \dots \rangle$ denotes an average over independent structured light patterns. By switching and averaging tens of thousands of $I_r(x,y)$ patterns, the contrast of the resultant $T(x,y)$ is incrementally improved. As this imaging method is predicated on the correlation between b_r and $I_r(x,y)$, it exhibits a noise tolerance analogous to lock-in detection. Moreover, by restricting the area of correlated absorption with $I_r(x,y)$ through the focusing of structured light, spatial resolution in the line-of-sight can be attained even in absorption spectroscopy.

The newly developed spectroscopy system has been employed to visualize the distribution of metastable helium atoms near the plasma endplate of a helicon-wave plasma device. Figure 2(a) presents a side-view image of the device, showing the plasma generated upstream of the device on the right side being terminated at the end plate. Structured lights illuminate a $27 \text{ mm} \times 17 \text{ mm}$ area indicated by the red square.

Figure 2(b) shows metastable helium distribution. The numbers on the horizontal and vertical axes represent the number of pixels in the image. The surface of the end plate is located around 40 on the horizontal axis, and an increase in the metastable density is observed towards the upstream of the device. Since the principle of CGI absorption spectroscopy has been verified, we intend to employ this measurement method to obtain the distribution of metastable atoms in detached plasmas.

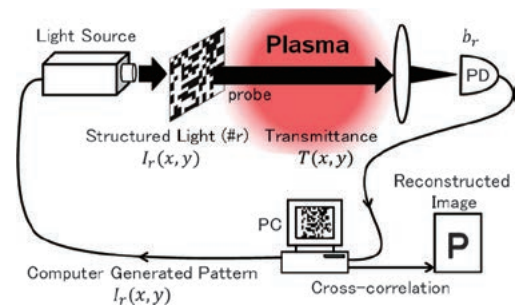


Fig. 1 Schematics of CGI absorption spectroscopy system.

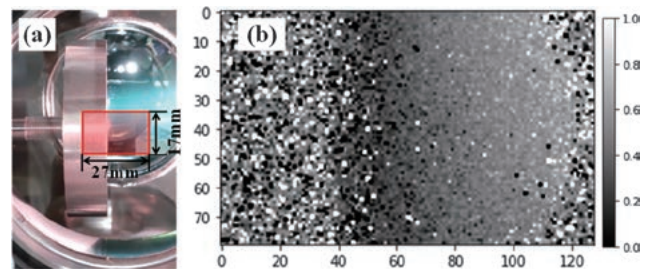


Fig. 2 (a) Measurement area by ghost imaging absorption spectroscopy. (b) Absorption distribution near the plasma end plate.

[1] J. H. Shapiro, Phys. Rev. A **78**, 061802(R) (2008).

2. Fusion Engineering Research Project

The Fusion Engineering Research Project (FERP), started in FY2010, accomplished its twelve-year mission in FY2022. In this report, the research activities of the FERP in its final year are briefly summarized with its highlights.

Along with conceptual design studies for the helical fusion reactor, the FERP has been developing technologies for key components in fusion reactors, such as the superconducting magnet, blanket, and divertor, as illustrated in Fig. 1. The research also focuses on materials used for blankets and divertors, the interaction between the plasma and the first wall, including atomic processes, handling of tritium, plasma control, heating, and diagnostics. The FERP was composed of 13 tasks and 44 sub-tasks with domestic and international collaborations. There has also been cooperation with the Large Helical Device Project and the Numerical Simulation Reactor Research Project. The research activities of the FERP have been succeeded by a couple of “Units” in the new structure of NIFS.

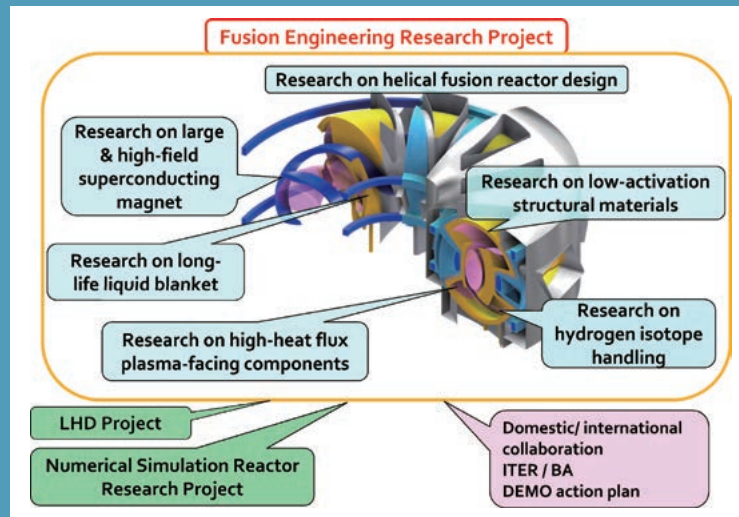


Fig. 1 Research areas of the Fusion Engineering Research Project with domestic and international collaborations.

(I. Murakami and N. Yanagi)

Design Studies on the Helical Fusion Reactor

Since the establishment of the Fusion Engineering Research Project (FERP) in FY2010, conceptual design studies for a steady-state helical fusion reactor have continued. Since FY2022 was the final year of the FERP, a summary of design studies has been conducted.

The conceptual design studies in the FERP have focused on the improvement of accuracy and feasibility of the design in cooperation with the Large Helical Device (LHD) Project and the Numerical Experimental Simulation Reactor Research Project, based on the achievements of previous design studies. While the conceptual design study has shown the feasibility of fusion reactor design utilizing the excellent features of the LHD-type heliotron device (steady-state operation capability, constructability, maintainability), it has also revealed various design issues. The two most significant ones identified are improvement of plasma performance (simultaneous achievement of MHD stability and good energy confinement) and ensuring sufficient blanket space.

To solve these problems, configuration optimization studies using the helical coil optimization code OP-THECS and engineering experiments on high-temperature superconductors and liquid blankets/divertors have been advanced. The R&D issues for improving the plant performance and public acceptance of fusion reactors have also been organized, leading to the systematization of fusion engineering as an academic field. The conceptual design study also led to collaborative research on three-dimensional neutron transport calculations, visualization of magnetic field lines, and an investigation of better magnetic field configurations using machine learning. It is expected that these research activities will be continued in the newly established “Units” as themes that lead to the solution of problems related to fusion reactors in general.

In the conceptual design of helical fusion reactors, structural analyses of the optimized helical magnet

system have been carried out. The basic geometry has been based on a similar expansion of the winding law of the helical coil (HC) as in the LHD. On the other hand, studies have been conducted to aim for better confinement performance, and optimization by changing the parameters of the winding law and geometry optimization by flexibly deforming the coil trajectory with spline curves. The effects of such changes in the geometry of the HC on the electromagnetic (EM) forces and the mechanical behavior of the coils were verified from the viewpoint of the integrity of the equipment. In the helical winding law, α is the HC pitch modulation parameter which determines the poloidal position of the coil, relative to the toroidal angle. The effect of the winding law optimization with α of 0.1, 0, and with the spline-based one were investigated. Although the changes in coil position due to these optimizations appear to be slight, they can result in relatively large changes in the generated magnetic field and electromagnetic force distribution. For the structural analysis, a major radius of 7.8 m and a plasma center field of 6.6 T were assumed. To compare stress distribution over a wide area, stress analysis was performed by applying the same support structure. The coils are supported by a torus shell and there are no openings. Table 1 and Fig. 2 show the results of the electromagnetic field and stress analysis. Even if the magnetomotive force of the HC is the same, the stress and displacement generated in the support structure are different, depending on the coil trajectory or the magnitude of the magnetomotive force of the vertical field coil.

Table 1 Coil specifications and electromagnetic properties

		LHD-type		Spline HC	
		$\alpha=0.1$	$\alpha=0$		
Magnetomotive force (MA)	HC	25.74	25.74	25.97	
	IV	15.03	15.37	19.46	
	OV	-14.59	-16.91	-14.43	
Magnetic stored energy (GJ)		85	89	93	
Maximum magnetic field (T)		18.57	18.91	19.51	
EM hoop force (MN/m)	HC	innermost	70.41	80.73	76.67
		outermost	53.73	44.36	50.10
	IV	77.36	75.59	113.94	
	OV	22.65	28.61	22.82	
Max. Mises stress (MPa)		506	549	553	
Max. displacement (mm)		7.1	7.3	8.1	

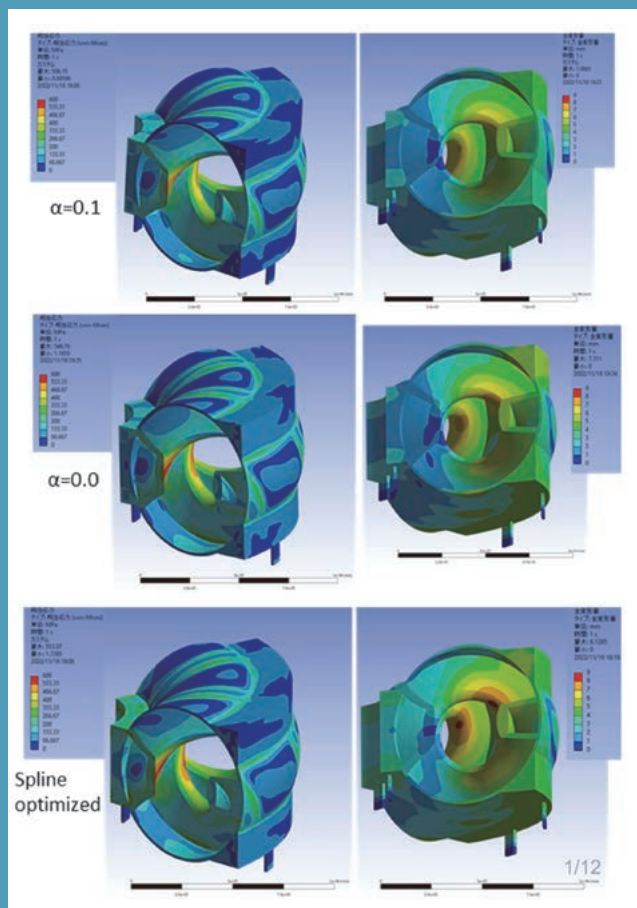


Fig. 2 Stress and displacement distributions of the magnet system of the helical fusion reactor with the helical coil configuration defined as (top) $\alpha = 0.1$, (middle) $\alpha = 0.0$, and (bottom) spline-optimized.

(T. Goto, H. Tamura and H. Yamaguchi)

Highlight

Research and Development on Divertor

A new type of divertor heat removal component with tungsten (W) armor and an oxide-dispersion-strengthened copper (GlidCop®) has been developed by original fabrication technology, so called Advanced Multi-Step Brazing (AMSB). The component has a rectangular-shaped cooling flow path channel with a V-shaped staggered-rib structure in the GlidCop® heat sink. This W/GlidCop® component showed an extremely high heat removal capability during a $\sim 30 \text{ MW/m}^2$ steady-state heat loading condition in our previous work. In this work, to investigate the durability and plasma wall interaction (PWI) phenomena of the new component against simultaneous loading of high-heat and high-particle flux under a large-sized plasma confinement device, the component was installed in the divertor strike position of the Large Helical Device (LHD), as shown in Fig. 3, and exposed to neutral beam heated plasma discharges with 1180 shots ($\sim 8000 \text{ s}$) in total. After the exposure, several microstructural analyses were conducted by using a dual-beam type of focused-ion beam/scanning electron microscopy (FIB-SEM) device, nanoDUE'T® NB5000 (Hitachi High-Technologies Corp.) on the W armor plate. An extremely high heat removal response in the component was demonstrated through the quick increase and decrease of the temperature of the W plate, located on the divertor strike point during discharges. Though submillimeter-scale damages such as unipolar arc trails and microscale cracks were identified on the W surface, such a high heat removal response did not show any sign of degradation during the 1180 shots ($\sim 8000 \text{ s}$) of plasma discharges. If these submillimeter-scale damages are evolved beyond a millimeter scale, the heat removal performance will be degraded. The improved component, which has tolerance against repetitive heat loading, will be required for a reactor environment.

From a viewpoint of microstructural damage on the surface of the W armor, remarkable sputtering erosion and redeposition phenomena, due to the strong influx of the divertor plasma, was confirmed on the side surface wall of the W armor. This phenomenon could be caused by the synergistic effects of high flux and long-time particle loading. Such a high fluence could also be easily reached in future fusion devices. This work has demonstrated one of the critical erosion phenomena of W armor for future fusion devices.

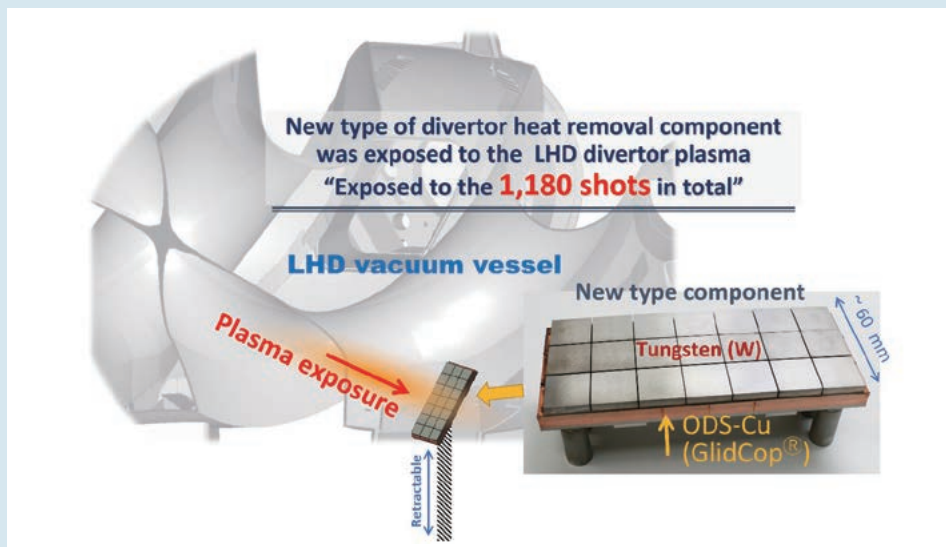


Fig. 3 Schematic figure for an exposure experiment of new type of divertor heat removal component to an LHD divertor plasma in the vicinity of the joint interfaces for W/Cu (b) and Cu/RAFM steel joint.

(M. Tokitani)

Development of oxide dispersion strengthened tungsten (ODS-W) including titanium oxide

For improvement of plasma facing tungsten on a fusion divertor, we have developed a new oxide dispersion strengthened tungsten (ODS-W), including titanium oxide as strengthening particles (Fig. 4), fabricated by mechanical alloying (MA)-hot isostatic pressing (HIP), which can inhibit the decrease of a mechanical property at high temperature, even after recrystallization occurs. In terms of its subsequent evaluation, it is therefore important to assess the material's soundness, whether it can withstand intense irradiation and high heat loads. We have researched the irradiation resistance of new oxide dispersion strengthened tungsten with a grain size of 1–2 μm and dispersed small titanium or titanium oxide nanoparticles. For the evaluation of irradiation resistance, tungsten ion irradiation experiments were carried out at 500 $^{\circ}\text{C}$ to about 0.66 dpa at the damage peak by 2.9 MeV W^{2+} ions from the Tandatron accelerator at the High Fluence Irradiation Facility, the University of Tokyo (HIT). A nano-hardness measurement was carried out using a Shimadzu nano-indenter with a Berkovich-type indenter. A nano-hardness of ODS-W was 6.4 ± 1.2 GPa and 6.4 ± 1.4 GPa before and after irradiation, respectively, and no irradiation hardening was observed. On the ODS-W, no void formation was observed after ion irradiation, as shown in Fig. 5. Therefore, according to the above results of a TEM observation and the hardness tests, this material is considered to have a high performance against irradiation.

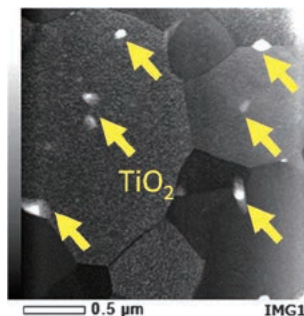


Fig. 4 Transmission Electron Microscope (TEM) image of nano-titanium oxide at grain boundaries after annealing at 1800 $^{\circ}\text{C}$.

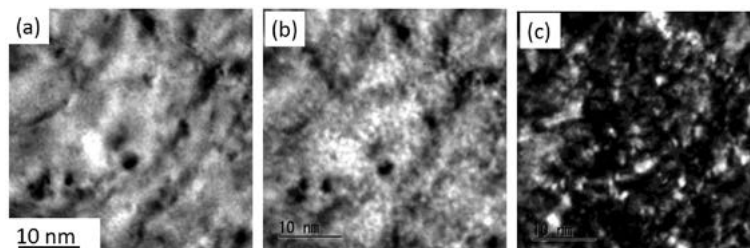


Fig. 5 (a) Bright-field image (in focus), (b) bright-field image (out of focus), (C) weak-beam dark field image in the irradiated W-TiC composite at 500 $^{\circ}\text{C}$ to 0.66 dpa. Copied from [1].

[1] E. Wakai, H. Noto *et al.*, “Titanium/titanium oxide particle dispersed W-TiC composites for high irradiation applications”, *Research & Development in Material Science* **16**, 1879–1885 (2022).

Tungsten is a strong candidate material for plasma-facing walls such as divertors in next-generation fusion devices. However, although the highly charged ion spectrum of tungsten is very important for plasma diagnostics, the identification of emission lines has not yet been established, due to the complexity of the excitation process. Therefore, we have been conducting a spectroscopic study of the highly charged tungsten ions using an Electron Beam Ion Trap (EBIT), in order to obtain atomic data on highly charged tungsten ions.

In highly-charged tungsten ion spectroscopy to date, quasi-continuous spectra (Unresolved Transition Array, UTA), which are formed by a large number of emission lines peculiar to highly charged ions, have been measured. These UTAs appear not only in tungsten but also in the emission lines of highly charged heavy ions and are widely observed in extreme ultraviolet light sources, fusion plasmas, and astronomical plasmas. However, there is still no quantitative diagnostic method for UTA spectra. Our research group has been focusing on UTA and analyzing its structure. We obtained UTA emission spectra from tungsten pellet injection at the LHD and compared them with the monoenergetic spectra at EBIT. The upper panel of Fig. 6 shows the spectrum at tungsten pellet injection. UTA appears at around 5 nm. The lower panel shows the electron energy dependence of the highly charged tungsten ion spectrum in the Tokyo-EBIT. Third-order light from diffraction grating (the wavelength is tripled) was used to obtain a high-resolution spectrum. In the future, we will analyze the spectral data using statistical theory to develop a new quantitative diagnostic method.

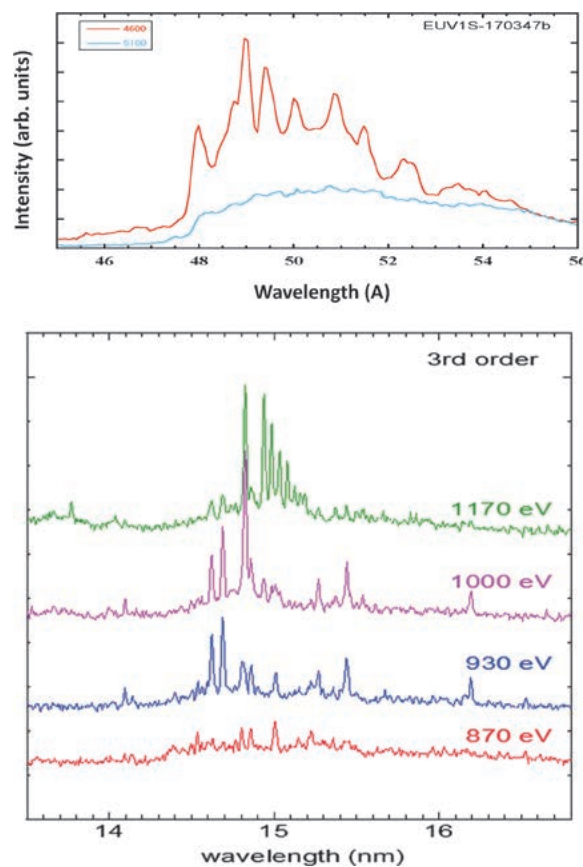


Fig. 6 (Upper) W pellet injection spectrum at LHD. (Lower) Energy dependence of highly charged W ion spectra in Tokyo-EBIT.

(H. Noto and H. Sakaue)

Research and Development on Superconducting Magnet

The NIFS-FERP has been developing three kinds of High-Temperature Superconducting (HTS) large-current conductors to apply to the next-generation fusion experimental devices, namely, STARS, FAIR, and WISE conductors. Here, the progress of the STARS conductor is briefly reported. The STARS conductor is characterized by its high current density (current amplitude divided by the cross-sectional area of the conductor). The target current density is 80 A/mm^2 , which is about twice that of an LTS conductor of the same size. The STARS conductor consists of 15 layers of REBCO tapes, encased in a stabilized copper jacket and strengthened by an outer stainless steel jacket (Fig. 7(a)). A coil-shaped sample having three turns of a diameter of 600 mm and a 6-m-long conductor (Fig. 7(b)) was fabricated by Metal Technology Co. Ltd. using the state-of-the-art EuBCO tapes manufactured by Fujikura Ltd. It was tested in the NIFS large-diameter high-field conductor testing facility and stably energized up to its rated current of 18 kA at a temperature of 20 K ($-253 \text{ }^\circ\text{C}$) and magnetic field strength of 8 T. This means that the target current density of 80 A/mm^2 was successfully achieved. In addition, it was confirmed that the coil was energized stably, even when the current was raised and lowered at a high speed of 1 kA/s and repeated a total of more than 200 times with no change, indicating that the STARS conductor is stable and robust.

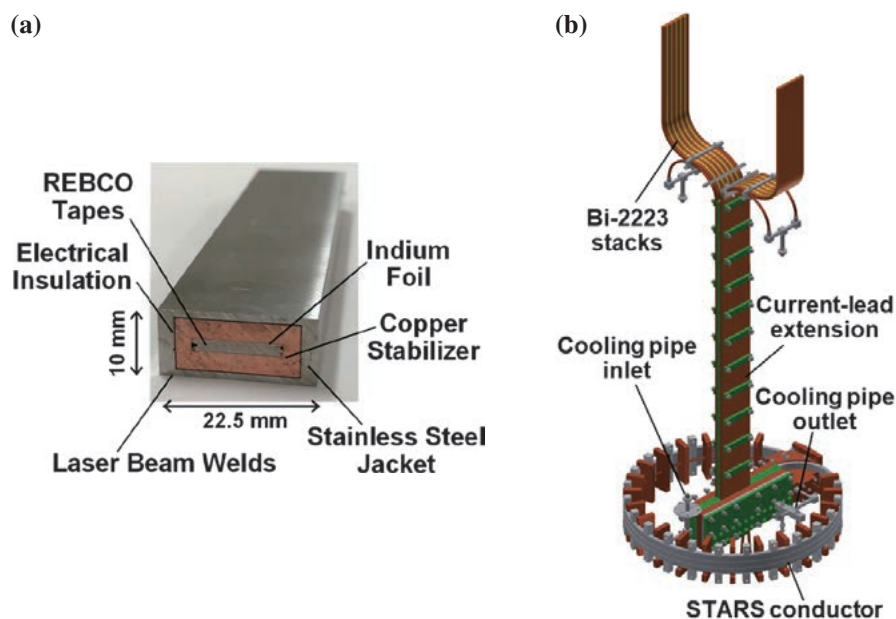


Fig. 7 (a) Photograph of a mock-up sample of the 20-kA-class STARS conductor with descriptions of internal layout, having a stack of 15 REBCO tapes (width: 12 mm) and internal electrical insulation between the copper stabilizer casing and stainless-steel jacket. (b) A three-dimensional drawing of the 6-m solenoid-coil sample without showing the stainless-steel supporting ring.

Magnesium diboride (MgB_2) wire is a promising alternative material to NbTi wire under a neutron irradiation environment such as fusion or accelerator applications. This is because MgB_2 has higher critical temperature (39 K) properties, lower cost, and low activation compared with NbTi wire. These factors will contribute to realizing a liquid hydrogen-cooled low-activation superconducting cable for future fusion magnets. We contemplated reconsidering the raw materials of in-situ processed MgB_2 wire in order to improve the low activation property. In the case of the in-situ process, generally, the MgB_2 phase is formed by the thermal diffusion reaction between magnesium (Mg) and amorphous boron (B). In particular, B material has two kinds of stable isotopes, i.e., ^{10}B

and ^{11}B , and the ^{11}B isotope is well known to have no nuclear transmutation by neutron irradiation. We thought that use of ^{11}B isotope as the raw B material in the in-situ processed MgB_2 wire could suppress the degradation of critical current density characteristics by nuclear transmutation, based on neutron irradiation.

Several in-situ processed MgB_2 wires using different ^{11}B isotope powders (crystallized or amorphous and coarse or fine) were fabricated, and their microstructures and critical current density (J_c) characteristics under a magnetic field were evaluated. A typical image obtained by the High-Angle Annular Dark Field Scanning Transmission Electron Microscope (HAADF-STEM) and the electron diffraction pattern after heat treatment are shown in Fig. 8(a). Formation of rectangular plate-like finer crystals was confirmed. The electron diffraction patterns indicate that plate-like crystals are an MgB_2 (Mg^{11}B_2) phase originated by the ^{11}B isotope. This tendency was also confirmed in in-situ wire samples using the other ^{11}B isotopic powder. The J_c - B performances of in-situ processed MgB_2 wires using a different ^{11}B isotope powder are shown in Fig. 8(b). In terms of the J_c - B properties, the amorphous ^{11}B powder was more suitable than the crystallized ^{11}B powder as the B raw material. Although the present J_c - B property of Mg^{11}B_2 wires is lower than those of NbTi wires, we believe that the J_c - B properties will be improved by optimizing various conditions, such as heat treatment and in-situ nominal composition in the future.

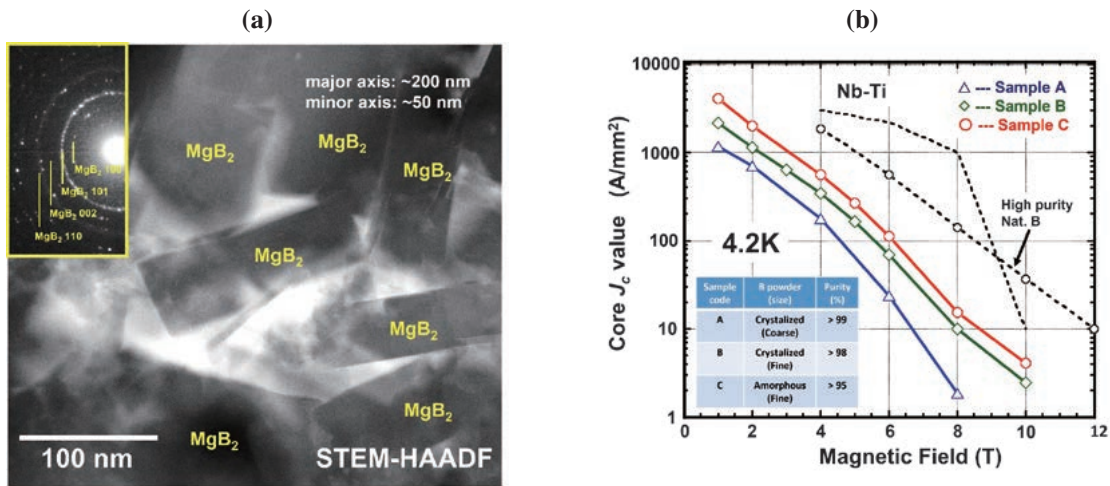


Fig. 8 (a) HAADF-STEM image and electron diffraction pattern after heat treatment and (b) J_c - B performances of in-situ processed MgB_2 wires using different ^{11}B isotope powder.

(N. Yanagi and Y. Hishinuma)

LHD-Project Research Collaboration

The LHD Project Research Collaboration program has been contributing to enhancing both the scientific and technological foundations of research related to the LHD project as well as to the future helical fusion reactors. A feature of this collaboration program is that all research is performed at universities and/or institutions outside NIFS. For the fusion engineering area, the following seven subjects were conducted in FY2022:

1. Evaluation of multi hydrogen isotope transfer behavior on plasma driven permeation for plasma facing materials
2. Studies on liquid hydrogen cooled HTC superconducting magnet
3. The analysis of biological effects elicited by organically bound tritium using life science techniques

4. Technological development of FeCrAl-ODS alloys coexisting with liquid metal cooling system of helical fusion reactor
5. Development of REBCO high Tc coated conductor with conductive micro-path
6. Fabrication technology development toward practical use of functional coating for helical reactor liquid blanket
7. Improvement of environmental tritium transfer model based on the observation near tritium released facilities

From the above seven collaborative research items, subject 5 is briefly reported below:

5. Development of REBCO high Tc coated conductor with conductive micro-path

In developing High-Temperature Superconducting (HTS) magnets for fusion and other applications, a drawback of REBCO tapes is that the buffer layer prevents current sharing between tapes, causing reduced conductor stability. We propose conductive micro-paths to improve conductor stability where the current is shared between the REBCO tapes. In this report, we fabricated the conductive micro-paths in REBCO tapes to investigate the current sharing in the tapes. Blind holes were made on REBCO tapes by Fujikura and SuperOx Japan, as non-conductive micro-paths, by using Nd:YAG lasers. Additional Ag films were deposited on the tapes by a sputtering method to make the micro-paths conductive. We observed the microscopic structure of the blind holes and conductive micro-paths by SEM microscopy. As a result, the blind holes reached the substrates of the REBCO tapes and the holes were filled by the deposited Ag films. Two and three REBCO tapes, one with degradation intentionally introduced, were prepared and stacked to investigate current sharing between them. Partial voltage in the tapes was measured with some voltage taps by sweeping the current at a temperature of 77 K. As a result, the current was shared between the REBCO tapes and successfully bypassed the damaged part. This phenomenon was confirmed with good reproducibility regardless of the sample type.

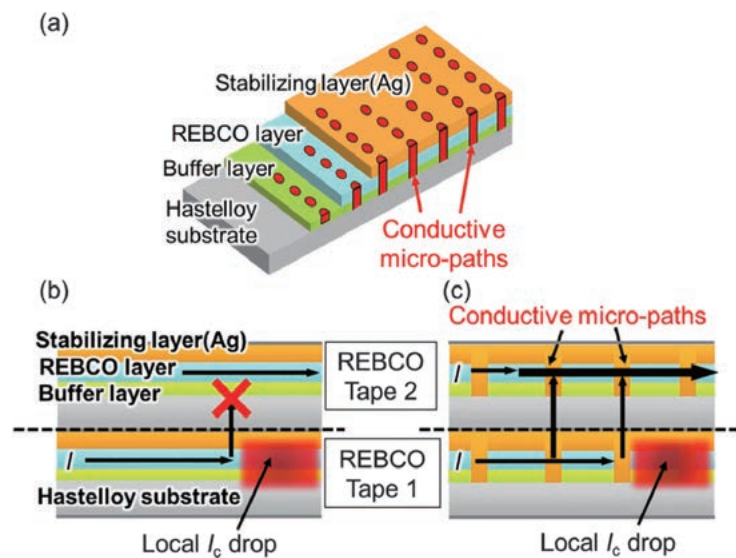


Fig. 9 (a) Schematic drawing of a REBCO tape with conductive micro-paths. Illustrative images of current sharing between the REBCO tapes including local defects with (b) and without (c) conductive micro-paths. Reproduced from [2].

[2] H. Yamada, Y. Tsuchiya, Y. Yoshida *et al.*, “Conductive micro-paths for current sharing between REBCO tapes in high-Tc superconducting conductors to improve stability”, *IEEE Transactions on Applied Superconductivity* **32**, 6602204 (2022).

(Y. Yoshida (Nagoya Univ.) and Y. Onodera)

3. Numerical Simulation Reactor Research Project

Fusion plasmas are complex systems which involve a variety of physical processes interacting with each other across wide ranges of spatiotemporal scales. The National Institute for Fusion Science (NIFS) has conducted the Numerical Simulation Reactor Research Project (NSRP) by utilizing the full capability of the supercomputer system, Plasma Simulator, and propelling domestic and international collaborations. Missions of the NSRP are (i) to systematize understandings of physical mechanisms in fusion plasmas for making fusion science a well-established discipline and (ii) to construct the Numerical Helical Test Reactor, which is an integrated system of simulation codes to predict behaviors of fusion plasmas over the whole machine range.

The Plasma Simulator “Raijin (雷神)” (Fig. 1) began operations in July 2020. It consists of 540 computers, each of which is equipped with eight “Vector Engine” processors. The 540 computers are connected to each other by a high-speed interconnect network. The computational performance is 10.5 petaflops. The capacities of the main memory and the external storage system are 202 terabytes and 32.1 petabytes, respectively.

Presented below in Figs. 2 and 3 are examples of successful results from collaborative simulation research in 2022-2023 on the Ion Cyclotron Range of Frequency (ICRF) heating of LHD plasmas and on ion velocity distribution functions formed in magnetic reconnection, respectively. Also, highlighted in the following pages are achievements of the NSRP research task groups on energetic-particle physics, turbulent transport, integrated transport code, and plasma-wall interaction. The NSRP was completed in March 2023 and its legacy is being carried over to the new organization of NIFS starting from April 2023.

(H. Sugama)



Fig. 1 The Plasma Simulator, “Raijin (雷神)”

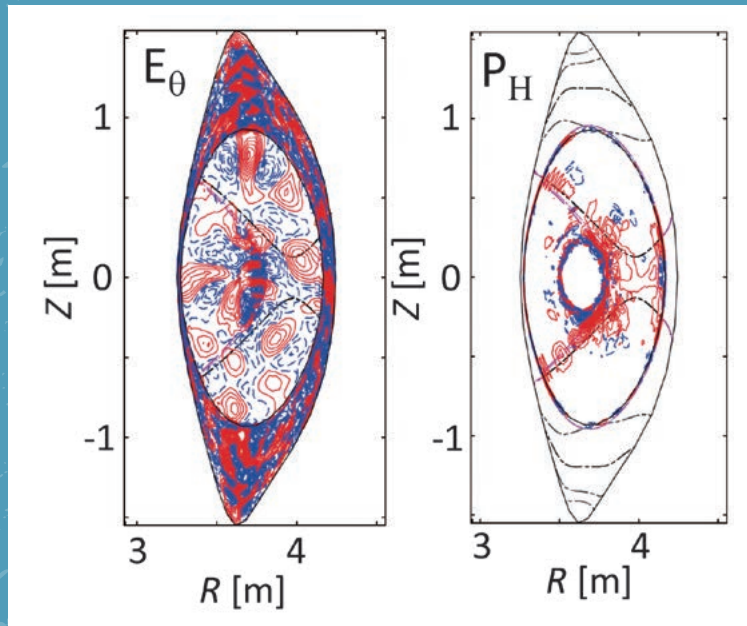


Fig. 2 Distributions of the electric field (left) and the absorbed power (right) obtained by the simulation of the Ion Cyclotron Range of Frequency (ICRF) heating of an LHD plasma [presented by Dr. R. Seki (NIFS)]. The TASK3D/WM code (A. Fukuyama and T. Tohnai, in 5th IAEA Technical Committee Meeting on Alpha Particles in Fusion Research, IAEA, Vienna, 1997) is used for the simulation.

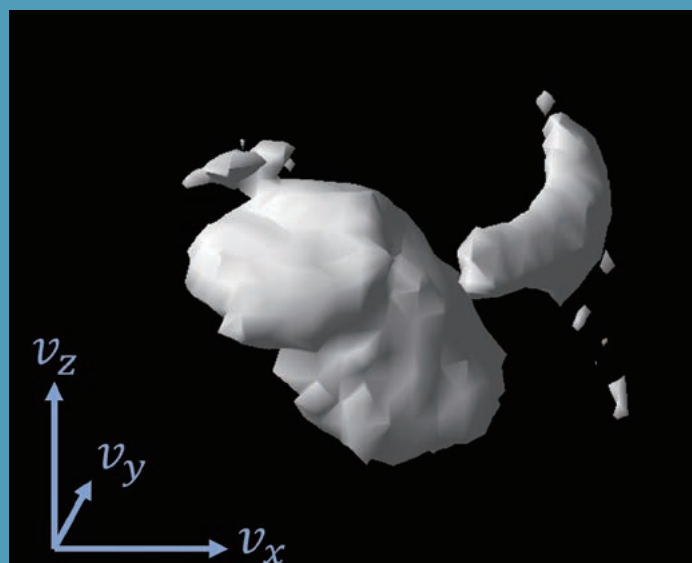


Fig. 3 An isosurface of the ion phase space density obtained by particle simulation of magnetic reconnection [presented by Dr. S. Usami (NIFS), Reference: S. Usami and S. Zenitani, in the Physical Society of Japan 2023 Sprint Meeting, Online, 2023]. This simulation was performed by using the PASMO code.

Energetic-particle Driven Instabilities and Energetic-particle Effects on Magnetohydrodynamic Instabilities

Highlight

Self-consistent simulations of ICRF-induced Alfvén eigenmodes in LHD

Self-consistent simulations which include ion-cyclotron-range-of-frequency (ICRF) acceleration and collisions were conducted with MEGA, which is a kinetic-magnetohydrodynamic (MHD) hybrid simulation code, to investigate the ICRF minority heating scenario in the LHD. Alfvén eigenmodes (AEs) were studied for the first time based on a realistic phase-space distribution of minority ions. It was shown that an AE can be driven unstable during on-axis ICRF heating, where ICRF-generated energetic localized trapped minority ions play a significant role in the AE destabilization. Firstly, a hundred-millisecond classical simulation, where the MHD perturbation is turned off, was performed to obtain the minority ion distribution in a steady state. Figures 1(b) and (c) show the energy distribution functions of minority ions in on-axis and off-axis heating cases, respectively. A considerable number of localized trapped (helically trapped) minority ions are accelerated to high energy (\sim MeV) in the on-axis (off-axis) heating case, as shown in Figs. 1(b) and (c). A localized trapped particle is toroidally trapped between two adjacent vertically elongated plasma cross-sections in the LHD, whose toroidal precession motion is almost zero, as shown in Fig. 1(a). Then, AE stability was investigated via a hybrid simulation based on the steady-state minority ion distributions. An unstable mode can only be found in an on-axis heating case. The unstable mode is identified as an energetic particle mode (EPM) localized in the plasma core with toroidal mode number $n=1$ and dominant poloidal harmonics $m=2,3$. The mode frequency is mainly between 80~100kHz, propagating in the ion diamagnetic drift direction. The resonance condition shows that localized trapped minority ions with energy 400~1000keV contribute to the EPM drive, whose poloidal drift orbit frequencies can match the mode frequency. Recent experimental observations of ICRF-induced modes during 2.5 MW on-axis ICRF heating in the LHD show good consistency with the simulation results of the mode frequency and both toroidal and poloidal mode numbers.

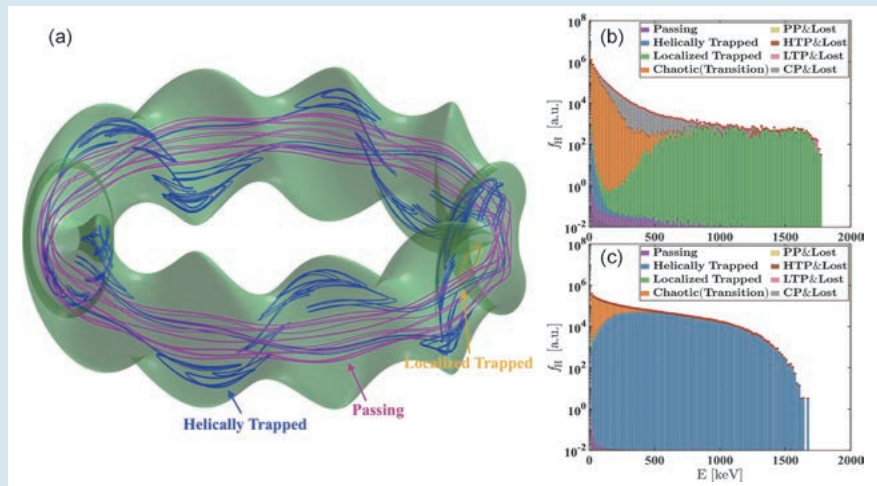


Fig. 1 (a) Typical ICRF-accelerated minority ion trajectories in the LHD. Minority ion energy distribution functions (red solid circles) in steady states for (b) on-axis heating ($B_{ax}=2.55T$), and (c) off-axis heating ($B_{ax}=2.80T$). Proportions of particles with different orbit types in each energy band are marked with different colors in panels (b) and (c).

[1] J. Wang *et al.*, “Self-consistent Simulations of ICRF-induced Alfvén Eigenmodes in the Large Helical Device”, in the 28th Meeting of ITPA Topical Group on Energetic Particle Physics (Nov. 21–25, 2022, ITER Headquarters).

Simulation study of interaction between energetic particles and magnetohydrodynamic modes in the JT-60SA inductive scenario with a flat $q \approx 1$ profile

Interactions between energetic particles (EPs), an internal kink mode, and other MHD instabilities in the JT-60SA inductive scenario were simulated with the MEGA code [2]. In this scenario, it was predicted by TOPICS, an integrated transport code, that the internal kink mode can be unstable, and the sawtooth relaxation results in a flat safety factor (q) profile with $q \approx 1$ for $r/a \leq 0.6$. In this equilibrium, it was found in the simulation results that the MHD stability depends strongly on the bulk plasma pressure gradient. In a simulation where toroidal mode numbers with $n \leq 8$ are retained, the most unstable modes are high- n interchange modes with a poloidal number $m=n$. The mode's frequency is less than 1 kHz because the toroidal and poloidal orbit frequencies of the co-passing EPs are approximately equal to each other within the $q \approx 1$ surface. During the linear growth phase, EP transfers energy to the mode. Due to the low mode frequency and the approximately equal toroidal and poloidal orbit frequencies, all passing EPs within the $q \approx 1$ surface can resonate with the mode. The resonance layer in the energy and canonical toroidal angular momentum phase space is parallel to the flux surfaces. The overlapping of these modes creates a stochastic magnetic field, leading to stronger EP and bulk plasma pressure redistributions. During the nonlinear phase, the transition from the high $m=n$ modes to the low $m=n$ ones is observed, as shown in Fig. 2, where the dominant mode is the $m/n=1/1$ mode with an internal kink-like structure. These low $m=n$ modes are generated by the nonlinear coupling of the high $m=n$ modes. The EP kinetic effect has a minor contribution to the dynamics of these nonlinearly generated $m=n$ modes.

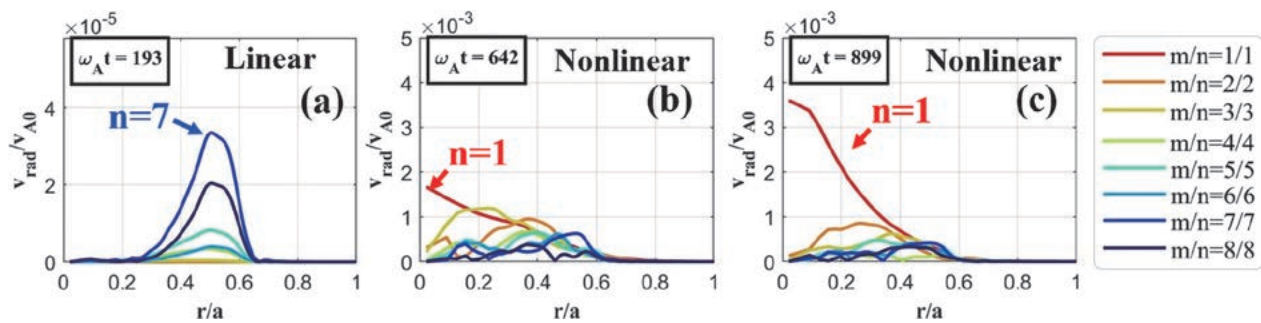


Fig. 2 Radial MHD velocity profiles for the $m=n$ modes in the JT-60SA inductive scenario at (a) the linear growth phase ($\omega_A t=193$), (b) the beginning of the nonlinear phase ($\omega_A t=642$), and (c) the final time of the simulation ($\omega_A t=899$).

[2] P. Adulsiriswad *et al.*, “Simulation Study of Interaction between Energetic Particles and Magnetohydrodynamic Modes in the JT-60SA Inductive Scenario with a Flat $q \approx 1$ Profile”, submitted to Nuclear Fusion.

(P. Adulsiriswad)

Waveform distortion of off-axis fishbone instability in the nonlinear magnetohydrodynamic evolution in tokamak plasmas

We conducted kinetic-MHD hybrid simulations to investigate the waveform distortion of off-axis fishbone modes (OFMs) driven by energetic particles in tokamak plasmas [3]. Building upon our previous work [4], we extended the simulations to include higher- n harmonics in the MHD fluid, where n represents the toroidal mode number. The simulations successfully reproduced the waveform distortion in both magnetic and temperature fluctuations which were observed in the experiments. Our analysis revealed that the waveform distortion originates from the combination of $n = 2$ harmonics and fundamental $n = 1$ OFM, while the $n = 2$ harmonics are generated by MHD nonlinearity resulting from the $n = 1$ OFM. Depending on the phase relationship between the $n = 1$ and $n = 2$ harmonics, as well as the relative amplitude of the $n = 2$ harmonic, two types of waveform distortion can occur, as shown in Figure 3. Lissajous curve analyses demonstrated that wave couplings between the $n = 1$ and $n = 2$ harmonics, with phase-lock approximately equal π and 0 , lead to “rising distortion” and “falling distortion,” respectively. These two waveform distortions can be attributed to the strong shearing profile of radial MHD velocity with $n = 2$ around the $q = 2$ magnetic flux surface. Additionally, we investigated the dependence of waveform distortion on viscosity and found that the viscosity required to reproduce the waveform distortion is higher than the classical value in the experiment.

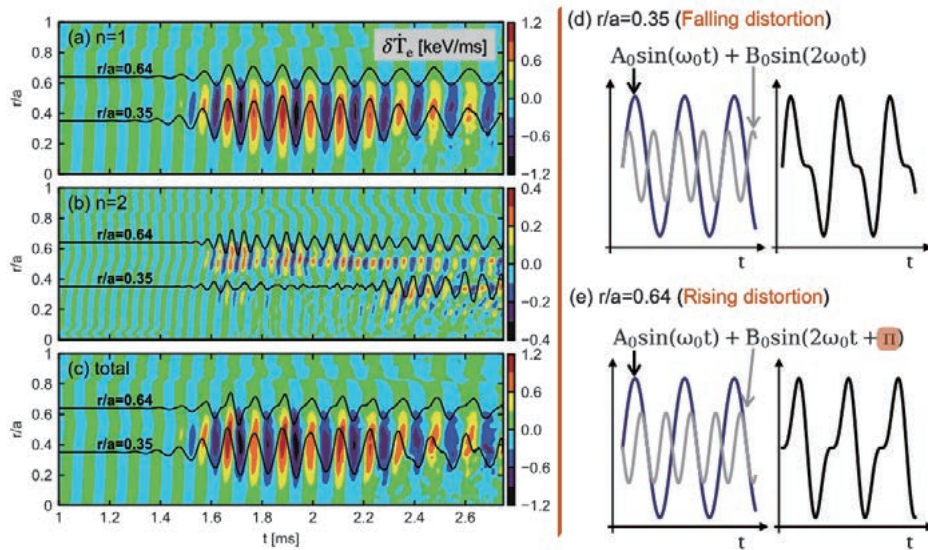


Fig. 3 Temporal evolution of the radial profile of the time-derivative of temperature perturbation at $\phi = 0$ on the outboard midplane for (a) $n = 1$, (b) $n = 2$, and (c) total with the oscillations at $r/a = 0.35$ and $r/a = 0.64$. Additionally, schematic figures (d) and (e) demonstrate how the phase difference between two sinusoidal waves generates two types of waveform distortion.

[3] H. Li *et al.*, Nuclear Fusion **63**, 086012 (2023).

[4] H. Li *et al.*, Nuclear Fusion **62**, 026013 (2022).

A Novel Simplified Model to Predict Nonlinear Turbulent Transport

Highlight

Nonlinear turbulent flows and transport in fusion plasmas are predicted by combination of mathematical model and linear computations.

One of the most important achievements toward realizing a fusion reactor is the clarification and prediction/control of “turbulence” in magnetically confined plasmas. Many efforts have been devoted to studies on the turbulent transport of thermal energy and particles, by means of large-scale numerical simulations based on kinetic and fluid models. Although supercomputing is a powerful approach, the high computational cost often discourages investigation of a wide range of physical states/conditions in the plasma. A simplified mathematical model is thus required to extract the predominant components in the turbulence dynamics. To this end, our research group has successfully constructed a novel, simplified model to predict nonlinear turbulent transport in plasmas. By applying mathematical optimization techniques to the big data obtained from large-scale “nonlinear” turbulence simulations, the newly developed mathematical model can predict the turbulent heat transport level only by a simplified “linear” calculation, which is about 1500 times faster than the conventional large-scale simulations. The mathematical model with linear-calculation quantities, e.g., the instability growth rate and the zonal-flow decay time, captures the complex functional structures of the turbulence simulation data, and resultingly the applicability and accuracy are significantly improved in comparison to those in previous studies (Fig. 1). Also, the present model can estimate the zonal-flow amplitude, which has a great impact on transport suppression. These studies not only accelerate turbulence research in fusion plasmas, but also the present method of predicting complex dynamics from simple calculations is expected to contribute to various research fields.

The results have been published as two papers [1-2], and further application to the development of a new global turbulent transport simulation is also underway.

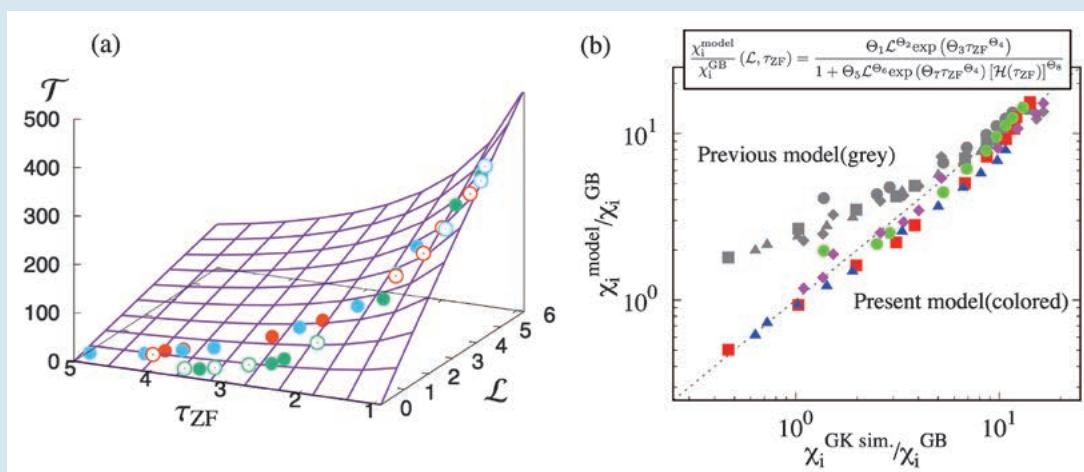


Fig. 1 (a) Nonlinear function (surface) to interpolate the turbulence simulation data (symbols). (b) Accuracy of the present simplified model.

- [1] T. Nakayama, M. Nakata, M. Honda, M. Nunami, and S. Matsuoka, *Plasma Physics and Controlled Fusion* **64**, 075007 (2022).
 [2] T. Nakayama, M. Nakata, M. Honda, E. Narita, M. Nunami, and S. Matsuoka, *Scientific Reports* **13**, 2319 (2023).

(M. Nakata)

Prediction of plasma profiles in helical plasmas by integrated code coupled with gyrokinetic transport models

Transport simulation is a challenging task, using the turbulent transport level evaluated by gyrokinetic simulation results. In this study, the transport simulation is performed by an integrated code using reduced gyrokinetic models [3]. Especially, the quasilinear flux model is used in helical plasmas. The turbulent transport is evaluated by reduced models using the linear gyrokinetic simulation results for kinetic electron response at each step of the integrated simulation. By performing the integrated simulation with the gyrokinetic models installed, multi time-scale simulation can be performed. The multi time-scale simulation is performed in the standard and inward shifted field configurations of the Large Helical Device (LHD). The multi time-scales consist of those for the gyrokinetic simulation ($\sim 1\mu s$) and for the transport simulation ($\sim 100ms$). The simulation using the quasilinear flux model based on the gyrokinetic simulation results, including effects of zonal flows and kinetic electrons, is performed for the first time to predict temperature profiles in the LHD. This is achieved by combining two codes, the integrated code, TASK3D and the local flux tube gyrokinetic code, GKV, developed for helical plasmas. The quasilinear flux model includes a cross-phase effect between fluctuating potential and temperature in addition to the linear growth rate and the zonal flow decay time. The stationary temperature profiles obtained by the transport simulation, using the reduced models, which reproduce the nonlinear simulation results, are predicted within a difference of 30%, at most, from the experimental results in the LHD, where the ion temperature gradient (ITG) mode is unstable. Some validations in the adiabatic electron condition for the other discharge in the LHD are done.

In this study are the cases for fixed heating power to obtain a stationary state where the power balance holds are focused. Validations over energy confinement time where the heating power varies in time are left for future research.

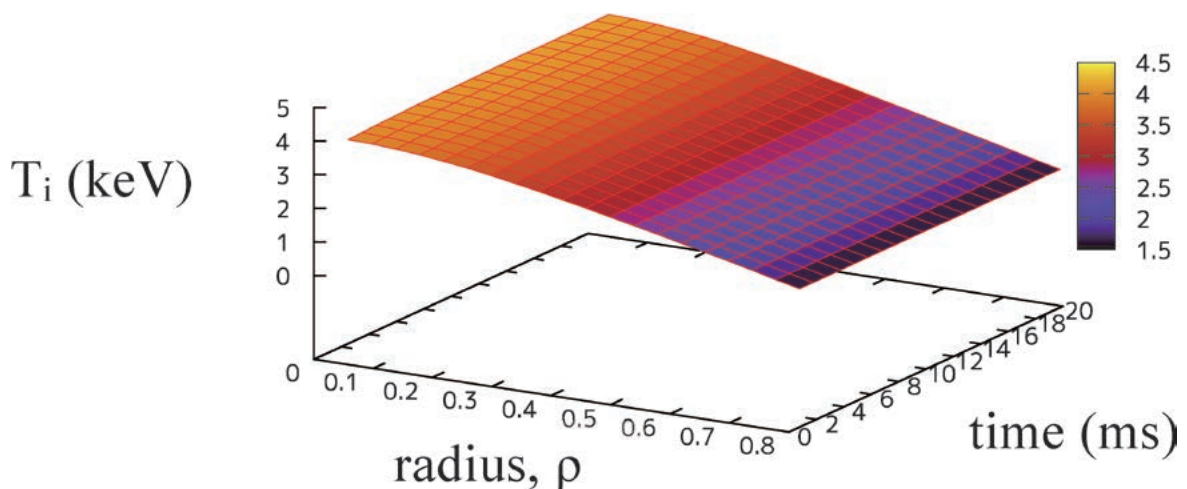


Fig. 1 Simulation results for time evolution of ion temperature profile, T_i are shown. State at $t=20ms$ is stationary.

[3] S. Toda *et al.*, Plasma Phys. Control. Fusion **64**, 085001 (2022).

Functional Extension of Integrated Transport Analysis Suite

Highlight

Developed Integrated Transport Analysis Suite, TASK3D-a, has been the Basis for Physics Analysis and Transport Modelling of LHD Plasmas

On the occasion of formulation of the Numerical Simulation Reactor Research Project, the first version of the integrated transport analysis suite for LHD plasmas, TASK3D-a01, was released in September 2012, after integrating various elemental analysis codes (modules) such as three-dimensional equilibrium, NBI heating, and heat transport processes. The construction of TASK3D-a01 has greatly advanced the automation of heat transport analysis. It is now possible to provide the results of dynamic transport analysis that take into account the temporal changes in temperature and density profiles. To apply TASK3D-a to a wider range of LHD experimental conditions, we have continuously added modules and improved the accuracy, and released it as TASK3D-a02. In TASK3D-a02, we incorporated a module to evaluate neoclassical thermal and particle diffusion fluxes. As a result, a neoclassical energy flux analysis was performed simultaneously with experimental energy balance analysis, which could provide a turbulent transport contribution in energy flux. In addition, by introducing ECH modules, energy balance analysis incorporating ECH absorption power could be performed, and then the analysis target was significantly expanded from the NBI-only heated plasmas to NBI and ECH-heated plasmas.

For large-scale simulation codes that are difficult to integrate in the framework of TASK3D-a, due to large differences in required computational resources, we have established a linkage function to provide LHD plasma equilibrium, temperature and density profiles, etc. from TASK3D-a to those simulation codes. As a result, TASK3D-a has enabled smooth implementation of LHD plasma analysis by large-scale simulations and furthermore enhanced international code benchmarking activities.

The third and fourth versions of TASK3D has enabled the capabilities of NBI heating calculations in the

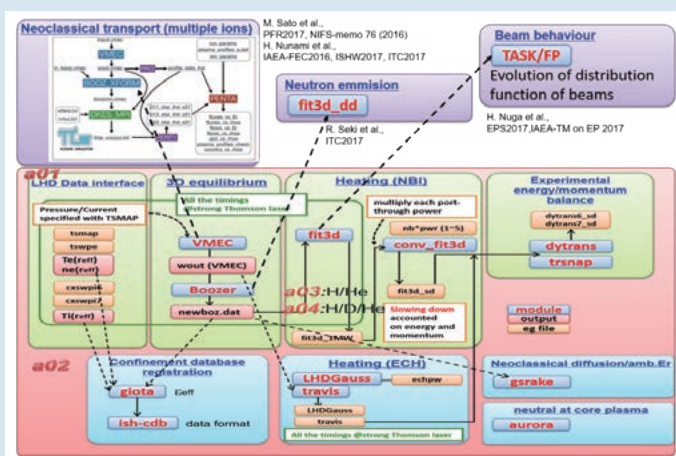


Fig. 1 Evolution of functional expansion of the integrated transport analysis suite, TASK3D-a, for LHD plasmas. From the first version (TASK3D-a01) shown in a horizontal row in the center, the function expansion (TASK3D-a02) written in the lower part, has been made to accommodate the existence of multiple ion species (hydrogen, helium, deuterium) for an NBI heating module (a03, a04). Other extensions have been made for Bayesian-calibrated density profiles, linkage with large-scale simulation codes, and energetic particles' behavior (upper part). (Reprinted from Ref. [1])

presence of multiple ion species: hydrogen, deuterium, and helium. The functions were expanded one after another, and TASK3D-a05 supported density profile measurement calibration based on Bayesian statistics. Including other upgrades, a version of TASK3D-a has now existed up to a07. This extension of functions has greatly contributed to the creation of an analysis database that serves as a basis for research on isotope effects. It also serves as a base for neutron measurement and quantitative evaluation of high-energy particle behavior in the LHD deuterium experiment. To improve the user's convenience, the TASK3D-a English manual was revised (in May 2021) and distributed to users in Japan and overseas.

[1] M. Yokoyama *et al.*, Journal of Plasma and Fusion Research **96**, 610 (2020).

(M. Yokoyama for TASK3D-a Users and Developers)

Development of ICRF Module for Further Extension of TASK3D-a

We are developing TASK/WM for evaluating wave propagation and heating of ICRF for non-axisymmetric configurations such as the LHD. In TASK/WM, the wave propagation is calculated by solving the wave equation with electric field components being spectrally expanded in toroidal and poloidal directions and being radially differentiated. Currently, to solve the wave propagation including second harmonic heating, we are applying a hot plasma model that considers the thermal motion of the plasma, and introducing a permittivity tensor in a differentional form in which a wave number can be given consistently with the wave electric field. After these implementations, results provided by TASK/WM will be verified against the experiment results in the LHD.

(R. Seki)

Integrated Transport Simulation of Fusion Plasmas based on the Data Assimilation Technique

We have developed a fusion plasma control method using data assimilation. First, we developed a new data assimilation framework, DACS [2], which integrates the optimization of the integrated simulation by assimilating the observation information and the estimation of the control input which is required to realize the target state. We extended the data assimilation system ASTI [3] to a control system based on DACS (adaptive model predictive control) and investigated its control capability by conducting numerical experiments to control virtual plasma created with the integrated code TASK3D. In addition, ASTI was accelerated so that it could be calculated in real time, and the control experiment of ECH plasma in the LHD was performed. The controllability of ASTI has been demonstrated in experiments in which the central electron temperature is controlled to approach the prescribed target temperature. This framework DACS can easily incorporate various observational information and control problems and is the basis for constructing a general-purpose and robust control system. Furthermore, while proceeding with a demonstration of the actual experiments, we will consider the development towards real-time plasma control.

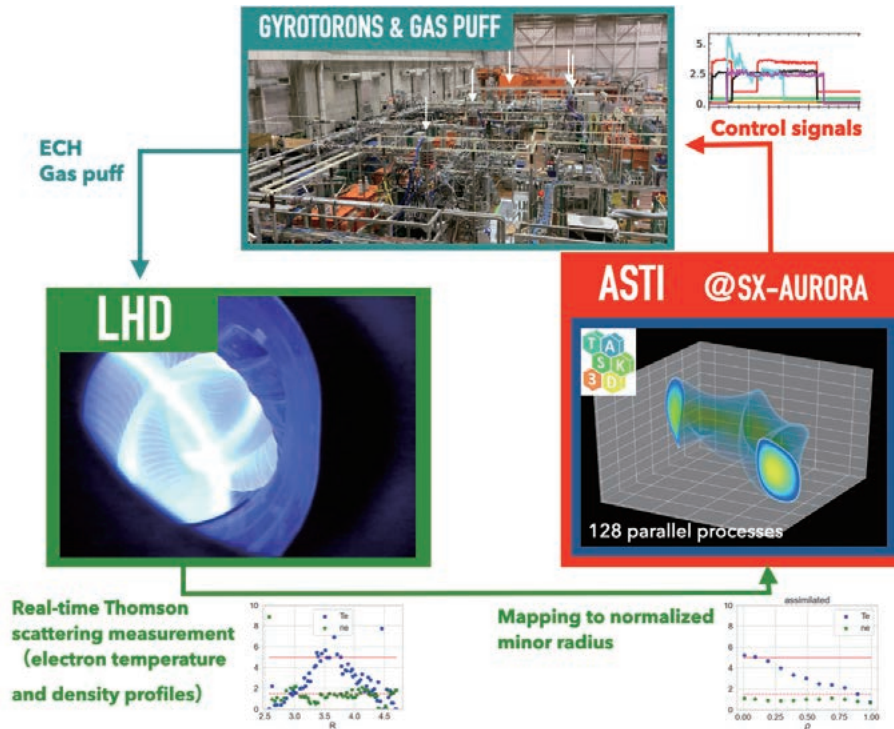


Fig. 2 Overview of the data assimilation-based control system for fusion plasmas (LHD in this case). The control signals for the gyrotrons (and the gas puff system) are estimated in the data assimilation system, ASTI, based on the prediction by the integrated code, TASK3D. In addition to the control estimation, ASTI processes Thomson scattering measurement data in real time to optimize the transport model sequentially along with the actual plasma experiment.

[2] Y. Morishita *et al.*, Computer Physics Communications **274**, 108287 (2022).

[3] Y. Morishita *et al.*, Journal of Computational Science **72**, 102079 (2023).

(Y. Morishita, Kyoto University)

Reactive Force Field Molecular Dynamics Simulations on Various Structural Transition Phenomena

Highlight

Molecular Dynamics Simulation on Hydrogen Trapping on Tungsten Vacancy

Tungsten (W) with its high melting point and thermal conductivity is one of the most promising candidates for plasma-facing materials including the divertor plate. In addition, W has lower hydrogen isotope solubility than carbon materials and is less prone to wear and tear due to hydrogen isotopes. On the other hand, defects such as atomic vacancies and voids in metals are known to act as trapping sites for hydrogen isotopes, and it has been suggested that tritium retention may be increased by neutron irradiation, which is a product of nuclear fusion.

Because hydrogen isotopes contain tritium, which is a radioactive material, this retention is limited in fusion reactor operation. Therefore, it is necessary to control this retention in the steady-state operation of fusion reactors. Elucidating the interaction between tungsten, vacancies, and hydrogen isotopes is one of the key issues, and various studies have been conducted through numerical calculations and experiments. The novel findings here, which were obtained in collaboration with Yamagata University, have been published in JASSE [1].

However, the effect of different exposure temperatures of hydrogen isotopes on the interaction between vacancies and hydrogen isotopes has not been fully elucidated. Therefore, we clarify the interaction effects between vacancies and hydrogen isotopes at different hydrogen isotope exposure temperatures using Molecular dynamics (MD) simulation. To achieve the objective of this study, we developed the tungsten-hydrogen code, developed and performed simulations of neutron-irradiated W with and without hydrogen isotopes shown in Fig. 1. Furthermore, the effects of varying the number of hydrogen isotopes and the temperature during hydrogen isotope irradiation on the displacement, fluctuation, and density distribution of W and H atoms are shown in this study.

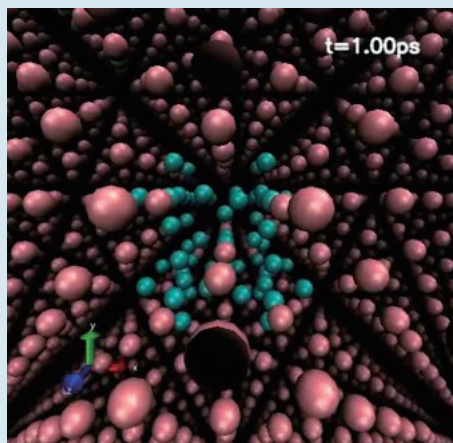


Fig. 1 Snapshot of hydrogen (green) filling a vacancy in a tungsten (brown) crystal.

[1] H. Nakamura, K. Takasan, M. Yajima and S. Saito, J. Adv. Simulat. Sci. Eng. **10**, 132 (2023).

Molecular dynamics simulation on fabrication of chiral nanoneedle by optical vortex

Toyoda *et al.* fabricated chiral nanoneedles by vortex laser ablation. They used 2 mm thick polished tantalum (Ta) as the target. According to their result, an optical vortex produced a chiral nanoneedle with a spiral conical surface at the center of the ablation zone. Inspired by this result, we attempted to elucidate the chiral nanoneedle structural formation process by the molecular dynamics (MD) simulation.

We have successfully generated tantalum chiral nanoneedles in silico using three-dimensional MD simulation to calculate the time evolution of the motion of atoms [2] shown in Fig. 2. Since current computer capabilities do not allow this nanostructure formation to be calculated at the electron level, the interaction between the optical vortex and tantalum atoms is approximated by a pseudo-electric force field, which is proportional to the electric field. The embedded atom method potential “2013_aem.alloy” is used for the interatomic forces between tantalum atoms. The dependence of a topological charge and helicity of the optical vortex beam on needle geometry, such as needle height and screw orientation, is quantitatively demonstrated. This dependence partially agrees with experimental measurements. Furthermore, we found that the presence of structure formation can be evaluated by extracting only the radial component of the force field and solving the one-dimensional equation of motion in the radial direction.

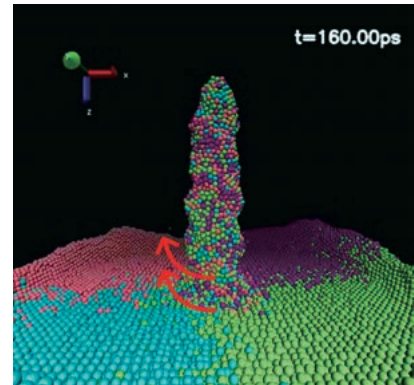


Fig. 2 Tantalum surface structures in the final state. The chiral structure is recognized, which is the same helicity of the force fields.

Isotope effect of the rovibrational distribution of hydrogen molecules desorbed from amorphous carbon

Plasma confinement experiments were carried out using deuterium in the LHD, and the isotope effects were reported. Motivated by these isotope experiments at the LHD, we aim to extend neutral transport and molecular dynamics codes, which had been developed for light hydrogen, to handle not only deuterium but also tritium.

When the hydrogen isotope atom is injected into amorphous carbon with the incident energies E of 20, 50, and 80 eV, we obtain the following physical quantities of hydrogen isotope atoms/molecules emitted from the amorphous carbon using molecular dynamics and heat conduction hybrid simulation [3]. The physical quantities are the time evolution of the emission rate, the depth distribution of the original location of the hydrogen emitted from the target, the polar angular dependence, and the translational, rotational, and vibrational energy distributions. In addition, the approximate analysis yields the emission distributions at vibrational (ν) and rotational (J) levels (Fig. 3). Using these distributions, we evaluate the rotational temperature T_{rot} for $\nu = 0$ and small J states. From the above, it is found that molecules with higher rotational levels J tend to be emitted as E increases or as the mass of hydrogen isotope increases. Moreover, the isotope effect appears in the mass dependence of T_{rot} .

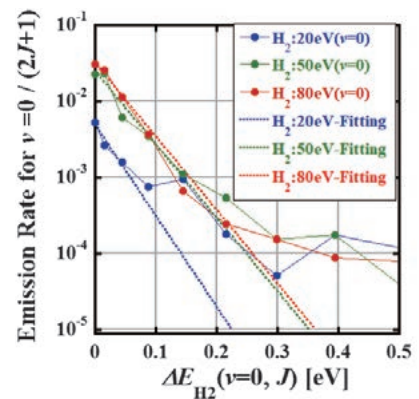


Fig. 3 The emission rate of hydrogen molecules from the graphite surface. The Boltzmann distribution is used as a fitting function. Fitting with the Boltzmann distributions is well done for low energy. However, for high energy, fitting is not well done with the Boltzmann distribution.

[2] H. Nakamura and S. Habu, *Jpn. J. Appl. Phys.* **62**, SA1013 (2022).

[3] H. Nakamura, S. Saito, T. Sawada, K. Sawada, G. Kawamura, M. Kobayashi and H. Hasuo, *Jpn. J. Appl. Phys.* **61**, SA1005 (2022).

4. Network-Type Collaboration Research

This research is eligible for study conducted by collaborating with facilities owned by NIFS and multiple universities. In this fiscal year, the research shown below was done. The titles and brief summaries of the research topics are listed below.

(1) Study of suppression and avoidance of vertical position shift phenomena in tokamaks using three-dimensional magnetic fields T. Fujita (Nagoya University)

In this study, we investigate methods to suppress and avoid vertical displacement (VDE), which is a problem in tokamaks, using a three-dimensional magnetic field from both experimental and theoretical perspectives. In tokamaks, high beta and confinement performance can be obtained by increasing plasma cross-sectional noncircularity (longitudinal elongation), but the vertical position tends to be unstable in highly noncircular plasmas, and stabilization of the vertical position (suppression of VDE) is an issue. It is theoretically predicted that the application of a helical magnetic field (three-dimensional magnetic field) can stabilize the vertical position, and this has been confirmed in several experiments. It would be more practical if this could be realized using local coils with simple layout and geometry. Therefore, plasma position stabilization experiments using 3D magnetic fields generated by local coils have been conducted in the TOKASTAR-2 system at Nagoya University and the PHiX system at Tokyo Institute of Technology. In previous studies, the strength condition of the 3-D magnetic field required for position stabilization was described by a rotational transformation of the 3-D magnetic field, but the transformation is not suitable for local coils because they do not necessarily form closed magnetic surfaces. A new index is needed to replace the rotational transformation. Therefore, the goal of this study is to create an identical index that can describe the stabilization conditions in the two devices with different local coils.

In addition, the interaction between a resonant perturbation magnetic field (RMP) and plasma, which is one of the three-dimensional magnetic field applications to confined plasmas, will be tested in the HYBTOK-II device at Nagoya University and in the LHD at the National Institute for Fusion Science, to establish a theoretical model of RMP propagation and a method to control peripheral MHD instabilities by RMP.

One of the objectives of this research is to support and stimulate experimental research on MHD equilibrium and stability in university laboratories through education for students by conducting this work mainly on small experimental devices at universities.

(2) New Developments in CT-derived Technologies for Space and Planetary Magnetospheric Plasma Science N. Fukumoto (University of Hyogo)

Spheromak (Spk) and field reversal coordination (FRC), which are called compact torus (CT) plasmas, have been applied to plasma collision/coalescence, injection, and irradiation in the field of fusion research, taking advantage of their features such as high density, high beta, and portability. This study aims to expand the CT-derived technology obtained in fusion research to interdisciplinary research. For example, Spk is used for planetary magnetospheres and space propulsion, and FRC is used for collisionless shock waves generated in space. Furthermore, through a comprehensive discussion of the results obtained in this research, we aim to share and promote new knowledge and research on high-beta plasma physics, etc., and to strengthen development capabilities by sharing information on equipment technology, such as continuous injection of magnetized coaxial plasma guns (MCPG) and improvement of injection performance. Interdisciplinary research topics with strong relevance

have been proposed in the units of the National Institute for Fusion Science, and they are expected to contribute to the progress of such research.

(3) Study on tritium, radon, and radium concentrations and dynamics of tritium, radon, and radium in environmental water in Japan T. Sanada (Hokkaido University of Science)

In order to clarify the dynamics of tritium in the environment of Japan, which has a long geographical feature from north to south, it is necessary to understand the tritium concentration in various regions through a wide-area field survey.

In this study, the National Institute for Fusion Science, which has a tritium precision measurement system, is the core of a network established by several research institutes to continuously observe tritium concentrations in environmental water over a wide area. In addition, we will also observe radon-222 Rn and radium-226 Ra, which are naturally occurring radionuclides, and investigate their usefulness as tracers of the causes of concentration fluctuations. Furthermore, these activities will be positioned as training for graduate students in the measurement and analysis of tritium and radon in water to foster young researchers in this field.

(4) Comprehensive study of hydrogen isotope behavior in plasma-facing walls for fusion reactors through inter-university collaboration Y. Oya (Shizuoka University)

In order to predict tritium behavior in future fusion reactors such as DEMO, it is efficient to conduct a systematic evaluation of hydrogen isotope behavior by effectively utilizing large plasma devices in the operation, small plasma devices in laboratories, and analytical instruments owned by each university.

In this study, W and W-10%Re alloys and their irradiation-damaged samples are prepared as common examples. These samples are used in experiments at each university and evaluated to obtain systematic knowledge. Physical constants related to hydrogen isotope behavior, which are necessary for DEMO reactor design, will be clarified. This study can contribute to understanding the hydrogen isotope behavior in JT-60SA and ITER.

5. Basic, Applied, and Innovative Research

FY2022 was a transition period in NIFS. Three projects were still conducted, although the NIFS collaboration categories were changed. The “Basic, Applied, and Innovative Research” category in FY2021 was included in “Interdisciplinary Fusion Science Research” in FY2022. In this section, we report highlights of collaborative research related to the basic, applied, and innovative research topics conducted in FY2022.

For basic plasma science, NIFS operates several experimental devices and offers opportunities to utilize them in a collaboration program for university researchers. A middle-size plasma experimental device the HYPER-I is available for basic plasma research. The compact electron beam ion trap (CoBIT) for spectroscopic study of highly charged ions, atmospheric-pressure plasma jet devices for basic study on plasma applications, and other equipment are all used for collaborations.

(I. Murakami)

Investigation of fine structure formation process of spectral line radiation during guide field reconnection in collaboration with NIFS spectroscopy database

Interpretation of the fine structure formation process of line-spectral emission is one of the major interests in plasma physics research. Both in astrophysical and laboratory plasmas such as in solar flares and merging spherical tokamak formation experiments, the line radiation profile typically forms a characteristic structure around the X-point where magnetic field lines reconnect. During the reconnection process, particles flow into the X-point region and are then ejected toward the downstream region. At the region of energy conversion, a plasmoid-like multiple blob structure is typically formed and such a structure tends to be referred to as evidence of plasmoid formation/ejection which contributes to acceleration of the reconnection speed (an open question of astrophysical plasma). Figure 1 is an example in laboratory plasma (TS-6: U-Tokyo reconnection experiment) under the influence of a high guide field. Around the X-point of magnetic reconnection, Ar II (480.6nm) spectral radiation forms two peaks around $t = 475\mu\text{s}$ and the peak positions move from around $r \sim 0.2\text{m}$ to the outflow direction and a flare-looptop like structure is formed at $r \sim 0.1\text{m}$ downstream in the microsecond time scale. The detected structure apparently shows that there is a particle acceleration process from the X-point region ($r \sim 0.2\text{m}$) to the radial direction; however, spectral line radiation is not simply proportional to electron density. For the proper interpretation of complex line radiation, NIFS is an important leading institution with a sufficient spectroscopy database and we are running a practical collaboration to extract more information, such as electron density and temperature, by monitoring the evolution of multiple spectral line radiation [1].

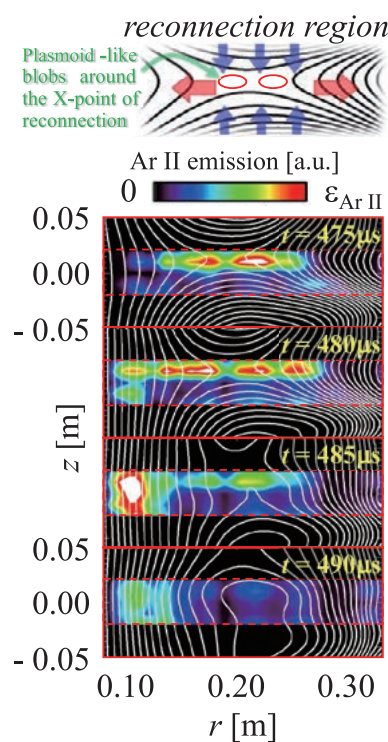


Fig. 1 Time evolution of 2D emission profiles of Ar II line spectrum (480.6nm) around the X-point of magnetic reconnection. At the region of where multiple plasmoids are expected to be formed, a blob-like structure is formed and the characteristic peaks are ejected to the outflow direction.

(H. Tanabe, Univ. of Tokyo)

Generalization for local oscillator integrated antenna array

Microwave diagnostics are key instruments for measuring electron density, electron temperature profiles, and their fluctuations in fusion plasma research. Our group has proposed an antenna array with an integrated local oscil-

lator. This antenna array uses frequency multiplication and superheterodyne techniques to reduce the number of expensive waveguide transmission lines and elements, making it inexpensive and easy to install. We have

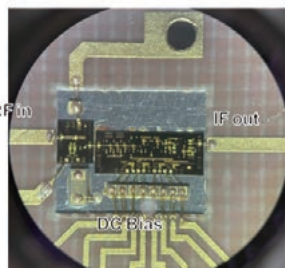


Fig. 2 MMIC board

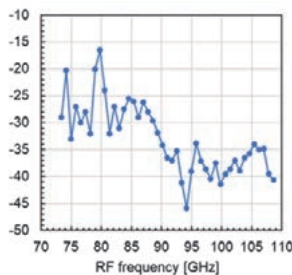


Fig. 3 Conversion loss

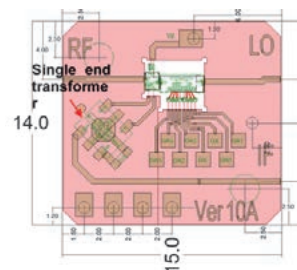


Fig. 4 Improved MMIC board

developed antennas in the 24–80 GHz range [2]. However, when considering microwave measurements in higher-density plasma devices, antennas that can be used at higher frequencies are needed. Therefore, in FY2022, we developed antennas in the W-band (80–110 GHz), which is an even higher frequency band. Figure 2 shows the implementation area of the Monolithic Microwave IC (MMIC) of the W-band receiver, in which a W-band mixer and a W-band frequency multiplier are mounted. Figure 3 shows the conversion gain of the receiver measured using the W-band transmitter developed at the same time. Although the efficiency is not high, the sensitivity is sufficient to confirm that phase measurement is possible. Figure 4 shows an improved version with a transformer implemented at the mixer output, which will be evaluated in FY2023.

(D. Kuwahara, Chubu Univ.)

Development of Random Laser for Fusion Environment Measurement

Solid-state lasers generally have excellent temporal and spatial coherence, but when they are used for full-field imaging, they cause spatial intensity irregularities (speckles), which reduce imaging accuracy. On the other hand, a random laser using multiple scattering in irregular structures has low spatial coherence and high intensity, making it a suitable light source for full-field imaging. In this study, we aim to realize a mid-infrared wavelength random laser for full-field imaging of trace molecules such as hydrogen isotopes in water.

In the FY2022 research, prior to the development of mid-infrared random lasers, we aimed to develop ultraviolet random lasers using plasma surface modification of gallium nitride. Using a plasma irradiation system (Co-NAGDIS) for divertor simulation at Nagoya University, random, sub-micrometer-sized surface irregularity structures were successfully formed on a gallium nitride substrate. Emission measurements of the surface-modified samples were performed with 355 nm excitation using a microspectroscopic system at Hokkai Gakuen University. The measured spectra are shown in Figure 5. Band-edge emission of gallium nitride was observed from 360 to 380 nm, and as the excitation power was increased, a spike-shaped emission peak appeared around 365 nm. The intensity of this emission peak had a threshold, indicating that an ultraviolet random laser was emitted. The author has succeeded in obtaining a strong correlation with the oscillation properties by newly defining size parameters such as projected area and representative length. This achievement was published in an original paper in the first issue of ACS Applied Optical Materials, and a joint press release was issued by NIFS, Hokkai Gakuen University, and Nagoya University [3].

(H. Fujiwara, Hokkai Gakuen Univ.)

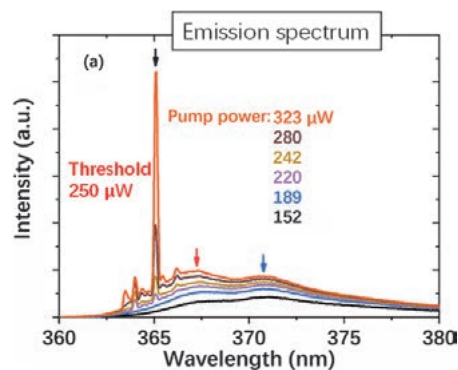


Fig. 5 Emission spectrum of gallium nitride after plasma surface modification.

- [1] H. Tanabe *et al.*, “Ion heating/transport characteristics of merging startup plasma scenario in the TS-6 spherical tokamak”, 29th IAEA fusion energy conference (FEC2023), EX/P7-26 (2023).
- [2] Y. Kondo *et al.*, *J. Instrum.* **17**, C05023 (2022).
- [3] Q. Shi *et al.*, *ACS Applied Optical Materials* **1**, 412–420 (2023).

6. Fusion Science Archives (FSA)

The Fusion Science Archives was established in 2005 to learn lessons from preserved past fusion science archives and to maintain collections of historical documents and materials that are related to fusion research in Japan. These activities are important from the viewpoint of the historical evaluation of fusion research, its social accountability, and making references for seeking future directions. Since then, historical materials on fusion research and/or organizations related to fusion research have been collected and preserved at the FSA. They are stored in acid-free folders and boxes. Catalogs of registered items are available to the public through the Internet in a hierarchical structure.

The following are summary of the collaborative works performed this fiscal year.

- **Construction of Digital Library of Husimi Kodi Archives**

H. Iguchi (NIFS, FSA) *et al.*

Research on the practical use of nuclear fission energy started in the 1950s. The first commercial nuclear power plant was put into operation in the early 1970s in Japan. On the other hand, nuclear fusion energy is still in the phase of research and development. Prospecting research and development in the future, it is useful or necessary to study the historical processes in fission energy development. Many historical documents related to the development of nuclear fission energy in Japan are archived as Kodi Husimi collections in NIFS Fusion Science Archives. The purpose of this research is to find related primary documents. Examples of the preliminary result are as follows with ID numbers of Fusion Science Archives. ○ “Energy Problem in Japan” published by Resources Council (Shigen-Chosakai; the governmental agency for research on energy problems in 1951 (FSA_ID:503-01). ○ Documents on Kaya-Husimi Proposal at Science Council in 1952 (FSA_ID:503-02-03, -05, 503-04-34). ○ Discussion at the 39th Committee on nuclear policy in early stage in Japan.

- **Studies on the history of the establishment of the Institute of Plasma Physics, Nagoya University**

T. Amemiya (CST Nihon Univ.) *et al.*

The Institute of Plasma Physics (IPP), Nagoya University is one of the previous bodies of the existing NIFS. In 1961, the IPP was established as the inter-university research institute of plasma physics and controlled fusion research in Japan. The purpose of this collaborative research is to find new historical interpretations of the IPP and the discussion about the Institute at the dawn of fusion research in Japan, based on the historical documents in NIFS FSA, CST Nihon University and other archives. This collaborative research of FY2022 consists of the following subjects: 1) “Analysis of the discussion about a proposal for the Institute of High Temperature in Osaka University at the dawn of fusion research in Japan”, 2) “On the drafting and background of the plan for the IPP” and 3) “History of the establishment of the Nuclear Fusion Research Group from the perspective of research funds.”

- **Improving name authority data about persons, groups, and organizations related to fusion science in Japan, for fusion science archives**

H. Gotoh (The Kyoto University Museum) *et al.*

This study aims to establish a methodology for improving archival name authority data related to fusion science in Japan, which is necessary for identifying names and of proper understanding of various materials. Information on researchers and visiting researchers at the Institute of Plasma Physics, Nagoya University (IPPJ), and groups or organizations that the researchers belonged to, was collected and analyzed (287 researchers and 80 visiting researchers; six groups and 55 organizations). The Fusion Science Archives staff also has attempted to extract the names of individuals and organizations that appear in the archival materials as part of the daily management of the archives. Further analysis of the extracted names and merging with the above information is still required.

- **Collaborative Activities at NIFS Fusion Science Archives (NIFS FSA)**

S. Kubo (Chubu Univ.) *et al.*

One of the topics of this fiscal year is that the catalog of a part of Kazuhisa MORI's collection accepted last year had been opened at the website of Yukawa Hall Archival Library, is being formally transferred and is agreed to be managed on the website of the NIFS-FSA web page. (<https://www.nifs.ac.jp/archives/mori/index.html>). A catalog of the non-cataloged part of this collection is underway.

The cataloged database of more than 26,000 items are accumulated in the form of FileMaker of Claris Co., under hierarchy layers (Collection layer, Box layer, File layer, Item layer) for internal use. Among them, just under 6,000 items are available from outside NIFS in the form of InfoLib of Infocom Co., because the transformation of the database had been performed manually. A transformation program written in Python has been developed.

- **Investigation on the progress of plasma spectroscopy in Japan from the chronicle of collaboration meeting on plasma spectroscopy**

N. Yamaguchi (Comprehensive Research Organization for Science and Society (CROSS)) *et al.*

A collaborative meeting on plasma spectroscopy has been hosted by the Institute of Plasma Physics, Nagoya University (IPPJ), and NIFS for over half of a century since 1969. Programs, abstracts, and meeting reports of the workshop have been compiled. Keywords have been extracted from about 1300 papers that were presented at meetings held from 1969 to 2017. Three keywords which are “Laser-induced fluorescence (LIF) measurement”, “Polarization spectroscopy” and “Collisional radiative (CR) model” have been analyzed. Their appearance frequency has been counted for the three keywords in each meeting. Statistics of the keyword appearance frequency show the trend of plasma spectroscopic research in Japan from 1969 to 2017.

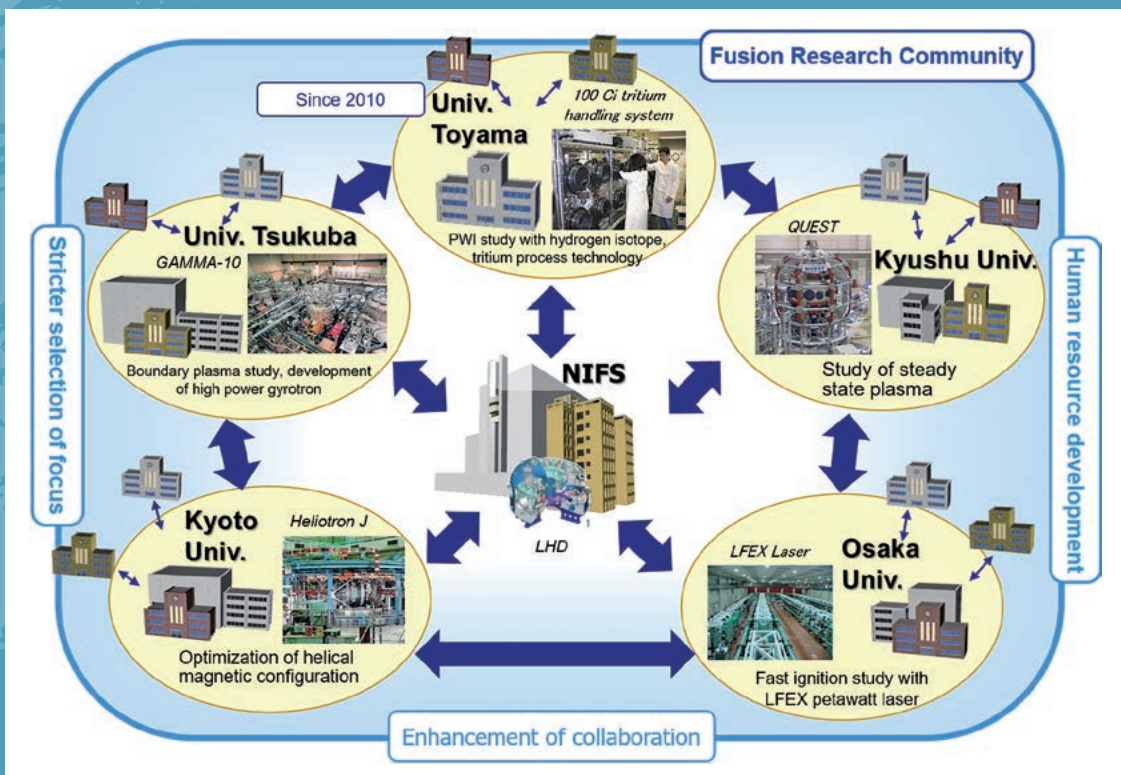
7. Bilateral Collaboration Research

The purpose of the Bilateral Collaboration Research Program (BCRP) is to reinforce the activities of nuclear fusion research in universities by using their middle-size experimental facilities of specific university research centers as joint-use facilities for all university researchers in Japan. The current program involves five university research centers as follows:

- Plasma Research Center, University of Tsukuba
- Laboratory of Complex Energy Process, Institute of Advanced Energy, Kyoto University
- Institute of Laser Engineering, Osaka University
- Advanced Fusion Research Center, Research Institute for Applied Mechanics, Kyushu University
- Hydrogen Isotope Research Center, University of Toyama

In the BCRP, each research center can have its own collaboration programs, using its main facility. Researchers at other universities can visit the research center and carry out their own collaboration research there, as if the facility belongs to NIFS. These collaboration research efforts are supported financially by NIFS as research subjects in the BCRP. They are proposed from all over Japan every year. The collaboration research committee, which is organized under the administrative board of NIFS, examines and selects the subjects.

(Y. Todo)



University of Tsukuba

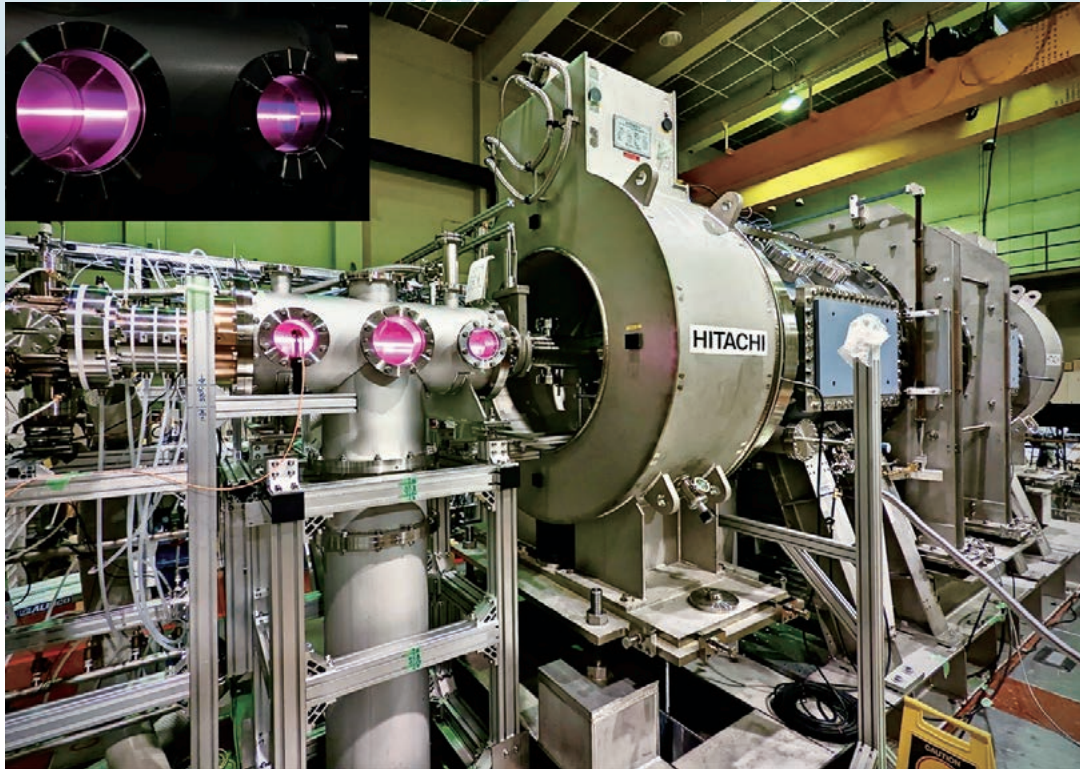


Fig. 1 Bird's eye view of GAMMA 10/PDX.

Highlight

Study of boundary plasmas by making use of open magnetic field configuration and development in high power gyrotrons towards the DEMO project

In the Plasma Research Center, University of Tsukuba, studies of boundary plasma and development of high-power gyrotrons have been performed under a bilateral collaboration research program. In GAMMA 10/PDX, processes of molecular activated recombination (MAR) have been studied by using a fast framing camera system with an arbaa prism to simultaneously measure spatio-temporal structures of four line-emissions in front of a V-shaped target, which is exposed to end-loss plasma. Advanced diagnostic systems such as a multichannel (multi-frequency) Doppler reflectometer and dual-path Thomson scattering have been developed.

A new linear plasma device Pilot GAMMA PDX-SC (Fig. 1) has been constructed. A pair of NbTi superconducting coils and a pair of Cu coils were installed to produce a simple mirror configuration. The first plasma was successfully achieved in October 2022. The source plasma was produced by a hot cathode arc plasma discharge with LaB_6 and it was injected into a main chamber (a central cell). After the first plasma operation, ICRF and ECH antennas were installed in the main chamber.

A divertor simulation study has been carried out by using end-loss plasma of GAMMA 10/PDX. A divertor simulation experimental module (D-module) was installed in the end region of GAMMA 10/PDX to be exposed to the end-loss plasma. Recently, we have developed a fast framing camera system with an arbaa prism to simultaneously measure spatio-temporal structures of four line-emissions in front of a V-shaped target in the D-module. In this time, the emissions of H_{α} (656 nm), H_{β} (486 nm), N_2 1st positive (760 nm) and NI (940 nm) lines were simultaneously measured to investigate processes of molecular activated recombination (MAR) due to additional supply of H_2 and N_2 gases. The intensity ratio of $I_{H_{\alpha}}$ and $I_{H_{\beta}}$ is a good indicator of the occurrence of hydrogen MAR (H-MAR), since $I_{H_{\alpha}}$ is enhanced by the chain processes of H-MAR but $I_{H_{\beta}}$ is not enhanced. When the H_2 gas was supplied in front of the V-shaped target, the intensity ratio of $I_{H_{\alpha}}$ and $I_{H_{\beta}}$ ($I_{H_{\alpha}} / I_{H_{\beta}}$) started to increase on the axis between the upper and lower targets and then the area with the high intensity ratio expanded to radial and upstream directions. This means the spatio-temporal progress of the H-MAR area. In the case of N_2 gas supply, on the other hand, the intensity ratio of $I_{H_{\alpha}}$ and $I_{H_{\beta}}$ did not increase, unlike the case of H_2 gas supply, indicating that H-MAR was suppressed. However, a microwave interference measurement indicated that the electron density at the central region between the targets was significantly decreased. This meant that H-MAR was suppressed but nitrogen MAR (N-MAR) was enhanced by the N_2 gas supply.

ECH experiments have been conducted to generate and control high heat flux to develop an edge localized mode (ELM)-like intermittent heat load pattern for divertor simulation studies. For higher heat flux study, a new mirror antenna was developed to generate higher heat flux and concentrate the heating power on the axis. More than 0.5 MW was injected into GAMMA 10/PDX plasma contributing to producing the endplate potential of above 5 kV and a heat flux of over 30 MW/m².

As for advanced diagnostic development, a multichannel (multi-frequency) Doppler reflectometer system has been developed to simultaneously measure turbulent fluctuation flows at different radial locations in the central cell of GAMMA 10/PDX. A flow profile was obtained during ICRF anchor heating, showing a radially sheared structure formation in the edge region. Both fluctuation flow and $E \times B$ flow profiles showed peaks at edge region which indicates the influence of E_r on flow structure formation. A dual-path Thomson scattering (DPTS) system has been developed to simultaneously measure the electron temperatures and densities in both the core and edge region of GAMMA 10/PDX. The laser path of the DPTS is divided in two to inject the central cell and end cell plasma. In the central cell TS, a multi-pass TS system has been constructed for improving the signal intensity and time resolution. Moreover, the dual-pass system has been developed in the end cell TS system.

Validation of a plasma fluid model based on an anisotropic ion pressure (AIP model) proceeded from both theoretical and experimental points of view. In GAMMA 10/PDX simulations with the AIP model, the effects of the heat-flux limiting coefficients and particle/heat sources on plasma profiles have been studied. An analytical ion transport model has been updated to compute the electrostatic potential self-consistently. The contribution of magnetic-moment conservation to the parallel ion energy increment in the end region was experimentally estimated by using two kinds of ion energy analyzers.

In order to further promote the divertor simulation study, a new linear plasma device, Pilot GAMMA PDX-SC, (Fig. 1) has been constructed. A pair of NbTi superconducting coils with a bore of 0.9m and a pair of Cu coils with a bore of ~1.5 m are utilized to produce a simple mirror configuration. The maximum magnetic field is 1.5 T and the mirror ratio is 20~30. The first plasma was successfully achieved in October 2022. The source plasma was produced by a hot cathode arc plasma discharge with LaB₆ and it was injected into a main chamber (a central cell). Operating parameters of the cascade arc plasma source were the following: discharge current 20 A, discharge voltage 180 V and gas pressure < 1Pa. After the first plasma operation, ICRF and ECH antennas were installed in the main chamber. Moreover, three concentric ring plates were installed at the end of the main chamber to apply the bias voltage to the peripheral plasma for suppression of MHD instability.

(M. Sakamoto)

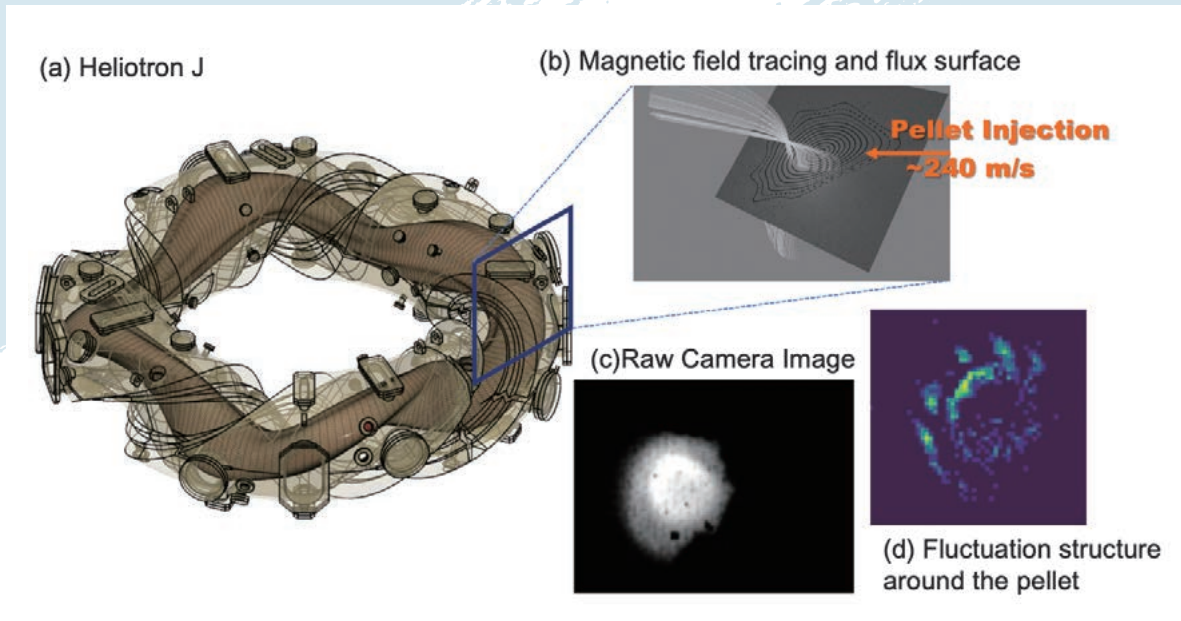


Fig 1. Heliotron J (a) and local magnetic field structure at pellet injection trajectory (b). Fluctuation structure appeared by signal processing of movie image (c) recorded using fast camera (d).

Highlight

Three-dimensional dynamics of fluctuations rotating around pellet appearing during pellet ablation process

The Heliotron J device features a wide flexibility of configuration control. Such flexibility also implies complexity in determining the propagation direction of a transient event in particle fuelling, such as gas puffing or pellet injection, concerning the magnetic field configuration.

This fiscal year, we have reported the formation of fluctuation structures in a pellet plasmoid during the pellet ablation process that had been observed using a fast camera. The fluctuation has a normalized fluctuation level of $\sim 15\%$ and propagates around the moving pellet across the magnetic field. Therefore, we applied an algorithm by comparing the fluctuation structures with the shape of magnetic field lines calculated with a field line tracing code, as shown in Fig. 1. We have successfully reconstructed the spatiotemporal structure of the fluctuations during the pellet ablation process. The fluctuations are at locations displaced toroidally from the pellet and propagate in the cross-field direction around the pellet axis along the field line, indicating a three-dimensional behavior and structure of fluctuations. They would be driven by a strong inhomogeneity formed around the pellet and invoke a relaxation of the gradient through a cross-field transport induced by the fluctuations, which could affect the pellet ablation and pellet fuelling processes. Such fluctuations can be ubiquitously present at the inhomogeneity formed around a pellet in the pellet ablation process in fusion devices, depending on the magnetic configuration. (S. Ohshima *et al.*, Sci Rep **12**, 14204 (2022))

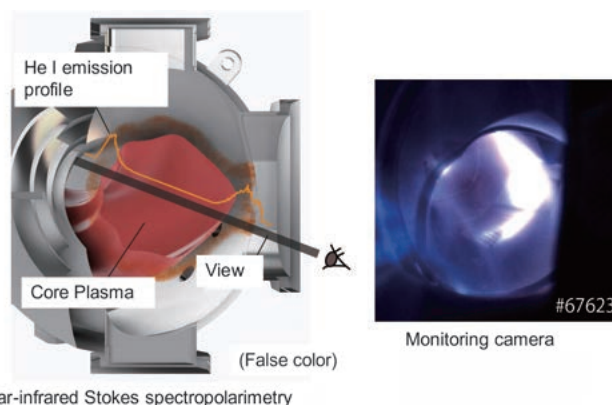
Research Topics from Bilateral Collaboration Program in Heliotron J

The main objectives of research in the Heliotron J device under this Bilateral Collaboration Program are to experimentally and theoretically investigate the transport and stability of fusion plasmas in an advanced helical field and to improve plasma performance through advanced helical-field control. Picked up in FY2022 are the following seven key topics; (1) plasma transport control by magnetic field coordination and related plasma structure formation control in advanced helical plasmas, (2) the ECH/EBW heating mechanism and its performance improvement, (3) high-density NBI plasma generation and high-beta plasma confinement, (4) boundary plasma control in advanced helical plasmas, (5) instability control by magnetic field coordination in advanced helical plasmas, (6) experimental study on plasma current control in advanced helical plasmas, and (7) study on new operating scenarios and a data analysis method.

Twenty-three projects, including our baseline one, were adopted. High magnetic field experiments were conducted for about four months, from late October to the beginning of February.

Spatially resolved measurement of helium atom emission line spectrum in scrape-off layer by near-infrared Stokes spectropolarimetry

Stokes spectropolarimetry is used to spatially invert the viewing-chord-integrated spectrum, based on the correspondence between the given magnetic field profile along the viewing chord and the Zeeman effect appearing on the spectrum. We increase the relative magnitude of the Zeeman effect by observing a near-infrared emission line based on the greater wavelength dependence of the Zeeman effect than of the Doppler effect. Utilizing the increased Zeeman effect, we can invert the measured spectrum with a high spatial resolution by a Monte Carlo particle transport simulation, reproducing the measured spectra with the semiempirical adjustment of the recycling condition at the first walls. The inversion result reveals that when momentum exchange collisions of atoms are negligible, the velocity distribution of core-fueling atoms is mainly determined by the initial distribution at the time of recycling. The inversion result is compared with that obtained using a two-point emission model used in previous studies. The latter approximately reflects the parameters of atoms near the emissivity peak. (T. Chatani *et al.*, Sci Rep **12**, 15567 (2022))



Schematic configuration of near-infrared Stokes spectropolarimetry

Many research topics have continuously made progress with collaborative researchers under the Bilateral Collaboration Program in the Heliotron J project. Progressing are (i) electromagnetic wave measurements such as multi-line-of-sight interferometry and multi-channel reflectometry, (ii) spectroscopic diagnostics such as high sensitivity beam emission spectroscopy for local turbulent fluctuation measurements and fast Stark spectroscopy for pellet ablation clouds, (iii) particle and heat measurements of peripheral plasma flow and heat flux, and (iv) active diagnostics such as multi-pass Thomson scattering measurements, event-triggered Thomson scattering, and laser blow-off spectroscopy.

(K. Nagasaki)

Study on Fusion Fast Ignition System with Ultra-High Dense Plasma

We have performed fundamental research on laser fusion with a fast ignition (FI) scheme, which enables us to separate the laser fusion process into three phases, i.e., compression, heating, and burning, using the GEKKO XII and LFEX laser systems at the Institute of Laser Engineering, Osaka University. The research included (a) a high-density implosion experiment, (b) a fast heating experiment using a mixed laser light of fundamental and second harmonics, and (c) the effects of a kilo-tesla magnetic field on ignition burning in the FI. In FY2022, the following is a summary of our achievements through the Bilateral Collaboration Research Program with NIFS and other collaborators from universities and institutes (NIFS12KUGK057 as the base project).

High-density implosion experiment

Laser fusion requires the generation of high-density plasma more than 1000 times the solid density. In the past, high-density plasma was generated by shell implosion, but in this study, a solid sphere is compressed by multi-stage shock waves because a hot spot in the center is not necessary in fast-ignition laser fusion. The solid sphere is resistant to hydrodynamic instability, but the inhomogeneity of the laser absorption intensity must be as high as that of shell implosion. A ray tracing code is used to calculate the bremsstrahlung absorption while varying the laser irradiation conditions. As shown in Figure 1, the implosion performance is getting better after improving the homogeneity of laser lights by introducing a random plate.

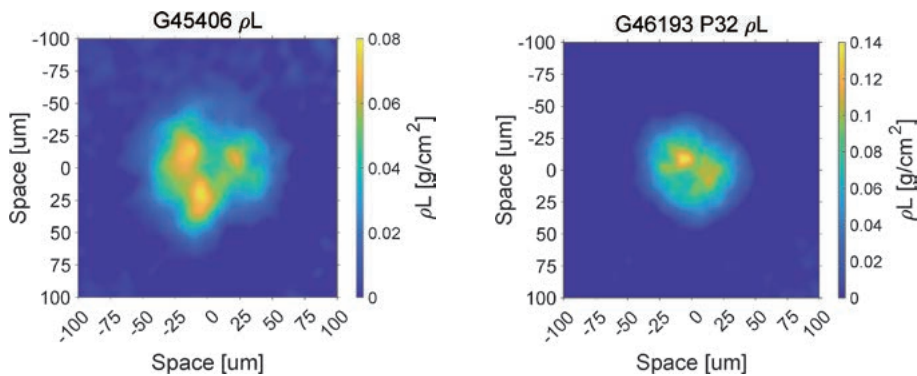


Fig. 1 Observed areal density (left) before improving the uniformity and (right) after improving the uniformity of laser light.

Fast heating experiment using a mixed laser light of fundamental and second harmonics

We have developed a system that can mix 50% second harmonics and 50% residual fundamentals by wavelength conversion of the LFEX laser just before the target. The four beams were successfully converted. In the four-beam experiment, the laser beam became poorly focused after transmission through the wavelength conversion crystal. Since it was not feasible, on a budget, to grind the wavelength conversion crystals for four beams with high precision, we prepared a wavelength conversion crystal with high precision grind for only one beam. The wavefront distortion was corrected using a full-size deformable mirror in the H2 beam of the LFEX, and the light focusing state was close to that of a normal LFEX. Even with wavelength conversion, energy was successfully injected within a diameter of 50 μm .

The most important aspect of heating in fast ignition is the electron energy spectrum, which affects the heating efficiency by increasing the number of electrons below 1 MeV. Figure 2 compares the electron energy spectra of a 5 μm Cu target shot with a wavelength-converted mixed beam and a shot without wavelength conversion. Comparison shots were performed with nearly identical laser energies on the target. The average energy of the electrons in both shots was significantly reduced. The expected result is that the red and green lines intersect at around 0.5 MeV, and the mixed wave produces more electrons in the low energy region. We will further analyze the data in detail to determine the effect on heating.

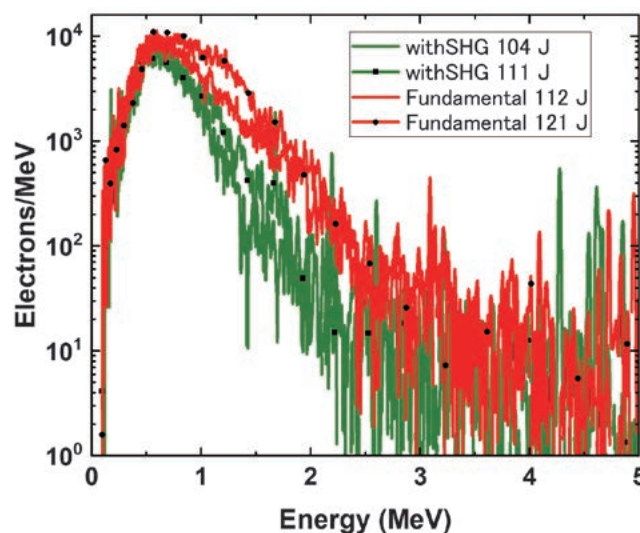


Fig. 2 Electron energy spectra induced by a normal LFEX laser (red) and the converted LFEX laser light (green.)

Effects of kilo-tesla magnetic field on ignition burning in the FI

When a kilo-Tesla magnetic field is applied near laser critical density to efficiently transport relativistic fast electrons to the fuel core, numerical simulations predict that the magnetic field would be compressed to 100 kT in the high density region of the fuel center. The effects of such a strong magnetic field on ignition and burnup characteristics through heat conduction and α -particle transport suppression are analyzed by numerical simulation. This year, we developed our own nuclear burnup code, FIBMET, so that the magnetic field effects could be taken into account in the heat conduction and α -particle transport, and performed the analysis for a high-gain target. Initial conditions for the calculations, after fuel compression and ignition zone formation, were a uniformly compressed ($r = 300 \text{ g/cm}^3$) DT plasma sphere (areal density $rR = 3 \text{ g/cm}^2$). FIBMET simulations were performed in two cases: one without an applied magnetic field ($B_0 = 0$) and the other with a uniform magnetic field of $B_0 = 100 \text{ kT}$, applied parallel to the axis of symmetry. In the case of applying a uniform magnetic field, it was found that the suppression of electron heat conduction and α -particle transport by the magnetic field (a) promoted temperature rise at the ignition site and increased the nuclear reaction rate during the ignition process, but (b) the opposite suppression delayed the propagation of the burnup wave from the ignition site to the vertical direction of the magnetic field, resulting in an increase in burnup time and a decrease in burnup rate. The results show that (a) the suppression of the nuclear reaction rate increased the nuclear reaction rate.

In the future, we will clarify the dependence of the magnetic field effect, including the ignition formation process, on the magnetic field strength and evaluate how the core heating energy required for ignition and the burn rate changes for compressed fuels of the current experimental class ($rR \sim 0.1 \text{ g/cm}^2$) to a high burn rate ($rR \sim 3 \text{ g/cm}^2$). The final result is an evaluation of the explosion process. Finally, an integrated simulation that takes into account the detonation process should be performed to evaluate the validity of the simulation results through comparison with experiments, and to improve the code to design a magnetic field-assisted fast ignition laser core with an external magnetic field applied for REB induction.

(Y. Sentoku)

Research activities on QUEST in FY2022

We will summarize the activities of the Advanced Fusion Research Center at the Research Institute for Applied Mechanics in Kyushu University during April 2022 – March 2023. The QUEST experiments were executed from 28th Jun. – 27th Oct. (2022 Spring/Summer, shot no. 48691-50556) and 1st Dec. – 28th Dec. (2022 Autumn/Winter, shot no. 50557-51205). The main topics of the QUEST experiments in FY2022 are listed below.

- 1) Co-axial helicity injection (CHI) was applied to achieve an efficient plasma start-up. Improvement of a gas-injection system for CHI worked well and clear formation of a closed flux surface could be achieved at an optimized condition of CHI.
- 2) In continuation from the previous FY, the effects of convection on particles and heat transport in liquid metals have been investigated this year, using a laboratory-scale steady state plasma facility at Chubu University. and an infrared spot heating gun at Kyushu University. The results have clearly indicated that both particles and heat transport are enhanced by liquid metal convection, the principle of which is believed to be applicable in designing liquid metal plasma-facing components (LM-PFCs) for a future DEMO reactor. These data were presented as part of an invited talk at the 7th International Symposium on Liquid Metals Applications for Fusion (ISLA-7), held at Chubu University. for the period: Dec. 12th – 16th, 2022.
- 3) A detection-side beamline of HIBP has been installed on QUEST. An injection-side beamline is being designed so that the probe beam can go through a small port. Although the injection port is as small as 30 mm in diameter, the incident angle of the beam needs to be changed by 25 degrees. Thus, two electrostatic deflectors will be used to sweep the beam with the port position as the center of the sweep.
- 4) A high temperature tungsten (W) first wall for QUEST has been developed by using the original fabrication methods of Advanced Multi-Step Brazing (AMSB). We successfully made a middle scale first wall sample of W/ODS-Cu/SUS joint structure in FY 2022. In addition, a W/ODS-Cu/SUS medium-scale sample was heated to 400°C to check uniform temperature increases and effects on vacuum properties. Consequently, the sample passed those qualifications without any problems.
- 5) In this study, the current profile of the injector current flowing into each part of the vessel wall during CHI discharge was investigated by installing a magnetic sensor array. The result enabled us to model the CHI flux evolution and to improve the discharge by optimizing the flux condition and electrode configuration. A closed flux formation plasma generated by CHI was measured by an inserted probe without significant disturbance.
- 6) Glow-discharge optical emission spectrometry has been extensively used to study the global distribution of deposition layers in QUEST and its change with operation history. One of the future tasks is to understand the correlation between the nature of the deposition layer and the recycling behavior of hydrogen. To reach this goal, it is necessary to establish a reliable technique to measure the depth profiles of hydrogen in deposition layers. One of the issues in hydrogen measurement is a high background signal in the measurement system. This year, we identified the origin of the high background signal and prepared a special sample holder to reduce its intensity.
- 7) The control and data acquisition system of the Thomson scattering measurement system was modified to measure profile evolutions during 1000-second discharges. The measurement comprised many short-period cycles, each of which consisted of 15 seconds of (10 Hz) data acquisition, and the cycle was repeated every minute. It was found that the profiles (six-spatial points) became steady after about 300 second from the start of discharge. The highest temperature and the highest density during the steady state were about 80 eV, $4 \times 10^{17} \text{ m}^{-3}$, respectively.
- 8) It has been proposed that the CT injector of UH-CTI for advanced fueling in QUEST is employed as a transient heat load simulator for liquid metal Sn. The injector has high performance to produce a CT plasmod with a power density of about 15 GW/m², and the direction of CT plasma irradiation can be changed

by using a curved drift tube. A site survey for setting up the injector with a curved tube was conducted and the latter was designed, then the several related parts were produced. A comparative experiment was also prepared at the University of Hyogo.

- 9) The hydrogen recycling process on a tungsten divertor has been investigated using molecular dynamics simulations. The results indicate the potential for the generation of significant quantities of hydrogen molecules in high rovibrational states on the surface of the tungsten wall when the incident energy is below a few electron volts (eV).
- 10) A Transient Co-axial Helicity Injection plasma startup was successfully achieved on QUEST. Closed flux surfaces of more than 50 kA were obtained using a simple reactor-relevant biased electrode configuration without needing large vacuum ceramic insulators as on NSTX and HIT-II. The solenoid-free plasma startup discharge evolution on QUEST is similar to that on NSTX.
- 11) The Ball-pen probe (BPP) is an innovative method for direct measuring space potential and electron temperature in magnetized plasmas. The BPP offers numerous advantages, including a simple and robust design, as well as high temporal resolution of the signals. Hence, we have conducted a feasibility study of the BPP for the QUEST spherical tokamak.
- 12) A 28-GHz electron cyclotron non-inductive plasma ramp-up involving bulk electron heating has been studied. The 28-GHz wave was quasi-perpendicularly injected and a retarding loop voltage was applied to suppress highly energetic electron growth. Relatively large-sized plasmas were attained with a 100-eV electron temperature with a low vertical magnetic field. High electron temperatures of 1 keV were attained in small-sized plasma with a high vertical field. In each case, electron densities were about 10^{18} m^{-3} .
- 13) Application of the plasma shape reconstruction code using the Cauchy condition surface method (CCS) to QUEST plasma has been launched. The latest CCS code for JT-60SA has been modified for QUEST. The accuracy of fluxloop signals, which are used in CCS calculation, were evaluated by the past data of a multiple coil energization test in QUEST.
- 14) A new combination diagnostic as a hydrogen recycling monitor based on a permeation membrane probe and a Langmuir probe has been developed. The membrane cleaning in Ar plasma and permeation flux calibration in a preparation chamber was tested. A visible spectroscopy of hydrogen emission was used to evaluate the hydrogen recombination coefficient of the membrane. The in-situ calibration results are in a good agreement with ones estimated with a nuclear reaction analysis.
- 15) A large electrode system (center and shield electrodes) which can withstand high heat flux by water cooling during steady state tokamak operations on QUEST was upgraded to use not only as a diagnostic but also as a low-field side limiter (limiter usage) simultaneously. It is expected that the upgrade enhances the amount of experimental data as a Langmuir probe. First, a movable range of the center electrode was extended, and heat flux to the center electrode could be significantly reduced by the shield electrode during the limiter usage. Second, the number of thermocouples was minimized to enhance vacuum compatibility of the system. Instead, a measurement system of cooling water flow and temperature is now under installation to measure total heat flux to the system during limiter usage.

HANADA Kazuaki (Kyushu University) 1)
 HIROOKA Yoshihiko (Chubu University) 2)
 IDO Takeshi (Kyushu University) 3)
 TOKITANI Masayuki (NIFS) 4)
 KURODA Kengoh (Kyushu University) 5)
 HATANO Yuji (University of Toyama) 6)
 EJIRI Akira (University of Tokyo) 7)
 FUKUMOTO Naoyuki (University of Hyogo) 8)

SAITO Seiki (Yamagata University) 9)
 RAMAN Roger (University of Washington) 10)
 MOON Chanho (Kyushu University) 11)
 IDEI Hiroshi (Kyushu University) 12)
 TAKECHI Manabu (QST) 13)
 KUZMIN Arseniy (Kyoto University) 14)
 NAGASHIMA Yoshihiko (Kyushu University) 15)

(K. Hanada)

University of Toyama

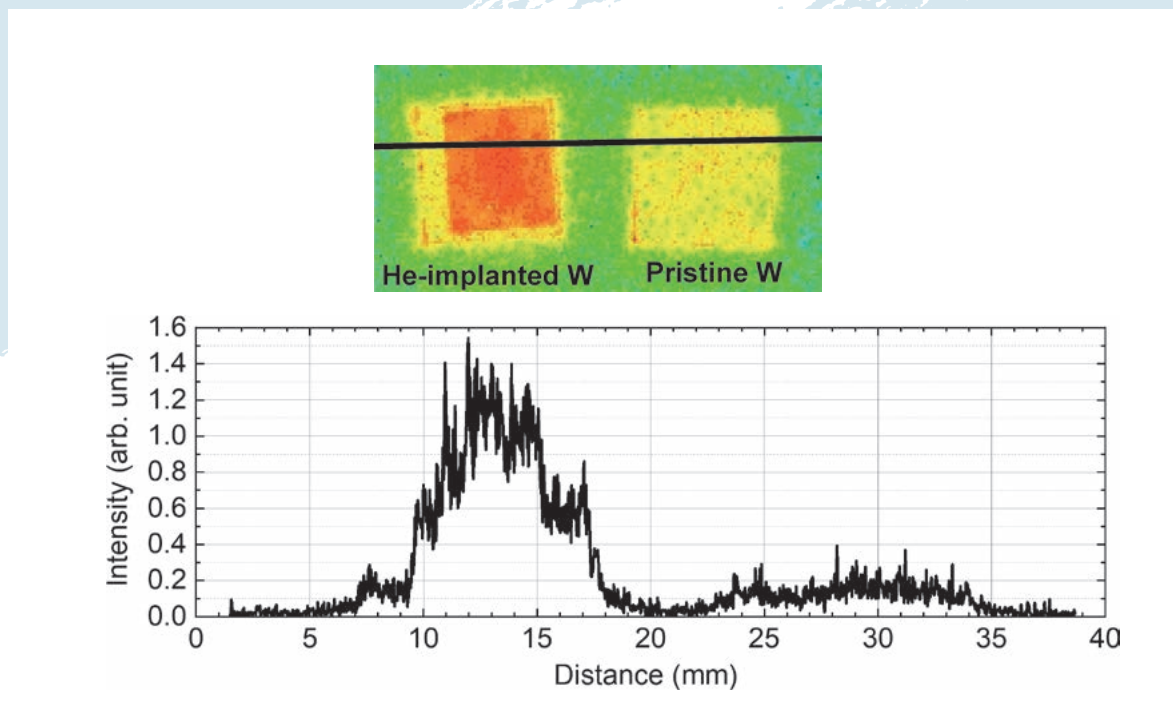


Fig. 1 (top) Two-dimensional (2D) image of photo-stimulated luminescence (PSL) intensity obtained using imaging plate (IP) for He-implanted and non-implanted W samples after exposure to deuterium-tritium (DT) mixture gas at 400°C and (bottom) profile of PSL intensity along black line in 2D image.

Highlight

Research Activities in Hydrogen Isotope Research Center, Organization for Promotion of Research, University of Toyama

Plasma-facing materials of a fusion reactor will be subjected to implantation of D, T and He ions from the plasma. The formation of He bubbles and trapping of T at those bubbles are important safety concerns. In this study, W and W-Mo alloy samples were irradiated with He ions and T trapping was examined using the IP technique after exposure to DT gas. Clear enrichment of T at the He-implanted zone was observed due to trapping effects, as shown in Fig. 1. The effects of Mo on the bubble growth and trapping are under investigation. [*Hydrogen isotope pick-up and retention in He-exposed W-Mo alloys* (E. Jimenez-Melero and J. Ashley, *The University of Manchester*)]

Tritium transport in fusion reactor materials (Y. Hatano, U. Toyama): A fusion power plant will use a steam turbine to generate electricity. Tritium (T) permeation through steam generator piping results in the risk of uncontrolled T leakage to the environment. Therefore, T permeation must be precisely evaluated and minimized. Nickel alloys are widely used as pipe materials. In this study, the permeation of T from/to high temperature, high pressure water through Inconel 600 film was examined.

Permeation devices made of type 316L stainless steel were used with fresh internal surfaces or those covered by protective oxide layers. The device was separated into two chambers by an Inconel 600 sample disk. The upstream chamber was filled with tritiated water (0.9 MBq/cm^3) and the downstream side was filled with non-radioactive water. The device was heated to 280°C in a forced convection oven for 14–60 hours. The vapor pressure of water at this temperature was 6.4 MPa. After heating, the downstream chamber was opened and the concentration of T in water was measured using a liquid scintillation counter. The effects of oxygen were examined by pressuring the water in both chambers by O_2 gas up to 3 MPa. A correlation between heating time and the amount of T permeated to the downstream side is shown in Fig. 2. The permeation rate was high with the fresh internal surfaces of the permeation device and 3 Bq/h on average. Nevertheless, an order of magnitude smaller permeation rate was observed with the internal surfaces covered by protective oxide layers. The addition of O_2 gas resulted in further reduction in the permeation rate. These results indicate that T permeation is sensitively dependent on the partial pressure of HT gas generated by the oxidation of co-existing material in the system (a stainless steel wall in the present case). The T permeation rate in a steam generator can be managed by controlling the oxidation of metals in a primary coolant loop and/or by addition of O_2 gas.

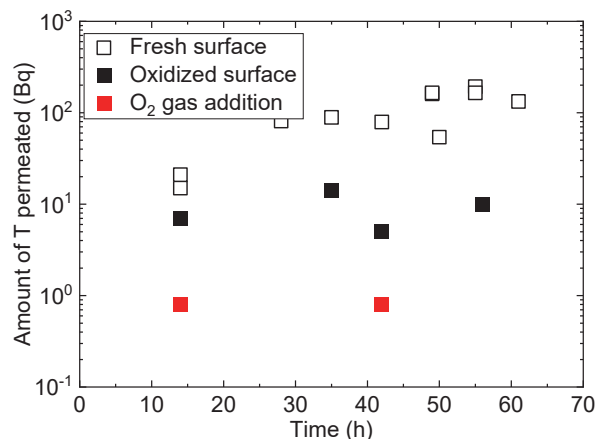


Fig. 2 Change in T permeation with elapse of time.

Other experimental studies performed in the Hydrogen Isotope Research Center in the fiscal year 2022 are the following:

- *Nano-fiber formation on tungsten alloy by helium plasma irradiation* (Y. Ueda, Osaka U.);
- *Effect of transmutation or irradiation damage on hydrogen isotope transport dynamics* (Y. Oya, Shizuoka U.);
- *Effective tritium removal under vacuum conditions* (N. Ashikawa, NIFS);
- *Effects of heat and particles load on hydrogen isotope retention in tungsten materials* (K. Tokunaga, Kyushu U.);
- *Release behaviors of hydrogen isotopes from tungsten materials exposed to hydrogen isotope plasma* (T. Otsuka, Kindai U.);
- *Depth analysis of co-deposited H, He and impurity atoms on plasma exposed W by means of GDOES* (N. Yoshida, Kyushu U.);
- *Precise evaluation of tritium profile in solid/liquid tin exposed to tritium plasma* (H. Toyoda, Nagoya U.);
- *Suppression of tritium permeation in metals by laser-doping of impurities* (Y. Nobuta, Hokkaido U.);
- *Measurement of transmission of liquid DT through polymer for development of laser fusion DT fuel* (Y. Arikawa, Osaka U.); and
- *Understanding and optimization of tritium absorption into titanium target for 14 MeV neutron irradiation experiments* (I. Murata, Osaka U.).

8. Activities of Rokkasho Research Center (RRC)

General Information on RRC

The Rokkasho Research Center (RRC, established in May 2007) promotes cooperation and joint research with the Broader Approach (BA) activities that are being undertaken in parallel with the ITER project and builds a technical foundation for the development of a prototype fusion reactor, by supporting the participation of collaborators of NIFS and universities, based on academic standpoints. The director of RRC serves as the leader of the general coordination group of the Joint Special Team for a Demonstration Fusion Reactor (DEMO) design, which is the organization of an all-Japan collaboration established in May 2015.

Furthermore, in order to promote the interdisciplinary expansion of issues being tackled in fusion research, we are focusing on disseminating research issues to a range of academic fields, inviting interdisciplinary meetings, and promoting interdisciplinary joint efforts. As an example, the fourth mid-term strategic project of the Research Organization of Information and Systems (ROIS), “Statistical-mathematical modeling for plasma data, complementary to plasma physics,” has been established and we are deepening/widening collaborations with communities involved in disciplines such as statistical-mathematics and data science.

In addition, we are actively working to contribute to human resource development based on the Graduate University for Advanced Studies (SOKENDAI), through establishing and deepening cooperation with neighboring educational institutions.

RRC’s Homepage: <https://www.nifs.ac.jp/en/about/rrc.html>

Highlighted Activities in FY2022

A number of individual collaboration research projects have been launched in the fields of nuclear fusion and statistical mathematics in order to extract useful information that can contribute to the promotion of fusion studies by making the most of large-scale/diverse data produced in nuclear fusion research. By aggregating them, the project, the Research Organization of Information and Systems (ROIS), the fourth mid-term strategic projects, “statistical-mathematical modelling on plasma data: complementary to plasma physics” was approved in FY2022, and NIFS RRC has been a research hub for promoting the project. The meeting for sharing research topics among those involved in fusion and statistical-mathematical research was held in Dec. 2022 at NIFS RRC/QST Rokkasho Institute and Hachinohe City Public Hall. This project has pursued synergetic development of both research communities by applying/improving a statistical-mathematical approach onto the fusion and plasma data. A report on the meeting was published in the Institute of Statistical Mathematics (ISM) News (No. 159, Feb. 2023) (in Japanese). The activities in FY2022 were highly evaluated in the ROIS Review Board, and a developmental extension was approved.

We are also promoting activities based on the SOKENDAI through promoting ties/collaborations with nearby educational institutions. In February 2023, the SOKENDAI Outreach Activities “training program for next-generation young researchers based the community at Aomori, in the Rokkasho area” was carried out by cooperation with the QST Rokkasho Institute. About 40 students of the National Institute of Technology (KOSEN), Hachinohe College, visited the Rokkasho site, and were conducted on a tour of cutting-edge facilities and had stimulating live discussions with researchers/engineers there.



Fig. 1 Group photo of the SOKENDAI Outreach Activities (at QST Rokkasho Institute).

We have created a clear file that incorporates the rich natural scenery of Rokkasho village. We are sure that visitors to RRC, from a wide range of academic fields either domestically or internationally, will recognize the beauty of Rokkasho village and Aomori Prefecture. The landscape photos (those published in the 2022 Rokkasho Village Handbook) were provided by the Rokkasho Village Office, and the wild bird photos were provided by Mr. Kazuaki Ichinohe (former executive officer of the Institute for Environmental Sciences, Public Interest Incorporated Foundation, located at Rokkasho Village).



Fig. 2 RRC clear files (3 types) created in FY2022.

(M. Yokoyama)

9. Research Enhancement Strategy Office

The Research Enhancement Strategy Office (RESO) was established on November 1, 2013, to strengthen the research activities of the Institute by planning various support programs for the researchers and conducting public relations programs for making fusion science more understandable in society. Three University Research Administrators (URAs) are working in the following five Task Groups:

- (1) IR (Institutional Research)/Evaluation Task Group
- (2) Young Researchers and their Career-path Development Task Group
- (3) Collaboration Research Enhancement Task Group
- (4) Public Relations Enhancement Task Group
- (5) Financial Basis Strengthening Task Group

(1) IR/Evaluation

The task group for the IR and evaluation continued its role to make systematic analyses of the present research activities of NIFS. Statistical data of publications and scientific reports were collected using the NIFS article information system (NAIS) with complementary data obtained through the Scopus and WoS public research resource supplying companies. The following candidates for unique indicators that can demonstrate the strength of the research capabilities of NIFS were investigated.

1. Total number of journals publishing NIFS articles
2. Percentage of internationally co-authored papers among total published papers
3. Total number of papers mentioning NIFS in acknowledgments
4. Increase in papers using keywords from different fields (examined through Text Mining)
5. Number of journals that publish papers citing NIFS papers

An IR Report No. 7 was edited and distributed, in which the evaluation indicators for NIFS specified in the Fourth Mid-term Goals and Plans were explained, and a policy to satisfy the indicators was proposed.

(2) Supporting Young Researchers

In the activities for supporting young researchers, their startup research was supported to enhance basic research skills. Applications were reviewed by the Young Researchers Development Task Group, and the following programs were supported in FY2022:

1. *Investigation of electron cyclotron (EC) motion and its resulting radiation processes* (Yuki Goto),
2. *Understanding and creation of applications for migration phenomena of supersaturated hydrogen in materials due to super-permeation of hydrogen* (Makoto Kobayashi),
3. *Creation of innovative forming method using Transformational Superplasticity* (Hiroyuki Noto).

A debriefing meeting was held in April 2022 for the three people who received support in FY2021.

RESO also assisted with the applications of young scientists to the ‘Grants-in-aid Scientific Research’ programs and other competitive external fundings.

(3) Supporting Enhanced Collaboration Research

NIFS has concluded international exchange agreements with many world-class research institutes. RESO supported the implementation of these international joint research activities.

W7-X of the Max-Planck Institute for Plasma Physics (Germany) is a modular stellar device and RESO supported joint research on common issues of helical devices. With Southwest Jiaotong University (China), we supported the construction of CFQS, a helical type quasi-axisymmetric magnetic field configuration confinement device, and supported research on differences in magnetic field configuration. RESO supported the implementation of joint research on helical devices at the University of Wisconsin (USA) and the CIEMAT Institute (Spain).

RESO dispatched researchers to explore new potential for joint research. NIFS researchers also actively par-

participated in international research activities such as ITER, and supported the strengthening of the presence of NIFS. Based on the Plasma Wall Interaction(PWI) Agreement, a multilateral compact of the International Energy Agency, we supported the implementation of joint research to understand plasma-wall interactions in nuclear fusion devices.

Through cooperation between Japan and China, RESO supported the implementation of joint research and personnel exchanges aimed at promoting nuclear fusion research. As a Japan-Korea nuclear fusion cooperation project, RESO supported a mutual exchange between KSTAR and the LHD, technical cooperation on measuring and heating equipment, implementation of workshops in each research field, and implementation of researcher exchanges.

(4) Enhancing public relations

- 1) Dissemination of research achievements through EurekAlert!

Six topics were released: (i) “Successful improvement of plasma thermal insulation layer with deuterium”, (ii) “Discovery of high-speed moving plasma turbulence for the first time in the world”, (iii) “The process of waves carrying plasma heat is observed for the first time in the world”, (iv) “Development of high-time-resolution measurement of electron temperature and density in a magnetically confined plasma”, (v) “Cooling 100 million degree plasma with a hydrogen-neon mixture ice pellet”, and (vi) “Simplified calculations reproduce complex plasma flows”. These topics were released to the media in Japan, too. Some topics attracted attention from the international media.

- 2) Information release about NIFS and fusion science

Sixteen research results were released in the press and disseminated on SNS (twitter and facebook) .

- 3) Outreach activities based on the fusion community

RESO joined a discussion on fusion science outreach headquarters with QST, universities and the Ministry of Education, Culture, Sports, Science and Technology.

- 4) Others

RESO introduced interesting science topics to the public on the occasion of the Science Talk at the Open Campus Online of NIFS, as shown in Figure 1. RESO produced movies briefly introducing researchers’ activities.

(5) Strengthening Financial Basis

Activities are being carried out with the aim of strengthening the financial base of the institute. Support activities were carried out by holding briefing sessions to obtain competitive research funds such as Grants-in-Aid for Scientific Research (KAKENHI), JST, and NEDO, and by supporting the preparation of application forms.

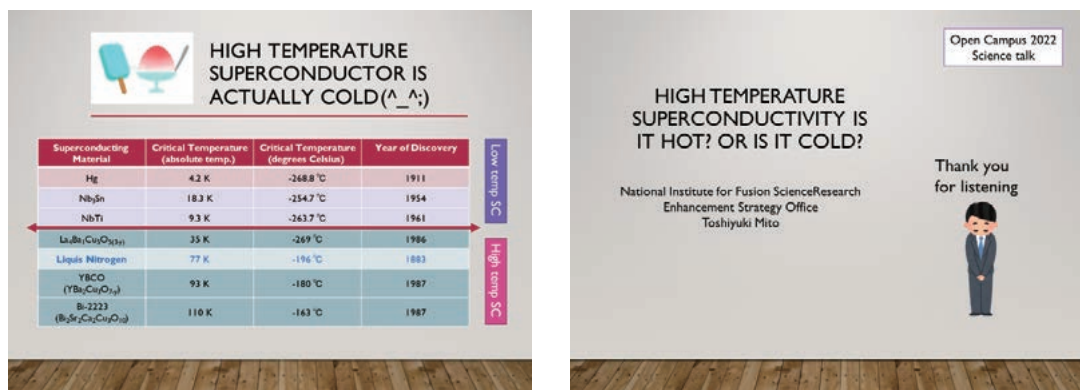


Fig. 1 Science Talk at Open Campus Online of NIFS. Prof. Mito talked about superconductivity to the public online.

(Y. Todo, T. Muroga and T. Mito)

10. Division of Health and Safety Promotion

The Division of Health and Safety Promotion is devoted to preventing work-related accidents, to ensuring safe and sound operation of machinery and equipment, and to maintaining a safe and healthful environment for researchers, technical staff, co-researchers, and students. This division consists of ten offices, and various subjects related to health and safety are discussed by office chiefs once a month.

1. Environmental Safety Control Office

This office has the responsibility to maintain a safe workspace and environment.

- A) Management to solve problems pointed out by the safety and health committee.
- B) Maintenance of a card-key system for the gateways of controlled areas.
- C) Maintenance and management of the vehicle gate at the entrance of the experimental zone.
- D) Maintenance of fluorescent signs of evacuation routes and caution marks.
- E) Management of sewage drainage from NIFS.
- F) Monitoring of discharging water to prevent water pollution.

2. Health Control Office

The main role of this office is to keep the workers in the institute healthy, including co-researchers and students.

- A) Medical checkups both for general and special purposes and immunization for influenza.
- B) Mental health care services and health consultation.
- C) Accompany inspections of the health administrator and the occupational physician.
- D) Maintenance of AEDs.
- E) Alerts and response to COVID-19.

Various lectures are held on physical and mental health. An online stress-check was held in October 2022.

3. Fire and Disaster Prevention Office

The main role of this office is to prevent or minimize damage caused by various disasters.

- A) Making self-defense plans for fires and disasters, and implementation of various training.
- B) Promotion of first-aid workshops and an AED class.
- C) Maintenance of fire-defense facilities and attending on-site inspections by the local fire department.
- D) Review and update disaster prevention rules and manuals.

All workers must attend disaster prevention training held every year, and a disaster simulation exercise is also held. Figure 1 shows fire-extinguisher training in the LHD.

4. Radiation Control Office

The main role of this office is to maintain radiation safety for researchers and the environment. Legal procedures for radiation safety and regular education for radiation area workers are also important roles.

- A) Maintain radiation safety for workers.
- B) Registration and dose control for radiation area workers.
- C) Observation of radiation in the radiation-controlled area and periphery.
- D) Maintenance of the radiation monitor.
- E) Applications for radiation equipment to national agencies and local governments.
- F) Revise official regulations and establish new rules.



Fig. 1 Fire extinguisher training in LHD

An educational lecture for the radiation area workers was held on March 2, 2023. We prepared an opportunity for DVD viewing for absentees. Non-Japanese workers were educated and trained in English.

5. Electrical Equipment and Work Control Office

The main role of this office is to maintain electrical safety for researchers, technical staff members and students.

- A) Check and control electrical facilities according to technical standards.
- B) Safety lecture for researchers and workers.
- C) Annual check of electrical equipment during blackouts.

The annual inspection of the academic zone was carried out on May 21, 2022, and that of the experimental zone on June 11 and June 12, 2022.

6. Machinery and Equipment Control Office

The main role of this office is to maintain the safe operation of cranes. Its tasks are as follows.

- A) Inspection and maintenance of cranes.
- B) Management of crane license holders and safety lectures for crane users.
- C) Schedule management of crane operations.

7. High Pressure Gas Control Office

The main role of this office is for safety operation and maintenance of high pressure facilities with cooling systems such as the LHD.

- A) Safety operation and maintenance of high-pressure gas handling facilities in NIFS.
- B) Daily operation, maintenance, system improvement, and safety education according to the law.
- C) Safety lectures for researchers and workers.

8. Hazardous Materials Control Office

The main role of this office is management of the safe treatment of hazardous materials and maintaining safety for researchers against hazardous events.

- A) Research requests for hazardous materials and their storage status.
- B) Management to ensure safe storage of waste.
- C) Implementation of chemical substance risk assessment.

9. New Experimental Safety Assessment Office

The main role of this office is to check the safety of experimental devices, except for the LHD. For this purpose, researchers who want to set up new experimental apparatus must apply for a safety review. Two reviewers are assigned from members of this office and other specialists to check the safety of these devices.

- A) Examine new experiments for safety problems and advise on safety measures.
- B) Improve safety in each experiment and reinforce a safety culture at NIFS by annual reviews by NIFS employees.

10. Safety Handbook Publishing Office

The tasks of this office are to publish the Safety Handbook in Japanese and in English, and it is updated every year. The regular safety lecture was held on May 13, 2022. All workers including co-researchers and students must attend this safety lecture every year.

(S. Sakakibara and M. Osakabe)

11. Division of Deuterium Experiments Management

Deuterium experiments have been carried out in the LHD since March 7th, 2017. Objectives of the deuterium experiments are (1) to realize high-performance plasmas by confinement improvement and by improved heating devices and other facilities, (2) to explore an isotope effect study, (3) to demonstrate the confinement capability of energetic particles (EPs) in a helical system and to explore their confinement studies in toroidal plasmas, and (4) to proceed with extended studies on plasma-material interactions (PMI) with longer time scales.

Division of Deuterium Experiments Management was founded to establish a safety management system and to consolidate experimental apparatus related to deuterium experiments. After the start of deuterium experiments in the LHD, the function of this division was shifted to the management of their safe and reliable operation. Under this division, a taskforce named ‘the deuterium experiment management assistance taskforce’ was founded. Its main jobs were: (1) the establishment and improvement of manuals to operate the LHD and peripheral devices safely during deuterium experiments, (2) check and improve regulations related to proceeding with the deuterium experiments safely, (3) an upgrade of the LHD itself, its peripheral devices and the interlock systems for safe operation during the deuterium experiments, (4) upgrade and optimize heating devices and diagnostic systems for the deuterium experiments, (5) remodel the LHD building and related facilities, and so on. These jobs proceeded with the cooperation of an LHD board meeting and the Division of Health and Safety Promotion. In addition, necessary tasks related to the safety evaluation committee founded by NIFS and those related to the Safety Inspection Committee of the National Institute for Fusion Science (NIFS) founded by local government bodies proceeded in this division. The publication of an annual report for radiation management of the LHD deuterium experiments is another of its important tasks.

Cooperation with the Safety Inspection Committee for NIFS, which is organized by local government bodies, such as those in Gifu Prefecture, Toki City, Tajimi City, and Mizunami City, is an important task of the Division of Deuterium Experiments Management. Environmental neutron dose monitoring at NIFS and tritium concentration monitoring in the water around the NIFS has been performed by the committee since 2015. In 2022 FY, these monitoring activities were performed twice, as scheduled with the cooperation of the Division of Deuterium Experiments Management.

Because deuterium experiments in the LHD ended in 2022 FY, the function of this division is going to merge with that of the Division of Health and Safety Promotion, as a part of its remit in 2023 FY.

(a)



(b)



(c)

LHD重水素実験放射線管理年報
(2022年4月1日~2023年3月31日)

2023年7月

大学共同利用機関法人 自然科学研究機構
核融合科学研究所 安全衛生推進センター

Photographs of (a) environmental water sampling and (b) environmental radiation dose rating with Secretariat of Safety Inspection Committee. (c) Front cover of Annual Report on radiation management at first LHD deuterium experiment (in Japanese).

(M. Osakabe and M. Isobe)

12. Division of Information and Communication Systems

NIFS handles a large amount of information, including experimental data. As a center of excellence in fusion science, NIFS is in a position to exchange information both domestically and internationally and is required to make open and protect such information. The Division of Information and Communication Systems (ICS) works to promote open science and network security by centralizing the development and operation of information and communication systems. Open science is an initiative that aims to “create new knowledge that transcends fields”, “ensure transparency in research”, and “return the results of studies to society” by making research data and results widely available. And it is becoming an important international trend. NIFS also provides open access to research data and results to researchers worldwide and to the public. Internet communication systems for handling various types of information are increasingly important to support open science. We are working on network security to ensure the safe and appropriate handling of information.

The Department of Information and Communication System (ICS) was founded in 2014 to efficiently develop and maintain the information and network systems of NIFS. All information system professionals in NIFS belong to the ICS. There is one office and three groups corresponding to the job classifications in NIFS. The Information Security Office, established in 2020, is responsible for the overall management and coordination of the work related to information security in the Institute. Members of the Information Security Office are also members of the Computer Security Incident Response Team, NIFS-CSIRT, and when an information security incident occurs, they cooperate with the institutional CISO, information system administrators, and information security managers to respond to the incident. The NIFS-CSIRT is also a member of the NINS-CSIRT, the CSIRT of the

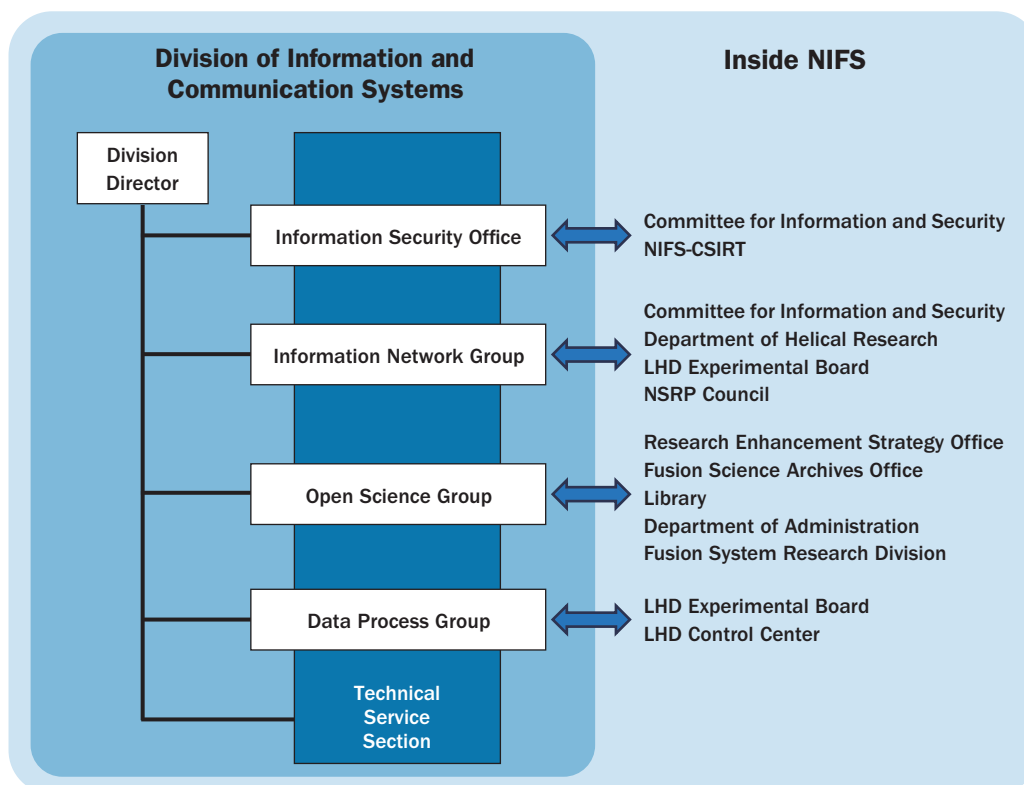


Fig. 1 Structure of Division for Information and Communication Systems.

National Institutes of Natural Sciences, and shares information with them in normal times. The Information Network Group operates and maintains the information network and related services, such as the e-mail system, in accordance with the Information Security Policy and Information Security Guidelines, and implements incident prevention measures. The Open Science Group, established in 2021, develops, operates, and maintains analytical information systems, atomic and molecular data systems, and various information systems that serve as the foundation of the Institute, and makes experimental and analytical data and atomic and molecular data available to the public. The Data Processing Group, established in 2021, develops, operates, and maintains the experimental information and data collection system.

The ICS works as follows: a request for the maintenance, improvement, and development of the information and communication system is submitted to the ICS by each section of the Institute. All requests are prioritized by a core member of the Technical Services Section of the ISC in consultation with the respective group leaders, and a team of practitioners is assigned to handle the request. Since all the experts belong to the Technical Service Section of the ICS, each group leader asks the section leader to allocate the necessary number of experts for a prescribed period to complete the task. Monthly leader meetings are held to review the progress of each group and the status of handling requests submitted to the ISC. Issues related to each group and the ISC as a whole are also discussed and coordinated with the appropriate organizations as necessary.

In NIFS, three research projects extend across the research divisions. It can be said that the ICS is another “project” which lies across all the divisions in the institute to keep the information and communication systems stable, secure, and up to date.

(T. Yamamoto)

13. International Collaboraiton

Many research activities in NIFS are strongly linked with international collaborations with institutes and universities around the world. These collaborations are carried out in various frameworks, as follows,

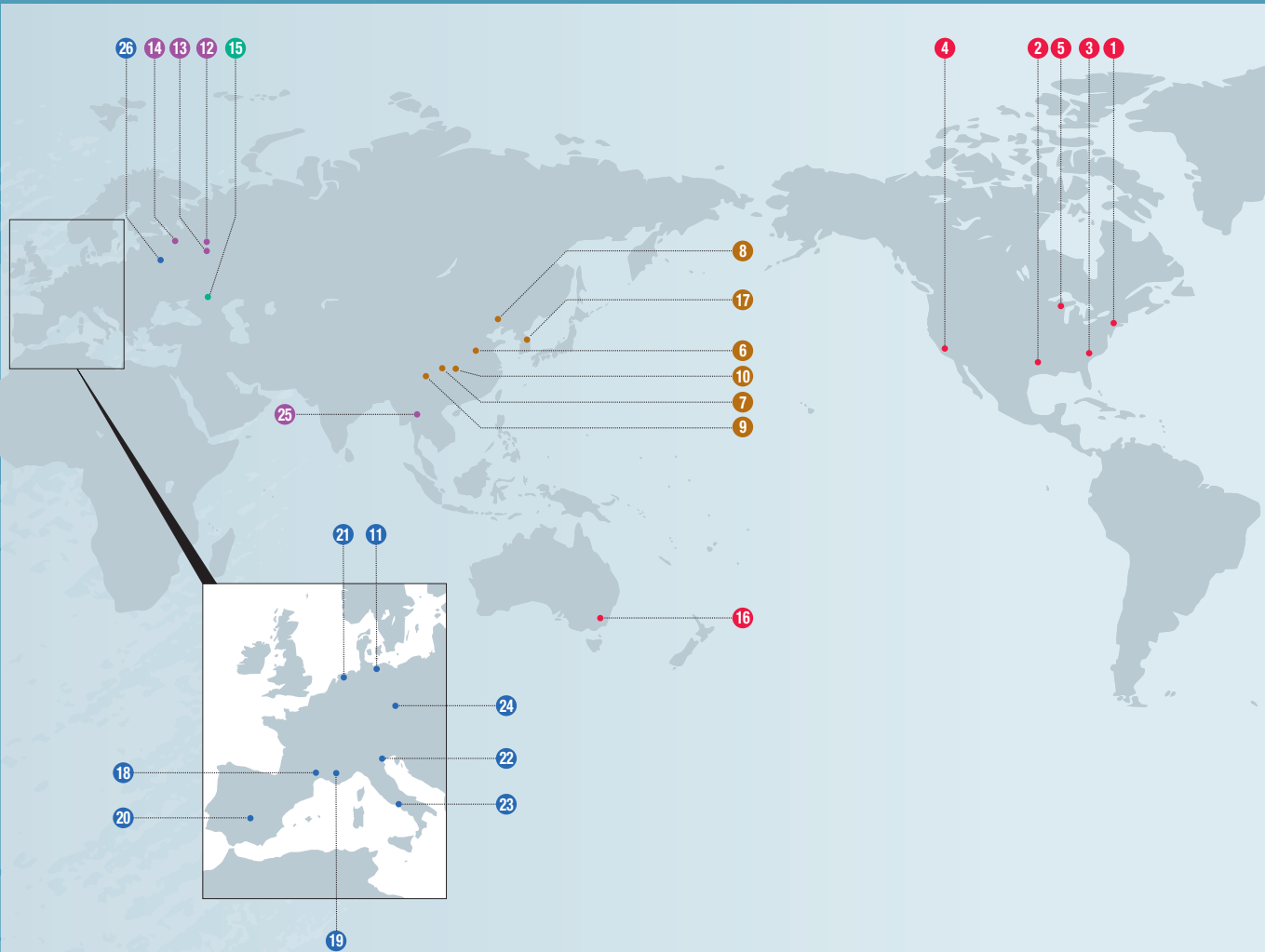
- 1) Multinational coordination in Fusion Power Coordinating Committee (FPCC) under International Energy Agency (IEA),
 - Stellarator-Heliotron Technology Cooperation Program (TCP)
 - Plasma-Wall Interactions TCP
 - Spherical Tori TCP
- 2) Binational coordination,
 - Japan-United States Collaborative Program
 - Japan-Korea Fusion Collaboration Programs
 - Japan-China Collaborative Program
 - Japan-EU Cooperation
- 3) Coordination with other institutions
 - 32 international academic exchange agreement

The geographical distribution of international collaborations and summary of each activity are shown in the following pages.

In FY2022, as the pandemic diminished, personal exchange with overseas organizations recovered gradually and the international collaborations became active, although it was still far from the situation before the pandemic.

(T. Morisaki)

Academic Exchange Agreements



- U.S.A.** 1 Princeton Plasma Physics Laboratory (PPPL)
- 2 Institute for Studies, The University of Texas at Austin (IFS)
- 3 Oak Ridge National Laboratory (ORNL)
- 4 Center for Energy Science and Technology Advanced Research, University of California, Los Angeles (UCLA)
- 5 College of Engineering, University of Wisconsin, Madison
- China** 6 Institute of Plasma Physics, Chinese Academy of Sciences (ASIPP)
- 7 Southwestern Institute of Physics (SWIP)
- 8 Peking University
- 9 Southwest Jiaotong University (SWJTU)
- 10 Huazhong University of Science and Technology
- Germany** 11 Max Planck Institute for Plasma Physics (IPP)
- Russia** 12 Russian Research Center, Kurchatov Institute (KI)
- 13 A. M. Prokhorov General Physics Institute, Russian Academy of Sciences (GPI)
- 14 Peter the Great St. Petersburg Polytechnic University
- Ukraine** 15 National Science Center of the Ukraine Khar'kov Institute of Physics and Technology Institute of Plasma Physics (KIPT)
- Australia** 16 Australian National University (ANU)
- South Korea** 17 National Fusion Research Institute (NFRI)
- France** 18 Aix-Marseille University (AMU)
- 19 Commissariat à l'énergie atomique et aux énergies alternatives (CEA)
- Spain** 20 National Research Center for Energy, Environment and Technology (CIEMAT)
- Netherlands** 21 Dutch Institute for Fundamental Energy Research (FOM)
- Italy** 22 CONSORZIO RFX
- 23 Institute of Ionized Gas (IGI)
- Czech** 24 HiLASE Center, Institute of Physics CAS (FZU)
- Poland** 25 Chiang Mai University
- Poland** 26 Institute of Plasma Physics and Laser Microfusion (IPPLM)

The ITER International Fusion Energy Organization (ITER)

US – Japan (Universities) Fusion Cooperation Program

US-Japan Joint Activity has continual from 1977. The 43rd CCFE (Coordinating Committee for Fusion Energy) meeting was held on April 21, 2023 via a video conference system. Representatives from the MEXT, the DOE, Universities and research Institutes from both Japan and the US participated. At the meeting, the current research status of both countries was reported together with bilateral technical highlights of the collaborations. FY 2022 cooperative activities were reviewed, and FY 2023 proposals were approved. As the pandemic diminished personal exchanges with overseas organizations recovered gradually. On the other hand, some collaborative activities still continued by remote participation and web meetings.

(1) Fusion Technology Planning Committee (FTPC)

In this category of US-Japan collaboration, there are six research fields: superconducting magnets, low-activation structural materials, plasma heating-related technology, blanket engineering, in-vessel/high heat flux materials and components, and power plant studies and related technologies. In fiscal year 2022, despite the continuation of the COVID-19 pandemic, two-thirds of proposed collaborations were accomplished, including three Japan to US personal exchanges and one US to Japan one. All the exchanges were in the research field of in-vessel/high heat flux materials and components, and the plasma-surface interactions research facility PISCES at UCLA was used for all of them. Fruitful experimental results were obtained in all these collaborations, and for the one US to Japan personal exchange with the title “Characterization of deuterium super-saturated surface layer in tungsten”, it was found, when using Transmission Electron Microscopy (TEM) at NIFS, that the deuterium plasma exposure of tungsten may cause formation of a Deuterium Supersaturated Surface Layer (DSSL), even at a low incident energy of ~ 75 eV. It has also been confirmed that this observation is consistent with a previous measurement using laser-induced breakdown spectroscopy (LIBS).

Although one Japan to US (in the research field of superconducting magnet) and one US to Japan (plasma heating-related technology) personal exchange were canceled, sufficient discussions have been held among the corresponding members via e-mails and/or video conferences to make agreements about the resumption of these programs in the coming fiscal year FY2023.

(2) Fusion Physics Planning Committee (FPPC)

In the area of fusion physics, two committee meetings, five workshops and 19 personnel exchanges were held. Notably, four of the workshops and 14 of the personnel exchanges were conducted on-site, as shown in Figs. 1 and 2.



Fig. 1 Magnetic Reconnection Workshop in Monterey.

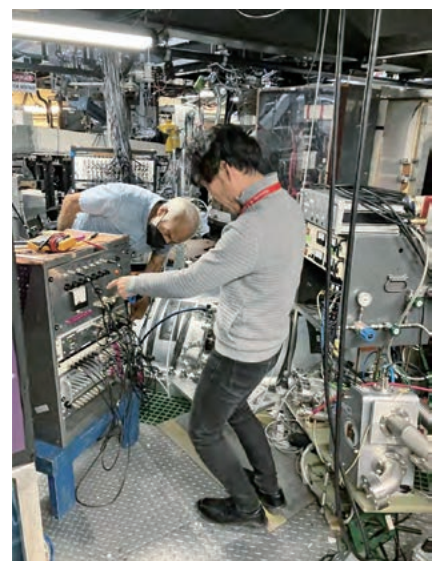


Fig. 2 Experiment in Univ. Wisconsin, Madison.

(3) Joint Institute for Fusion Theory (JIFT)

A workshop “Theory and simulation on high field and high energy density physics” was held at Spokane in October 2022. In the category of personal exchange, one US to Japan exchange visit for “Kinetic-MHD hybrid simulations of energetic-particle driven instabilities” and one Japan to US exchange visit for “Collaboration on Tokamak boundary plasma turbulence simulations for divertor heat flux width” were successfully completed. The latter exchange visit resulted in publication in *Computer Physics Communications* (Figure 1). Three Japan to US and three US to Japan personnel exchange programs were carried out as remote collaborations. A JIFT discussion meeting was held online on September 30, 2022 in the Plasma Simulator Symposium. The status of JIFT activities for 2022–2023 was reviewed and recommendation plans for 2023-2024 were discussed by email among members of the JIFT Steering Committee in December 2022.

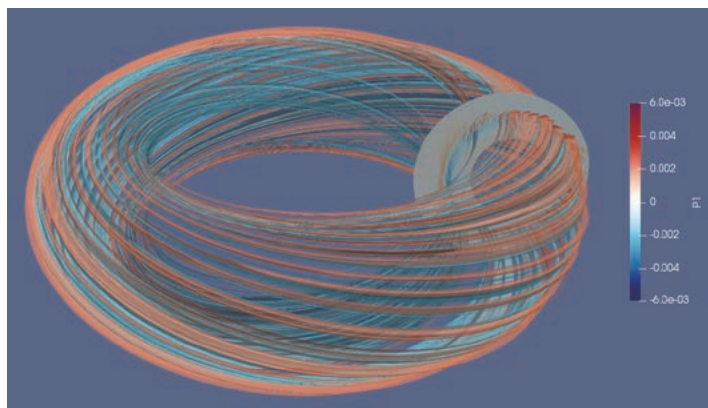
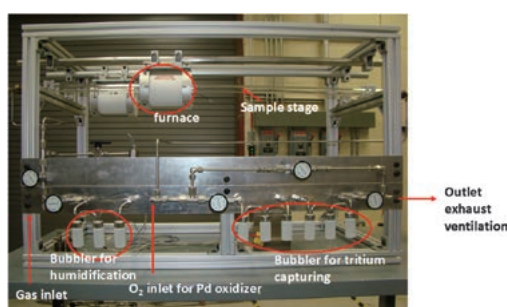


Fig. 1 Three-dimensional structure of perturbed pressure during pedestal collapse in full annular torus ELM crash simulation [H. Seto *et al.*, *Comput. Phys. Commun.* **283**, 108568 (2023)]

(4) US-Japan Joint Project: FRONTIER

The FRONTIER collaboration started in April 2019 to provide the scientific foundations for reaction dynamics in interfaces of plasma facing components for DEMO reactors. This project consists of four tasks: Irradiation Effects on Reaction Dynamics at Plasma-Facing Material/Structural Material Interfaces (Task 1), Tritium Transport through Interface and Reaction Dynamics in Accidental Conditions (Task 2), Corrosion Dynamics on Liquid-Solid Interface under Neutron Irradiation for Liquid Divertor Concepts (Task 3) and Engineering Modeling (Task 4). To examine liquid metal-structural material compatibility under neutron irradiation, five Sn capsules were exposed to neutrons for 10.5 days in a High Flux Isotope Reactor at Oak Ridge National Laboratory (ORNL) in cycle 500, after an extensive approval process for this unique experiment. The irradiated capsules were transported to the hot cells in March 2023 for starting post-irradiation examinations. In the Safety and Tritium Applied Research (STAR) Facility at Idaho National Laboratory (INL), a mobilization device and a thermogravimeter were installed to examine high temperature oxidation of neutron-irradiated tungsten and consequent emissions of radioisotopes under accidental conditions.



Mobilization device (left) and thermogravimeter (right) installed in INL to examine high temperature oxidation of neutron-irradiated tungsten and consequent emissions of radioisotopes under accidental conditions.

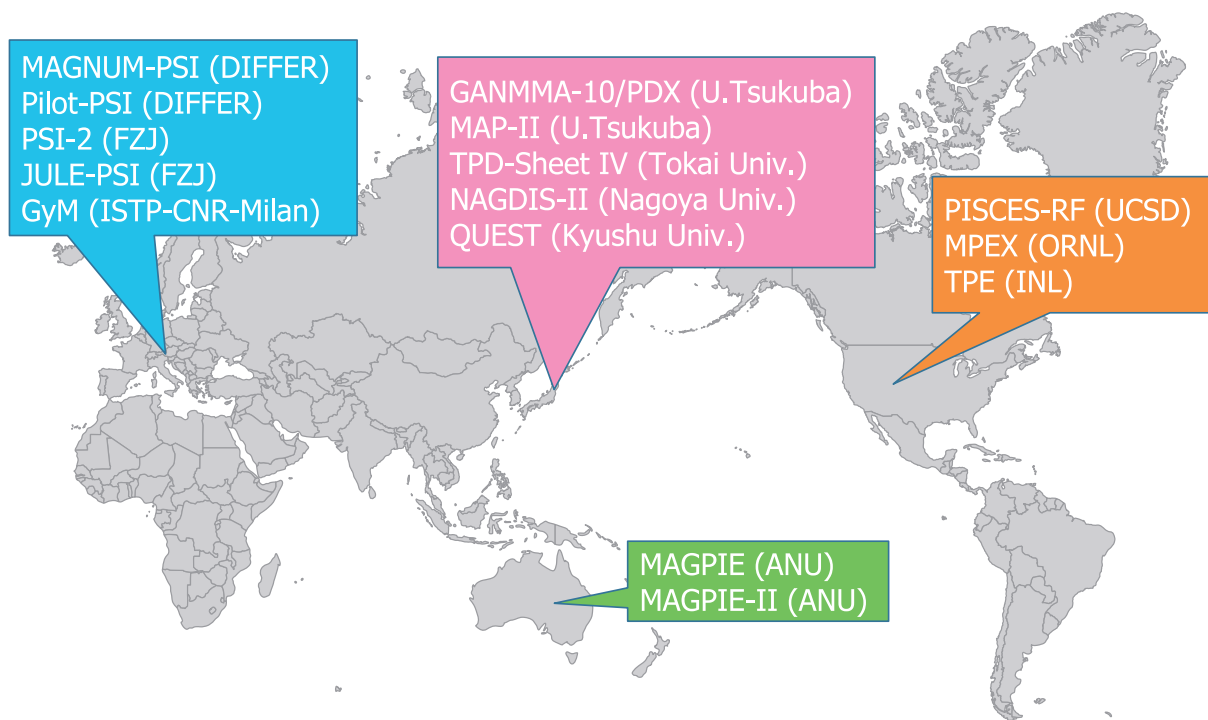
(T. Morisaki, S. Masuzaki, N. Yanagi, H. Sugama and Y. Hatano)

Plasma Wall Interaction (PWI) Collaboration

This collaboration is based on the IEA Technical Collaboration Programme (TCP) of the “Development and Research on Plasma Wall Interaction Facilities for Fusion Reactors” (PWI TCP) which involves Japan, Europe, the United States, and Australia. The objective of this program is to advance the physics and technologies of plasma-wall interaction research by strengthening cooperation among plasma-wall interaction facilities (in particular, by using dedicated linear plasma devices), to enhance the research and development effort related to a fusion reactor’s first wall materials and components, shown in the figure below.

NIFS collects proposals for international collaborative studies based on the PWI TCP, from domestic universities every year. The proposals are reviewed by the PWI technical committee whose members are domestic senior researchers in universities, QST, and NIFS, and some of the proposals are approved. Proponents of the approved collaborative research go to foreign institutes with support from NIFS and conduct the studies.

In this fiscal year, a collaboration on PWI experimentation was conducted.



Main Plasma-Wall Interaction facilities in member countries

Observation of Spontaneous Arcing on Tungsten Surface Structure by High-Density Plasma Irradiation with Impurity Gas

D. Hwangbo (University of Tsukuba)

Impurity gases used for cooling in the divertor region have recently been found to mix with helium (He) plasma to form nano-structure bundles (NTBs) on a tungsten (W) surface, i.e., protruding structures with a length of more than 100 m. Isolated protrusions of NTBs are a source of field electron emission in high-density plasmas. In particular, under the sheath electric field that soars in high-density plasma, there is a very high possibility of generating spontaneous arcing, even in the absence of an external heat load supply. In this study, we conducted experiments at DIFFER in the Netherlands from February to March 2023 to clarify the relationship between the frequency of arcing and the surface topography of a sample by adjusting the electric potential of the sample placed in a high-density plasma.

(S. Masuzaki)



IEA (International Energy Agency) Technology Collaboration Programme for Cooperation in Development of the Stellarator-Heliotron (SH) Concept (“IEA SH-TCP”)

Highlight

The restrictions put in place by Covid-19 have been relaxed, and direct international collaboration has been reinstated

The objective of the Stellarator-Heliotron Technology Collaboration Programme (TCP) is to improve the physical basis of the Stellarator-Heliotron concept and to increase the effectiveness and productivity of research and development efforts related to that concept by strengthening cooperation among IEA Member Countries. The cooperation program will consist of the following activities: exchange of information; dispatch of experts to facilities or research groups of the Parties; joint planning and coordination of experimental programs in specific fields; workshops, seminars, and symposia; joint theoretical design and systems studies; exchange of computer codes; joint experiments.

The various activity restriction measures taken to prevent the spread of Covid-19 beginning in 2020 were hampering not only the execution of direct international collaborative research, which is the main activity of the IEA SH-TCP but also the research activities of each country. However, with the start of 2022, the restrictions on Covid-19 in each country were significantly relaxed. For example, the easing of the limit on the number of people in the control room has made it easier to conduct and participate in face-to-face experiments. As a result, active international exchange is returning, and it is expected that the SH TCP will once again become more active in the future.

Major achievements in 2022–2023

Significant events in the IEA SH-TCP from 2022 to 2023 include: (1) the completion of the Large Helical Device (LHD) project, which has been carried out since FY2012 as part of the Ministry of Education, Culture, Sports, Science and Technology (MEXT) Large-Scale Academic Frontier Promotion Project. In conjunction with this, the last deuterium experiment was performed at the LHD, and the experiment was safely completed; (2) experiments were resumed and completed at W7-X in Germany, where numerous improvements were made, including the installation of forced cooling divertors for high-heat fluxes. It is also worth mentioning that, as highlighted above, the relaxation of various regulations by Covid-19 that started in 2020 in multiple countries has made it possible to conduct and participate in experiments face-to-face, and active international exchanges are returning.

At the LHD, the 24th cycle experiment was initially scheduled to be conducted from the end of September 2022 to the beginning of February 2023. However, due to the rising cost of electricity, the duration of the experiment had to be shortened, and the experiment was terminated at the end of 2022. Although the period of the experiment was shortened, experiments to clarify isotope effects in helical plasmas were steadily conducted in both hydrogen and deuterium plasmas. The analysis results are expected to be presented at important international conferences scheduled in the future, for example, IAEA FEC2023. At Heliotron J at Kyoto University in Japan, plasma experiments were conducted as usual, focusing on control of structure formation and improvement of transport based on the detailed control of magnetic configuration, and various international joint experiments

were carried out. In W7-X, after about three years of extensive modifications, experiments resumed, and the plasma experiment phase OP2.1 was conducted. W7-X succeeded in producing plasma with an average heating power of 2.7 MW and a plasma duration of 480 s, i.e., 1.3 GJ of injection energy. This is 17 times higher than the previous record by W7-X. These results will also be presented at important international conferences, such as IAEA FEC2023, scheduled shortly.

Summary of 51st S-H TCP executive committee meeting

The 51st Executive Committee (ExCo) meeting of the S-H TCP was held on June 21, 2022, in Warsaw, Poland, during the following 23rd International Stellarator-Heliotron Workshop (ISHW), with hybrid face-to-face and remote participation. The meeting discussed the status of SH TCP legal document amendments, reports from the Fusion Power Coordinated Committee (FPCC), additional TCP members such as Costa Rica and sponsoring members, and the timing and location of the 24th ISHW.

23rd International Stellarator-Heliotron Workshop (ISHW)

The 23rd International Stellarator-Heliotron Workshop (ISHW), postponed due to Covid-19, was held in Warsaw, Poland, from June 20 to 24, 2022, hosted by the Institute of Plasma Physics and Laser Microfusion (IPPLM). Due to the easing of Covid-19 travel restrictions in Europe, the workshop was held in person. Still, for those unable to come to Warsaw, Poland, there was an opportunity to participate remotely for various reasons. The topics of this workshop were: 3D effects on transport and confinement; impurity sources and transport; plasma edge physics and plasma wall interaction; energetic particles, MHD, and plasma stability; theory and simulation; energy, particle, and momentum transport; stellarator and heliotron reactor design studies, and 3D effects in tokamaks and reversed field pinches. The total number of participants in the workshop was just over 130, mainly from Europe, with seven from Japan. The number of participants from Japan was minimal compared to previous workshops. This may have been because the easing of Covid-19 travel restrictions in Europe was recently concluded, and Poland is a neighbor of Ukraine, a country at war with Russia.

There were 29 invited talks, 16 oral talks, and 67 poster presentations at the workshop, including six invited talks from Japan (five from NIFS and one from Kyoto University). Four invited talks reported the latest experimental results from the LHD, including the initial results of the He beam injection experiments in LHD by N. Tamura (NIFS). Also, five invited talks reported on stellarator optimization, including one from H. Yamaguchi (NIFS). In this workshop, a student poster award was given to three young researchers. The next ISHW will be held in Hiroshima, Japan, in 2024.

22nd Coordinated Working Group Meeting (CWGM)

The 22nd Coordinated Working Group Meeting (CWGM) was held on June 24, 2022, in Warsaw, Poland, following the 23rd ISHW. The CWGM, like the ISHW, was a hybrid of face-to-face and remote participation, and because it was held right after the ISHW, it was shorter than the regular CWGM. The meeting was also held as an international seminar of the Japan Society for the Promotion of Science (JSPS) Core-to-Core Program “Advanced Core-to-Core Network for High-Temperature Plasma Dynamics and Structure Formation Based on Magnetic Field Diversity (PLADyS)”, in which the Institute of Energy Science and Engineering, Kyoto University, serves as the Japanese base institution. A. Dinklage (IPP) introduced the status of the CWGM, which had been temporarily suspended due to Covid-19, as well as expected future joint experiments. Next, Y. Suzuki (Hiroshima Univ.) and S. Inagaki (Kyoto Univ.) remotely introduced the concept of the META-stellarator and experiments for it. Finally, the plans for each country’s experiment device (LHD, W7-X, TJ-II, Heliotron J and HSX) for FY2022 were introduced, and the possibility of international joint experiments was discussed. The next CWGM will be held in Kyoto, and a concrete action plan for the CWGM will be discussed remotely before the next meeting.

(N. Tamura, K. Ida and K. Nagasaki (Kyoto Univ.))

Japan–China Collaboration for Fusion Research (Post–CUP Collaboration)

I. Post–CUP collaboration

The post-Core University Program (Post-CUP) collaboration is motivated by cooperation on fusion research with institutes and universities in China including the Institute of Plasma Physics Chinese Academy of Science (ASIPP), Southwestern Institute of Physics (SWIP), Peking University, the Southwestern Jiaotong University (SWJTU), Huazhong University of Science and Technology (HUST) and other universities both in Japan and China. The Post-CUP collaboration is carried out for both studies on plasma physics and fusion engineering. Based on the following implementation system, the Post-CUP collaboration in FY 2022 was executed.

Table 1 Implementation system of Japan-China collaboration for fusion research

Category	① Plasma experiment				② Theory and simulation	③ Fusion engineering research
Subcategory	①-1	①-2	①-3	①-4	—	—
Operator	A. Shimizu	Y. Yoshimura/ H. Takahashi	M. Isobe	T. Oishi/ M. Goto	G. Kawamura	T. Tanaka

①-1: Configuration optimization, transport, and magnetohydrodynamics, ①-2: Plasma heating and steady-state physics, ①-3: Energetic particles and plasma diagnostics, ①-4: Edge plasma and divertor physics, and atomic process

II. Primary research activities of collaboration in FY 2022

The fifth Steering Committee meeting for the NIFS-SWJTU joint project for the CFQS quasi-axisymmetric stellarator, was held on Dec. 9, 2022 online, as shown in Fig. 1. The progress of engineering design, current status of the construction of modular coils (MCs), and the vacuum vessel (VV) were reviewed [1]. At this time, in a total of 16 MCs, the first vacuum pressure impregnation (VPI) process of 15 MCs, and the second VPI of four MCs



Fig. 1 The fifth Steering Committee meeting of the NIFS-SWJTU joint project for CFQS held on Dec. 9, 2022 online. Top left, top right, and bottom pictures show participants from NIFS, Hefei Keye, and SWJTU, respectively.

have been finished. For the VV, the manufacturing of the first quarter toroidal section was finished and its vacuum leak test was in progress. The first plasma will be produced in 2024 in a condition of 0.1 T operation.

In research on energetic particles, the results of joint experiments in the Large Helical Device (LHD) were summarized as an invited talk in the Asia-Pacific Conference on Plasma Physics 2022 [2]. NIFS and ASIPP performed experiments to study the classical confinement of beam ions in EAST by means of short pulse neutral beam injection (NBI) in July 2022. Also, NIFS and ASIPP have been discussing implementation of collaborative research to measure lost energetic ions for EAST and BEST. Development of a gamma ray spectrometer with Compton suppression on the HL-2A tokamak was published as a joint outcome between NIFS and SWIP [3]. NIFS and SWIP have been discussing the design of neutral particle analyzers in HL-2M for phase space resolved measurement of energetic particles.

In research on plasma heating, the property of second harmonic ECCD with 54.5 GHz and 400 kW was investigated for the CFQS physics experiments. According to TRAVIS calculations with proper profiles of T_e and n_e , more than 30 kA of EC-driven currents, which is larger than the expected neoclassical bootstrap current (BSC) of 26 kA, was obtained in a standard QAS configuration and even in an extreme one with $\pm 20\%$ magnetic field ripples [4]. Thus, it is confirmed that at least in absolute value, sufficient EC-driven current will be available to compensate for the possible BSC. As for collaboration on NBI, NIFS accepted two internship students from the University of Science and Technology of China. One of them has been working on the COMSOL simulation relevant to the production and spatial distribution of n_e and T_e in a RF ion source, and the other student has been analyzing the beamlet profiles from experimental data. The NIFS NBI group also had a meeting with the SWIP NBI one to discuss and plan next year's DC-RF hybrid ion sources constructed at SWIP and NIFS.

In research on edge and divertor plasmas, collaborative work on extreme ultraviolet (EUV) and vacuum ultraviolet (VUV) spectroscopy has progressed. The emission line spectra of intrinsic impurities in the wavelength range of 5-2400 Å were identified in detail at the LHD. The EUV spectrometers developed at the LHD have been installed and are still in operation at EAST and HL-2A, and discussions have been initiated for comparison studies with the intrinsic and externally injected impurity spectra measured at those devices.

In research on theory and simulation, two collaborative papers were published. A multiscale particle simulation model was developed based on the Particle-in-Cell (PIC) simulation codes PICS1 and PICS2, and the transient heat load during an ELM pulse was investigated [5]. Heat flux deposition around the leading edge of castellated divertor blocks in KSTAR was investigated with the PIC simulation code PICS2 [6].

- [1] CFQS TEAM, “NIFS-SWJTU JOINT PROJECT FOR CFQS – PHYSICS AND ENGINEERING DESIGN – VER. 5.0.” December, 2022.
- [2] K. Ogawa, H. Nuga, R. Seki, J. Jo, G.Q. Zhong, Y.P. Zhang, S. Sangaroon *et al.*, “Progress in energetic particle confinement research in the Large Helical Device deuterium experiments using integrated neutron diagnostics”, 6th Asia-Pacific Conference on Plasma Physics on-line e-conference, Oct 9–14, 2022 (AAPPS-DPP2022), MF1-I27.
- [3] Y.P. Zhang, J. Zhang, S.K. Cheng, J.J. Zhu, M. Isobe, P.F. Zhang, G.L. Yuan *et al.*, “A gamma ray spectrometer with Compton suppression on the HL-2A tokamak”, *Review of Scientific Instruments* **93**, 123509 (2022).
- [4] Y. Yoshimura, M. Kanda, R. Yanai, A. Shimizu, S. Kinoshita, M. Isobe, S. Okamura, K. Ogawa, H. Takahashi, T. Murase, S. Nakagawa, H. Tanoue, H.F. Liu, and Y. Xu, “Investigation of Capability of Current Control by Electron Cyclotron Waves in the Quasiasymmetric Stellarator CFQS”, *Plasma and Fusion Research* **17**, 2402039 (2022).
- [5] G. Niu, G. Kawamura, S. Dai, Q. Xu, T. He, F. Nian *et al.*, “Multiscale particle simulation of the temporal evolution of heat flux into poloidal gaps of castellated divertor with edge-localized modes” *Nuclear Fusion*, **63**, 066036 (2023).
- [6] Q. Xu, G. Kawamura, E. Bang, Z. Yang, G. Niu, F. Ding, S. Hong, and G. Luo, “Heat load inside the gaps of castellated tungsten blocks with different shapes in KSTAR”, *Nuclear Materials and Energy* **34**, 101390 (2023).

(M. Isobe, A. Shimizu, K. Tsumori, H. Takahashi, K. Ogawa, T. Oishi, M. Goto and G. Kawamura)

Japan-Korea Fusion Collaboration Programs

FY 2022 Japan-Korea Diagnostics Collaboration

Japan and Korea have been collaborating on the development of plasma diagnostics since 2004. The topics have included Thomson scattering, ECE, CXS, bolometer, energetic ion and neutron diagnostics, ECEI and RF diagnostics, SXCCD and VUV cameras and automated integrated data analysis. On January 26th – 27th, 2023, Prof. Peterson visited NFRI in Korea and we held a hybrid meeting to discuss the collaboration (See Figure 1). There were approximately 10 participants from each country.



Fig. 1 Image from hybrid meeting regarding the Japan-Korea diagnostics collaboration.

Time-resolved triton burnup study in KSTAR

Further analysis was carried out of triton burnup experiments performed in FY2020 and 2021 in the relatively high I_p condition using a Sci-Fi detector developed under the Japan-Korea collaboration. A higher triton burnup ratio was obtained in the off-axis ECRH case (shot # 30287) compared to the on-axis ECRH case (shot # 30285) as seen in Figure 2. The amplitude of the MHD instabilities was suppressed in the off-axis ECRH case, indicating that triton transport due to MHD instabilities is reduced.

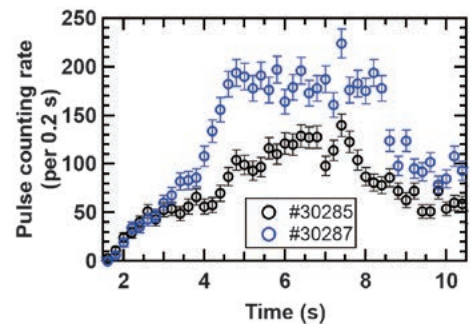


Fig. 2 Time evolution of D-T neutron counts by the Sci-Fi detector.

Real-time Thomson scattering diagnostics on KSTAR and LHD

The real-time Thomson scattering system on KSTAR provides the electron temperature data to the PCS (plasma control system). The fast digitizers produced by CAEN are used. The GPU system is used for the signal processing with Fourier transformation in the signal fitting and the neural network calculation of the electron temperature. Real-time measurement on LHD with digitizers from TechnoAP started on November 2022. Real-time display of electron density and temperature profiles was made possible. The data were transferred to the ASTI (Data Assimilation system), which is developed by S. Murakami and Y. Morishita (Kyoto University). The following problems remained and discussion with the KFE group was useful for resolving them: (1) Data transfer time between the digitizers and the analysis PC: The multi-thread processing for each digitizer will be tried in the next LHD experiment. (2) Excluding noise components mainly due to the digitizer: Detailed discussions were

made about the errors and the fitting methods.

10th Korea-Japan Seminar on Advanced Diagnostics for Steady-State Fusion Plasmas

On the 15th and 16th of September, 2022 Seoul National University hosted the 10th Korea-Japan Seminar on Advanced Diagnostics for Steady-State Fusion Plasmas online. There were 9 lectures from Korean Scientists, 8 lectures from Japanese experts and one lecture from a scientist in the United States of America. The number of students attending the seminar were 20 from Japan and 19 from South Korea, some of whom can be seen in Figure 3.

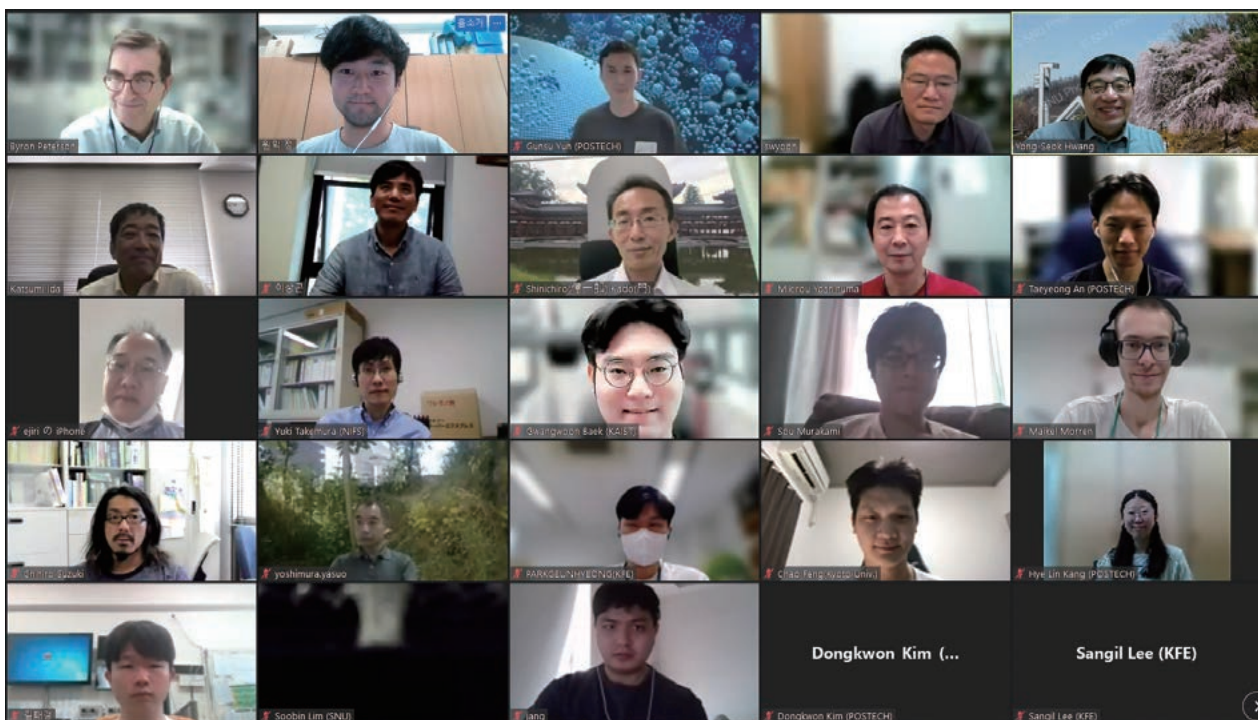


Fig. 3 Screen image of 10th Korea-Japan Seminar on Advanced Diagnostics for Steady-State Fusion Plasmas held online September 15th – 16th, 2022 and hosted by Seoul National University.

- [1] Yamada, H. Funaba, J. H. Lee, Y. Huang, and C. Liu, “Neural Network Data Analysis in the Large Helical Device Thomson Scattering System”, *Plasma and Fusion Research* **17**, pp. 2402061-1–2402061-4 (2022).
- [2] H. Funaba, I. Yamada, R. Yasuhara, H. Uehara, H. Tojo, E. Yatsuka, J.H. Lee, and Y. Huang, “Fast Signal Modeling for Thomson Scattering Diagnostics and Effects on Electron Temperature Evaluation”, *Plasma and Fusion Research* **17**, pp. 2402032-1–2402032-4 (2022).
- [3] K. Ogawa, M. Isobe, S. Kamio, H. Nuga, R. Seki, S. Sangaroon, H. Yamaguchi, Y. Fujiwara, E. Takada, S. Murakami, J. Jo, Y. Takemura, H. Sakai, K. Tanaka, T. Tokuzawa, R. Yasuhara, and M. Osakabe, “Studies of energetic particle transport induced by multiple Alfvén eigenmodes using neutron and escaping energetic particle diagnostics in Large Helical Device deuterium plasmas”, *Nuclear Fusion* **62**, 112001 (2022).

(B. Peterson, I. Yamada and K. Ogawa)

14. Division of External Affairs

The Division of External Affairs, as a core organization responsible for public relations and outreach activities, promotes “dialogue” with society, including the local area, through a variety of activities. The organization underwent a review in 2019 and consists of five offices: the Society Cooperation Office, the Content Production Office, the Event Planning Office, the Public Relations and Tour Guide Office, and the Outreach Promotion Office. A summary of the offices is depicted in Fig. 1. Many NIFS staff are active as members of the department. Its main activities are : holding online tours of the facilities (Fig. 2), providing on-site tours of NIFS facilities (Fig. 3), and science classroom activities (Fig. 4). Face-to-face activities have been limited due to COVID-19, but new activities online have been initiated.



Fig. 1 Organization chart of Division of External Affairs

Activities held in 2022 include the following.

- Tours of NIFS facilities (any time) held 288 times; 2,177 people participated
- Open academic lectures and tours of the facilities for the public, held online
- Science classroom activities, held 19 times
- Release of information through web pages, mailing lists, and SNS (X and Facebook)
- Publication of NIFS official pamphlet (in Japanese and English)
- Publication of public relations magazine: NIFS News (3 issues) (Fig. 5)
- Publication of public relations magazine: Letters from Helica-chan (4 issues)



Fig. 2 Online tours of the NIFS facilities



Fig. 3 Tour of the NIFS facilities



Fig. 4 Science classroom



Fig. 5 Public relations magazine: NIFS News

15. Department of Engineering and Technical Services

The Department of Engineering and Technical Services is involved in the operation and maintenance of research platforms such as the Large Helical Device (LHD) and information facilities such as the research infrastructure network, as well as the design, development, and fabrication of equipment, radiation control, and safety promotion. The Department of Engineering and Technical Services contributes greatly to the creation of results in fusion research through advanced and specialized technical support. The department consists of five divisions, and the total number of staff is now 56 (2022).

And as shown in Chapter 6, the 2022 NIFS External Peer Review Committee conducted an external evaluation of the “Department of Engineering and Technical Services.”

(H. Hayashi)

1. Fabrication Technology Division

The main work of this division is the fabrication of experimental equipment. We also take care of technical consultation and experimental parts supplies related to the LHD experiment. In addition, we manage the administrative procedures of the department.

The number of machined requests was 76, and the production parts total number was 278 in this fiscal year (FY). The total numbers of electronic engineering requests and articles were 13 and 22, respectively. The details of some of this division’s activities follow below.

(M. Yokota)

(1) 2.5-inch corrugated miter bend for microwave at a frequency of 70–330 GHz

We have fabricated 22 corrugated miter bends (Fig. 1). The miter bend is a component of a vacuum waveguide system that is installed in part of the 90-degree bend. In order to improve the transmission efficiency of a 2.5-inch corrugated waveguide, it is necessary to cut corrugated slots on the surface of the inside diameter of the miter bend. The parameters of the rectangular corrugation are a width of 0.3 mm, a depth of 0.3 mm, and a period length of 0.46 mm. These are going to be used in joint research with QST.

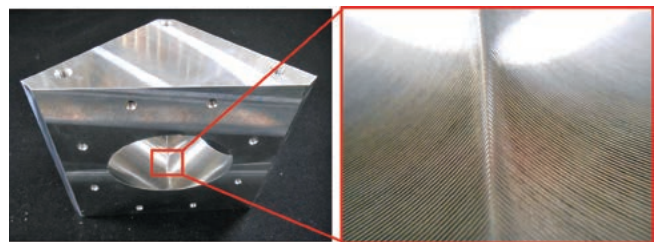


Fig. 1 2.5-inch corrugated miter bend

(K. Okada)

(2) 74.6 GHz Notch filter

We have fabricated a Notch filter (Fig. 2) for CTS. It has 24 cavities and an internal waveguide.

In order to determine a parameter of the cavity, we have analyzed the electromagnetic field. The cavity has a diameter of 3.0 mm and a depth of 3.05 mm to 3.10 mm. The rectangular waveguide has a length of 3.10 mm and a width of 1.55 mm.

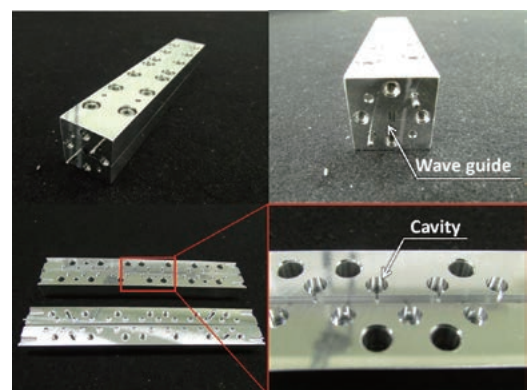


Fig. 2 74.6 GHz Notch filter

(T. Shimizu)

(3) Improvement of a 35-channel PN photodiode array amplifier

A 35-channel PN photodiode array amplifier is used to amplify the emission spectral signal when solid hydrogen pellets melt in plasma (Fig. 3). By dividing the previously constructed amplifier circuit board into separate boards for each of the two channels, we were able to reduce the noise by half.

(Y. Ito)

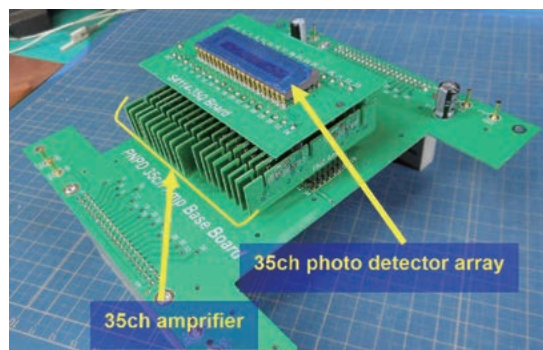


Fig. 3 35-channel PN photo diode array amplifier

(4) 16-channel level converter

We made a 16-channel level converter (Fig. 4). The vertical column is one channel, and each channel is implemented on an independent board with a shared power supply.

Each channel has voltage input, contact input, voltage output, and contact output from top to bottom. An internal switch changes the output between inverted and non-inverted.

(H. Furuta)

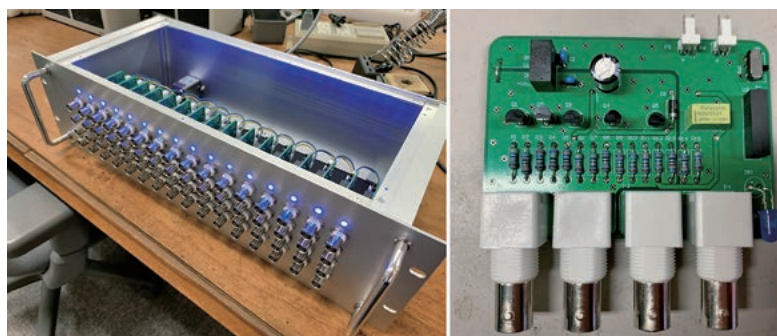


Fig. 4 16-channel level converter

2. Device Technology Division

This Division provides support for the operation, improvement, and maintenance of the LHD, as well as support for collaborative and commissioned research.

(1) LHD operation

We started pumping a cryostat vessel for cryogenic components on August 10, 2022, and a plasma vacuum vessel on August 12, 2022. Subsequently, we checked for air leakage from the maintained flanges installed on the plasma vacuum vessel. As a result, we found leakage at a gate valve and repaired it.

The vacuum pressure of the cryostat vessel reached an adiabatic condition ($< 2 \times 10^{-2}$ Pa) on August 12, 2022, and the vacuum pressure of the plasma vacuum vessel was below 1×10^{-5} Pa on August 30, 2022.

The 24th LHD experimental campaign started on September 29, 2022, and was carried out until December 27, 2022. The total number of days of the plasma experiments was 53.

During this experimental campaign, the vacuum pumping system and the LHD utilities (for example, compressed air, water cooling, and GN₂-supply systems) continued operating without problems. The 24th LHD operation was completed on January 27, 2023.

(N. Suzuki)

(2) Technical cooperation with universities and research institutions

We provided technical cooperation to universities and research institutions through numerical analysis and instrument development. An example of our achievement is shown below.

Based on the request of the Research Institute for Applied Mechanics at Kyushu University, we calculated the electromagnetic force generated on aluminum bus bars when the current for magnetic field coils flows through the bus bars installed in QUEST. The calculation was performed by the finite element analysis software ANSYS. An example of the analysis result is shown in Fig. 5. Based on the result of this analysis, we recommended that the material of the supporting structure for the aluminum bus bars be changed from SS400 to SUS.

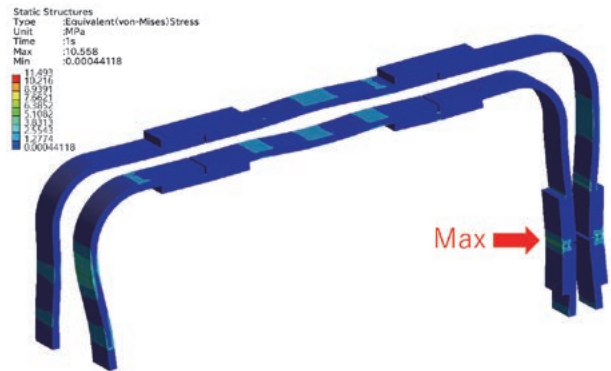


Fig. 5 Example of electromagnetic force analysis results for aluminum bus bars

(N. Suzuki and Y. Yanagihara)

(3) Development of an Electrostatic Deflector in a New Negative Ion Source for a Heavy Ion Beam Probe

Plasma potential, which is an important parameter for studying plasma, can be measured by a Heavy Ion Beam Probe (HIBP). A new ion source has been developed and installed in the actual HIBP to enable measurement even in high-density regions of plasma. Although the beam current was increased from 23 μA to 45 μA compared to the old ion source, it could not reach the target of 100 μA . The reason for the lack of current was found to be that the beam was off-center by about 6 mm from the short-tube center by measuring the beam profile. Therefore, we fabricated a new electrostatic deflector and installed it to adjust the beam alignment. The 3D-CAD drawing and photo of the electrostatic deflector are shown in Fig. 6. As a result of the modification, the effective beam current increased by about 1.38 times.

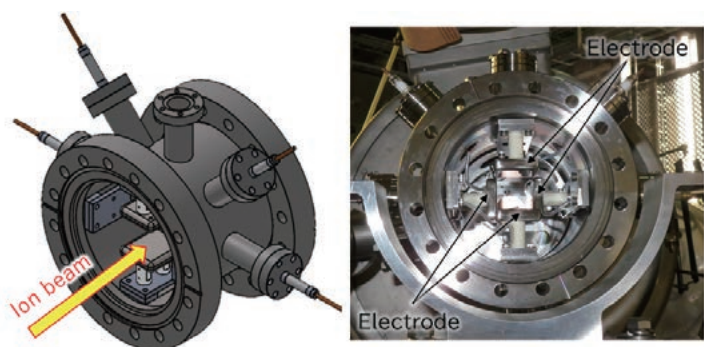


Fig. 6 Electrostatic Deflector for HIBP

(H. Takubo)

3. Plasma Heating Technology Division

The main tasks of this division are the operation and maintenance of three different types of plasma heating devices and their common facilities. We have also provided technical support for improving, developing, and newly installing these devices. In this fiscal year, we mainly carried out device improvement and modification for the LHD plasma experiment and common facilities. The details of these activities are as follows.

(T. Kondo)

(1) ECH

During the 24th experimental campaign, we injected power up to 5 MW to assist plasma experiments. That contributed to the high performance of plasma with high ion and electron temperatures. Low power and long pulse injections could sustain the ECH plasma. One of the 77 GHz gyrotrons did not work well because of minor damage to the ceramic insulator for the hot cathode. Its operation was difficult because the electron beam current was unstable.

(Y. Mizuno)

(2) ICH

(a) The operation of ICH in the 24th experimental campaign of LHD experiments

In this campaign, we carried out the LHD experiment in total with two antennas with four antenna straps, that is, the HAS (Handshake type) antenna with two antenna straps at the 3.5U&L ports and the FAIT (Field-Aligned Impedance-Transforming) antenna with two antenna straps at the 4.5U&L ports of the LHD.

We decided on the combination of an RF transmitter and an antenna strap. Then the transmitters of #3 and #4 were connected to the 3.5U&L antenna straps, and the transmitters of #6A and #5B were connected to the 4.5U&L antenna straps. The total injection power from the four antenna straps into the plasma reached about 3.35 MW in a short pulse of four seconds at an RF wave frequency of 38.47 MHz.

(b) Installation of magnetostrictive type silicon oil level sensors for liquid stub tuners

A differential pressure gauge had been used to measure the oil level inside a liquid stub tuner until the 23rd cycle experiment. However, several noise problems caused by plasma discharge caused an error in the oil level measurement of up to 200 mm. In the 24th cycle experiment, magnetostrictive type oil level sensors were installed in oil tanks and, as a result, could measure the oil level without problems during plasma discharge.

(G. Nomura and M. Kanda)

(3) NBI

(a) The operation of NBI in the 24th campaign of LHD experiments

In this campaign, approximately 8,000 shots of beams were injected into LHD plasmas with three negative-NBIs (BL1, BL2, and BL3). The maximum injection power in this campaign was about 12 MW. As for positive-NBIs (BL4 and BL5), the maximum total injection power was about 18 MW. The NBIs had a few problems. For example, BL1 had a water leak in the extraction grids for ion sources and had to be injected with one out of two ion sources in the last two weeks of this campaign, and BL3 had a failure of a roughing vacuum pump.

(b) Installation of the small cooling water pumps for electric power savings

The NBI test facility has a 250 kW cooling water pump for the NBI heat load. While the cryopump is running, the cooling water pump cannot be stopped because the liquid nitrogen for the cryopump freezes the water inside the cooling pipes near the cryopump. The night electric power had been too much, so we added a 22 kW pump only for the cryopump operation at night. This small cooling water pump reduced electric power by about 70% compared with the past.

(M. Sato and M. Shibuya)



Fig. 7 Cooling water pumps

(4) Motor-Generator (MG) and cooling water facility for plasma heating devices

(a) MG

An MG is used to supply pulsed power to the NBI and the ECH for the LHD. The MG has supplied power for 15,794 shots in this fiscal year and 710,258 shots since its construction. The operation time was 864 hours.

(b) Cooling water facility

Three pump motors had been factory refurbished. The overhaul maintenance for pump motors, which has continued since last year, is over.

(Y. Mizuno)

4. Diagnostics Technology Division

Some plasma diagnostics devices have functioned for more than 20 years and thus require maintenance. This division mainly supports the operation, maintenance, and development of plasma diagnostics devices and radiation measurement devices for the LHD. In the LHD experimental campaign, we operated the diagnostics shutter system on experimental days. In addition, we have taken charge of radiation control.

(T. Kobuchi)

(1) Plasma diagnostic device

We supported the fast Thomson scattering diagnostic that measures the electron temperature and density in the LHD plasma. We have started up and shut down the operation of the system and changed its settings. We have also adjusted the schedule of measurement requests.

(H. Hashimoto)

(2) LHD data acquisition (DAQ) system

In the 24th LHD experimental campaign, the LHD DAQ system acquired data for about 8,000 plasma shots, and the total data generated was approximately 292 TB in compressed size. During the campaign, two DAQ PCs failed, and we responded by replacing one with a new computer and the other with a new storage disk. In addition, several DAQ PCs were migrated from Windows to Linux operating systems. Since this will lead to cost reduction, we plan to migrate them one by one in the future. The remaining capacity of the optical disks for long-term storage is about 30 TB, so it will be necessary to switch to new media for the next campaign.

(M. Ohsuna)

(3) Fusion Diagnostics Data Repository System and NIFS Article Information System (NAIS) development

We have developed a worldwide web system to publish raw data acquired in LHD plasma experiments. This system allows users to view and download the data via the Internet. Fig. 8 and Fig. 9 show search pages for acquired LHD experimental data.

To log in to the NIFS Article Information System (NAIS), you used to need this system account. But we have

LHD : Search for Acquired Shot Data

The screenshot shows a web form titled "LHD : Search for Acquired Shot Data". It contains the following fields and controls:

- Diagnostic name:** A dropdown menu with a downward arrow and the text "Select from the list." to its right.
- Shot number:** A text input field with the label "Enter start/end number(s): (default: 0 -- last)". Below it, there are two smaller input fields labeled "From" and "to" with a right-pointing arrow between them.
- Media type:** Two radio buttons, one labeled "RAID Disk" (which is selected) and one labeled "Any".
- Buttons:** Two buttons labeled "Query" and "Reset" are positioned at the bottom right of the form.
- Footnote:** A small note below the shot number fields reads "[The number of results is limited by 10000.]".

Fig. 8 Searching page for acquired shot data

introduced Shibboleth authentication to achieve a single sign-in. Therefore, users can log in with an account that is common to other systems.

(Link: <https://nais.nifs.ac.jp/article/center>)

(M. Nonomura)

LHD : Search for Acquired Diagnostic Data

Fig. 9 Searching page for acquired diagnostic data

(4) Radiation control

In order to control the safety of radioactivity, we carried out the operation and maintenance of three high-purity germanium (HPGe) detectors, seven liquid scintillation counters, a 2π gas-flow counter, and an auto well gamma system.

The concentration of drainage water, which is generated in the radiation controlled area, is measured using a liquid scintillation counter and an auto well gamma system. After confirming that the radioactivity concentration of drainage water is below the management value of NIFS, it is discharged. In the 2022 fiscal year, the radioactivity concentration of drainage water was measured 45 times.

To assess the impact of the deuterium experiments, we monitored the environmental radiation in the atmosphere, depositions, and river water. Among these results, the ^7Be concentrations in atmospheric aerosols and depositions from January 2014 to January 2023 showed that there was no impact on the surrounding environment due to the deuterium experiments, because the concentrations were within the range of environmental variations and ranged as other locations near NIFS.

Furthermore, atmospheric tritiated water vapor (HTO) has been collected every month by using a passive-type sampler since June 2015. The results of monitoring suggested that there were no clear experimental impacts in the vicinity of NIFS.

These monitoring reports were presented at the 24th Environmental Radiology Conference held at the High Energy Accelerator Research Organization in March 2023.

(M. Nakada, S. Kurita and C. Iwata)

5. Control Technology Division

The Control Technology Division is in charge of the important engineering tasks in the LHD project, such as system development, project management, and system operation, which are mainly targeted at central control systems, cryogenic systems, coil power supply, and super-conducting coils.

We are also responsible for the IT infrastructure, e.g., the LHD experiment network, the NIFS campus information network, and internet servers, in every phase of the project, including requirements analysis, system design, implementation, operation, and user support.

The essential topics of the activities for the last fiscal year are described below.

(T. Inoue)

(1) LHD cryogenic system for superconducting coils

We have been making databases with maintenance information for all components of the LHD cryogenic system since 2020. So far, the database has found some components of the cryogenic system that require replacement. As a result, the cryogenic system operation in the 24th experimental campaign was performed without a significant accident. Fig. 10 shows the operation result. On August 19th, 2022, the He purification operation was

begun. After that, the coil cool-down operation was performed in 607 hours. After approximately three months of plasma experiments, the coil warm-up operation was performed from December 28th to January 18th, 2023. The total operation period of the He compressors was 3628 hours, and their operation rates were 100%.

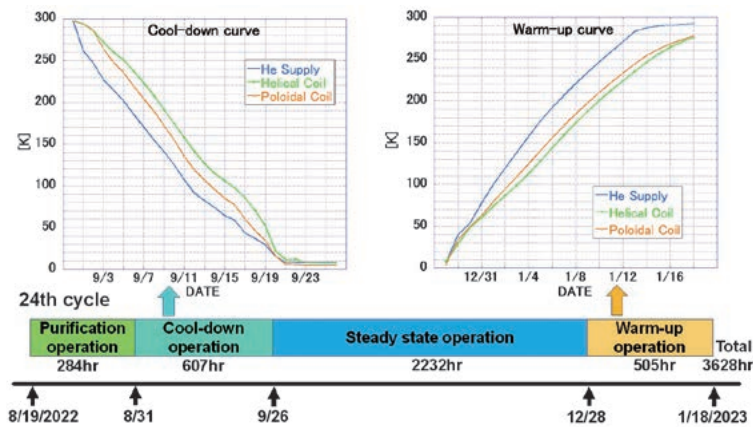


Fig. 10 The operation results of the LHD Cryogenic system for the 24th experimental campaign

(H. Tanoue and H. Noguchi)

(2) Management of utilities at the control building

We are in charge of managing the various utilities installed at the control building.

A 150-inch projector, an audio system, and personal computers for presentation are the most essential utilities for LHD operation and collaboration. And we also maintain a multi-function printer (MFP) for general purposes, four printers for experiment summary output, and a copy machine in the control room (Fig. 11). This fiscal year, the degraded MFP and two printers were updated.

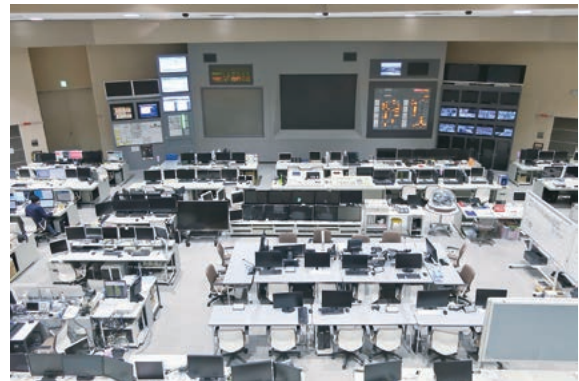


Fig. 11 Overview of the control room

There is a dedicated UPS on the first basement floor. It supplies electric power up to 200kVA/10min stably to the experimental infrastructure systems, such as the LABCOM data acquisition system, the Central Control System, and LHD-LAN devices.

We are responsible for not only device management but also fiscal budget management, user support, and IT system development for efficient administration. We will continue to maintain the control building as a center for research activities.

(H. Ogawa)

(3) Network Management

The NIFS campus information networks consist of several clusters. We manage the Research Information Cluster (NIFS-LAN) and the LHD Experiment Cluster (LHD-LAN).

The achievements in FY 2022 are as follows:

(a) Replacement of the edge switch

The edge switches in a research building, an administration building, and an experimental building have been replaced.

(b) SSL-VPN system update

Updated the SSL-VPN system from PSA5000 (Ivanti) to ISA8000 (Ivanti) (Fig. 12).



Fig. 12 SSL-VPN System

The number of simultaneous connections has been upgraded from 2500 to 25000, and the interface has been upgraded from 1G to 10G. As a security measure, we continued to use two-factor authentication with client certificates.

(c) LHD-LAN

It is required in our security policy that the network management staff be present when connecting a new device to LHD-LAN. In FY2022, 22 new devices were connected to LHD-LAN, 59 devices were updated, and 16 IP addresses were made available due to device removal.

(T. Inoue and O. Nakamura)

6. An external evaluation of the Department of Engineering and Technical Services (DETS)

DETS was externally evaluated by the “2022 NIFS External Peer Review Committee” from the following six perspectives. Overall, we received high ratings of Excellent, outstanding, and Commendable. And we also received many suggestions and comments.

Evaluation perspectives

- 1) Contributed to deuterium experiments in LHD?
- 2) Contributed to the maintenance and utilization of the research platform in NIFS?
- 3) Are safety and health initiatives sufficient?
- 4) As an Inter-University Research Institution, have they conducted technical collaboration, exchange, and cooperation with universities and research institutes?
- 5) Has the technical experience and knowledge accumulated so far been utilized in industry-academia cooperation activities?
- 6) Is there an environment that supports the autonomy of individual technical staff members, together with a systematic effort to improve and pass on techniques?

(H. Hayashi)

7. Mission realization strategy project

The National Institutes of Natural Sciences started the “Mission Realization Strategy Project” in FY2022. The project was invited as a development project with the theme of contributing to the SDGs through the social implementation of fusion technology.

We proposed a six-year project on unutilized biomass as agricultural waste, and as a result of the screening, the project was adopted in June 2022. In this project, we aim to create biomass-derived high-performance activated carbon by utilizing our knowledge of activated carbon through the development of the closed divertor

pumping system and metal bonding and sintering technology.

In FY2022, the experimental environment was improved by installing a tube heating device for carbonizing rice straw and a rotary kiln device (Fig. 13(a)) for the activation process, as well as a spark plasma sintering device (Fig. 13(b)) for conducting silica removal tests. In parallel, research on removing silica from the inside of rice straws was conducted, and as a result, efficient silica removal was successfully achieved using a vacuum heating device. We applied for a domestic patent for this achievement. We also made an oral presentation for our project at the International Symposium “KRIS2023” held by the National Institution of Technology, Japan (Fig. 13(c)). We have also started collaborative research with Walailak University in Thailand for international joint research (Fig. 13(d)).



Fig. 13 (a) Rotary kiln device (b) Spark plasma sintering device (c) Presentation in KRIS2023 (d) Group photo at the visit to Walailak University

(T. Murase)

8. Technical Exchanges

(1) Technical Exchanges to improve technical skills

Technical exchanges between our department and other institutes or universities were held in order to improve the technical skills of the staff. In this FY, we invited Mr. Sugisawa and Mr. Nakajima (Tohoku University) on February 13–16, 2023 (Fig. 14), and Mr. Aida and Mr. Haga (Tohoku University) on February 20–22, 2023 (Fig. 15).

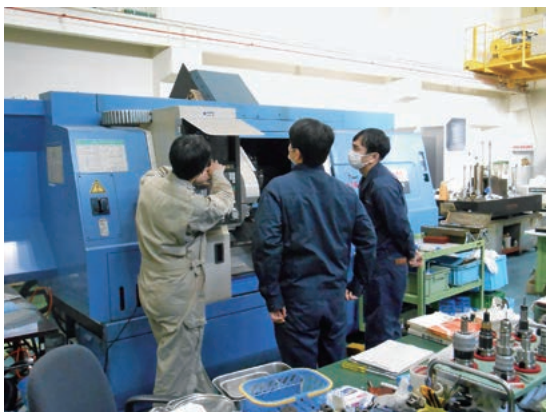


Fig. 14 NC machine



Fig. 15 Measurement and control

(M. Yokota)

(2) Sixth technical exchange meeting: “Computational technology using the finite element method”

On February 17, 2023, we held a technical exchange meeting to discuss numerical computational technology based on the finite element method. This meeting, which was the sixth held hitherto, was attended by seven presenters and 41 participants, including those who used a remote web conference application (ZOOM), as shown in Fig. 16. In this meeting, two invited talks were presented under the titles “Possibilities of Ansys” and “Generation and propagation of electron cyclotron waves in the millimeter wave band with helical wavefronts.” In addition, five general talks were presented, all of which resulted in lively discussions.

(T. Murase)



Fig. 16 Group photos of the technical exchange meeting (a) at the NIFS site and (b) at the ZOOM system

16. Department of Administration

The Department of Administration handles planning and external affairs, general affairs, accounting, research support, and facility management work.

The major operations of this department are to support the promotion of the Institute's regular research and the development of the collaborative research.

The department consists of the following four divisions, namely, the General Affairs Division, the Financial Affairs Division, the Research Support Division, and the Facilities and Safety Management Division. Details of these divisions are described below.

General Affairs Division

The General Affairs Division handles administrative work and serves as the contact point with the outside. This Division consists of four sections. The General Affairs Section is in charge of secretarial work for the Director General and the Deputy Director General, support for the Advisory Committee meetings, and enacting rules and regulations. The Planning and Evaluation Section is in support for assessment of the institution's performance including scientific achievement and management efficiency. The Personnel and Payroll Section is in charge of general personnel affairs, salary, and public welfare. And the Communications and Public Affairs Section focuses on outreach and publicity activities.

Number of Staff Members

Director General	1
Researchers	105
Technical and Engineering Staff	45
Administrative Staff	41
Employee on Annual Salary System	11
Research Administrator Staff	4
Visiting Scientists	0
Total	207

Financial Affairs Division

The Financial Affairs Division consists of six sections: The Audit Section, the Financial Planning Section, the Accounts and Properties Administration Section, the Contracts Section, the Procurement Section, and the Purchase Validation Section.

The major responsibilities of the division are to manage and execute the budget, to manage corporate property, revenue/expenditure, and traveling expenses of staff, and to purchase supplies and receive articles.

The budget is 8,300,000,000 yen. (JFY 2021)

Research Support Division

The Research Support Division consists of four sections and one center. These are the Graduate Student Affairs Section, the Academic Information Section which includes the Library at NIFS, the Research Support Section and the International Collaboration Section, which is in charge of inter-university coordination and arranging international cooperation. The Visitor Center assists collaborating researchers and visitors.

Collaboration Research Programs

	Applications Applied	Applications Accepted	Researchers Accepted
LHD Project Collaboration Research	17	17	214
Joint Research	250	250	2,305
Joint Research Using Computers	79	79	482
Workshops	32	32	1,013
Bilateral Collaboration Research	103	103	1,497
Total	481	481	5,511

Number of Graduate School Students

(SOKENDAI: The Graduate University for Advanced Studies)

Doctoral Course					
Grade 1	Grade 2	Grade 3	Grade 4	Grade 5	Total
3	4	8	3	5	23

(The Joint Program of Graduate Education)

Graduate course education is given in NIFS apart from SOKENDAI in joint programs with the Department of Energy Science and Engineering of the Graduate School at Nagoya University, Division of Particle and Astrophysical Science of the Graduate School of Science at Nagoya University, Division of Quantum Science of the Graduate School of Engineering at Hokkaido University, Department of Energy Science of the Graduate School of Science and Engineering at University of Toyama, Interdisciplinary Graduate School of Engineering Science in Kyushu University and the Graduate School of Engineering at Tohoku University. In total, 34 graduate students are involved in the programs as of March 31, 2021.

The Special Research Collaboration Program for Education

Affiliation	Degree	Bachelor's Course	Master's Course	Doctoral Course	Total
	National Graduate School		5	16	13
Public Graduate School		0	0	0	0
Private Graduate School		0	0	0	0
Total		5	16	13	34

Books and Journals

Books in Japanese	20,457
Books in Other Languages	51,171
Total (volumes)	71,628
Journals in Japanese	283
Journals in Other Languages	844
Total (titles)	1,127

Facilities and Safety Management Division

The Facilities and Safety Management Division consists of three sections: The Safety and Health Management Section, the Facilities Planning Section, and the Facilities Maintenance Section. They are in charge of planning, designing, making contracts, supervising the construction and maintenance of all facilities at NIFS, such as buildings, campus roads, electricity, telephone, power station, air conditioning, water service, gas service, elevators, and cranes. The Facilities and Safety Management Division submits a budget request and administers the budget for those facilities.

The Safety and Health Management Section also arranges medical examination and disaster drills. These three sections promote facilities' environment better for all staff.

Site and Buildings

Toki	
Site	464,445 m ²
Buildings	
Total Building Area	39,557 m ²
Total Floor Space	71,830 m ²

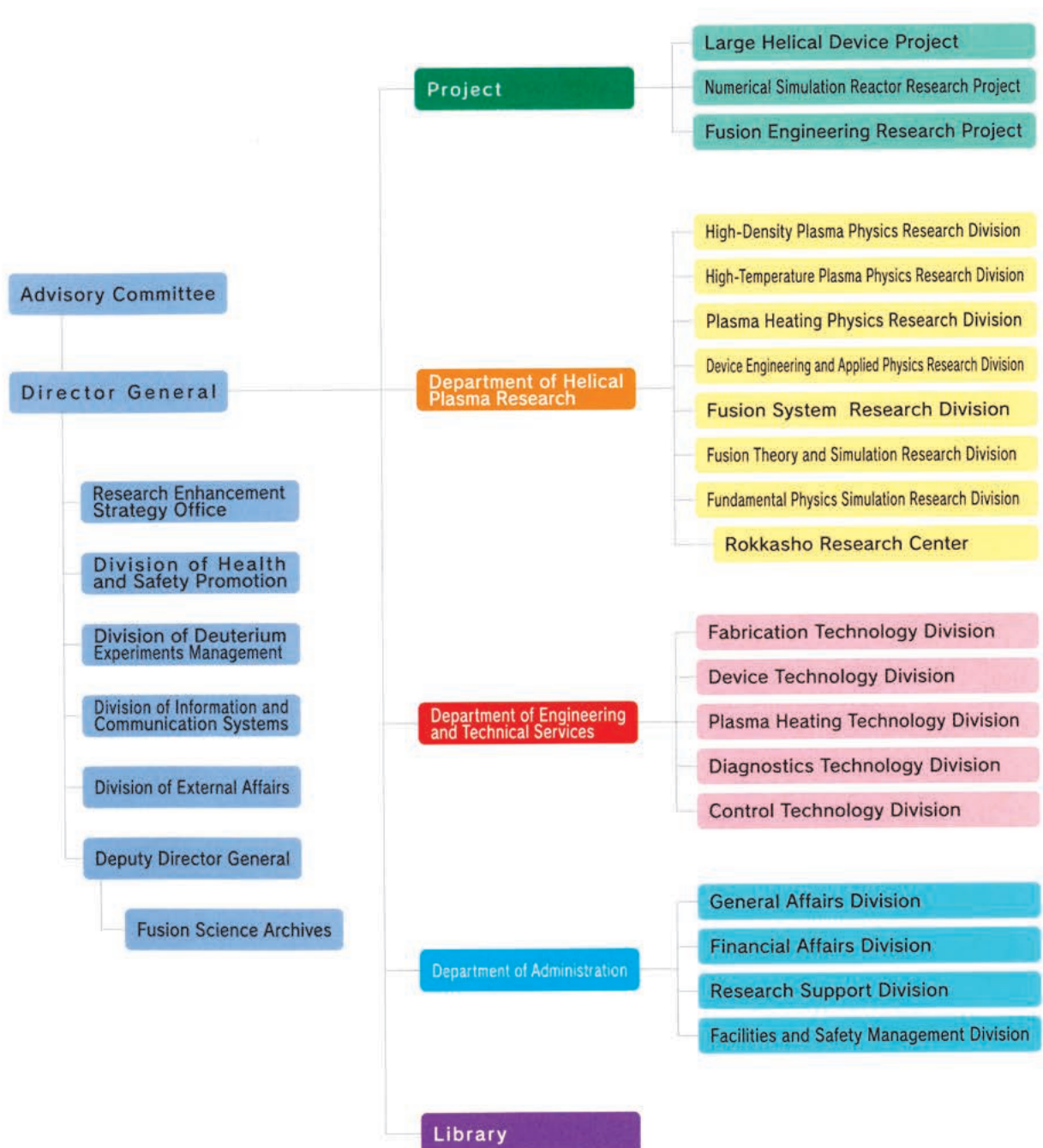
※ All statistical data is as of March 31, 2023

APPENDIX

APPENDIX 1. Organization of the Institute

NATIONAL INSTITUTE for FUSION SCIENCE

Organization



APPENDIX 2. Members of Committees

Advisory Committee

UEDA, Yoshio	Professor Graduate School of Engineering, Osaka University
OHNO, Noriyasu	Professor Graduate School of Engineering, Nagoya University
OZAWA, Tohru	Professor Department of Applied Physics, Waseda University
KANEKO, Toshiro	Professor Graduate School of Engineering, Tohoku University
KISHIMOTO, Yasuaki	Professor Graduate School of Energy Science, Kyoto University
KURIHARA, Kenichi	Managing Director, Fusion Energy Research and Development Directorate, National Institutes for Quantum and Radiological Science and Technology
FUJISAWA, Akihide	Professor Research Institute for Applied Mechanics, Kyushu University
MATSUOKA, Ayako	Professor Graduate School of Science, Kyoto University
YAMADA, Hiroshi	Professor Graduate School of Frontier Sciences, The University of Tokyo
YONEDA, Hitoki	Professor Institute for laser science, The University of Electro-Communications
WATANABE, Tomo-hiko	Professor Department of Physics, Nagoya University

※ This list was compiled as of March 31, 2023

APPENDIX 3. Advisors, Fellows, and Professors Emeritus

Professors Emeritus

ICHIKAWA, Yoshihiko (1993)
MIZUNO, Yukio (1994)
FUJITA, Junji (1996)
KURODA, Tsutomu (1997)
AMANO, Tsuneo (1998)
MOMOTA, Hiromu (1998)
IIYOSHI, Atsuo (1999)
HATORI, Tadatsugu (1999)
TANAHASHI, Shugo (2000)
KAWAMURA, Takaichi (2000)
SATO, Tetsuya (2001)
FUJIWARA, Masami (2002)
KAMIMURA, Tetsuo (2003)
HAMADA, Yasuji (2007)
KATO, Takako (2007)
NODA, Nobuaki (2008)
WATARI, Tetsuo (2008)
MOTOJIMA, Osamu (2009)
SATO, Kohnosuke (2010)
OHYABU, Nobuyoshi (2010)
MATSUOKA, Keisuke (2010)
TOI, Kazuo (2012)
NARIHARA, Kazumichi (2012)
KUMAZAWA, Ryuhei (2012)

UDA, Tatsuhiko (2012)
SATO, Motoyasu (2012)
YAMAZAKI, Kozo (2013)
KAWAHATA, Kazuo (2013)
OKAMURA Shoichi (2014)
KOMORI, Akio (2015)
SUDO, Shigeru (2015)
SKORIC, Milos (2015)
MUTO, Takashi (2016)
NAGAYAMA, Yoshio (2017)
NAKAMURA, Yukio (2017)
SAGARA, Akio (2017)
ITOH, Kimitaka (2017)
HORIUCHI, Ritoku (2017)
HIROOKA, Yoshihiko (2018)
MORITA, Shigeru (2019)
NISHIMURA, Arata (2019)
KUBO, Shin (2020)
MITO, Toshiyuki (2020)
NISHIMURA, Kiyohiko (2020)
ISHIGURO, Seiji (2021)
MUROGA, Takeo (2021)
NAKAJIMA, Noriyoshi (2021)
SHIMOZUMA, Takashi (2021)

※ This list was compiled as of March 31, 2023

APPENDIX 4. List of Staff

Director General

YOSHIDA, Zensho

Deputy Director General

MORISAKI, Tomohiro

Department of Helical Plasma Research

Prof. IDA, Katsumi (Director)

High-Density Plasma Physics Research Division

Prof. SAKAMOTO, Ryuichi

Prof. OHDACHI, Satoshi

Prof. WATANABE, Kiyomasa

Assoc. Prof. KOBAYASHI, Masahiro

Assoc. Prof. MOTOJIMA, Gen

Assoc. Prof. SHOJI, Mamoru

Assoc. Prof. TOKUZAWA, Tokihiko

Assoc. Prof. YOSHIMURA, Shinji

Asst. Prof. NARUSHIMA, Yoshiro

Asst. Prof. TAKEMURA, Yuki

Asst. Prof. NISHIMURA, Shin

Asst. Prof. HAYASHI, Yuki

Asst. Prof. KAWAMOTO, Yasuko

Asst. Prof. GOTO, Yuki

Project Asst. Prof. OHTSUBO, Yohko

High-Temperature Plasma Physics Research Division

Prof. IDA, Katsumi (Director)

Prof. SAKAKIBARA, Satoru

Prof. TANAKA, Kenji

Prof. ISOBE, Mitsutaka

Prof. PETERSON, Byron Jay

Assoc. Prof. GOTO, Motoshi

Assoc. Prof. TAMURA, Naoki

Assoc. Prof. YAMADA, Ichihiko

Assoc. Prof. YASUHARA, Ryo

Assoc. Prof. OZAKI, Tetsuo

Assoc. Prof. NAKANISHI, Hideya

Assoc. Prof. OGAWA, Kunihiro

Asst. Prof. KOBAYASHI, Tatsuya

Asst. Prof. MUTO, Sadatsugu

Asst. Prof. FUNABA, Hisamichi

Asst. Prof. YOSHINUMA, Mikirou

Asst. Prof. SUZUKI, Chihiro

Asst. Prof. SHIMIZU, Akihiro

Asst. Prof. EMOTO, Masahiko

Asst. Prof. MUKAI, Kiyofumi

Asst. Prof. UEHARA, Hiyori

Proj. Res. Staff ZHAO, Mingzhong

Plasma Heating Physics Research Division

Prof. NAGAOKA, Kenichi (Director)

Prof. OSAKABE, Masaki

Prof. TSUMORI, Katsuyoshi

Assoc. Prof. IGAMI, Hiroe

Assoc. Prof. KASAHARA, Hiroshi

Assoc. Prof. NAKANO, Haruhisa

Assoc. Prof. NISHIURA, Masaki

Assoc. Prof. SAITO, Kenji

Assoc. Prof. SEKI, Tetsuo

Assoc. Prof. TAKAHASHI, Hiromi

Assoc. Prof. YOSHIMURA, Yasuo

Asst. Prof. IKEDA, Katsunori

Asst. Prof. KENMOCHI, Naoki

Asst. Prof. NUGA, Hideo

Asst. Prof. SEKI, Ryosuke

Asst. Prof. YANAI Ryohma

Project Asst. Prof. KAWACHI Yuichi

Device Engineering and Applied Physics Research Division

Prof. IMAGAWA, Shinsaku
Prof. HIRANO, Naoki
Prof. TAKAHATA, Kazuya
Prof. YANAGI, Nagato
Assoc. Prof. CHIKARAISHI, Hirotaka
Assoc. Prof. HAMAGUCHI, Shinji
Assoc. Prof. IWAMOTO, Akifumi

Assoc. Prof. SAZE, Takuya
Assoc. Prof. TAKAYAMA, Sadatsugu
Assoc. Prof. TANAKA, Masahiro
Asst. Prof. KOBAYASHI, Makoto
Asst. Prof. OBANA, Tetsuhiro
Asst. Prof. ONODERA, Yuta
Asst. Prof. TAKADA, Suguru

Fusion Systems Research Division

Prof. MURAKAMI, Izumi (Director)
Prof. MASUZAKI, Suguru
Prof. NAGASAKA, Takuya
Assoc. Prof. ASHIKAWA, Naoko
Assoc. Prof. HISHINUMA, Yoshimitsu
Assoc. Prof. KATO, Daiji
Assoc. Prof. TAMURA, Hitoshi
Assoc. Prof. TANAKA, Teruya
Assoc. Prof. TOKITANI, Masayuki

Asst. Prof. GOTO, Takuya
Asst. Prof. HAMAJI, Yukinori
Asst. Prof. KAWATE, Tomoko
Asst. Prof. NOTO, Hiroyuki
Asst. Prof. SAKAUE, Hiroyuki
Asst. Prof. SHEN, Jingjie
Asst. Prof. YAJIMA, Miyuki
Specially Appointed Prof. NAGATA, Daisuke

Fusion Theory and Simulation Research Division

Prof. TODO, Yasushi (Director)
Prof. ICHIGUCHI, Katsuji
Assoc. Prof. KANNO, Ryutaro
Assoc. Prof. MIZUGUCHI, Naoki
Assoc. Prof. NAKATA, Motoki
Assoc. Prof. NUNAMI, Masanori
Assoc. Prof. SATAKE, Shinsuke
Assoc. Prof. TODA, Shinichiro
Asst. Prof. ISHIZAKI, Ryuichi

Asst. Prof. KAWAMURA, Gakushi
Asst. Prof. MATSUOKA, Seikichi
Asst. Prof. SATO, Masahiko
Asst. Prof. WANG, Hao
Asst. Prof. YAMAGISHI, Osamu
Asst. Prof. YAMAGUCHI, Hiroyuki
Proj. Asst. Pro. WANG, Jialei
Proj. Res. Staff ADULSIRISWAD, Panith
Proj. Res. Staff IDOUKASS, Malik

Fundamental Physics Simulation Research Division

Prof. SUGAMA, Hideo
Prof. MIURA, Hideaki
Prof. NAKAMURA, Hiroaki
Prof. SAKAGAMI, Hitoshi
Assoc. Prof. ITO, Atsushi M.
Assoc. Prof. OHTANI, Hiroaki
Assoc. Prof. TOIDA, Mieko

Assoc. Prof. USAMI, Shunsuke
Assoc. Prof. YAMAMOTO, Takashi
Asst. Prof. HASEGAWA, Hiroki
Asst. Prof. ITO, Atsushi
Asst. Prof. MORITAKA, Toseo
Asst. Prof. TAKAYAMA, Arimichi

Rokkasho Research Center

Prof. YOKOYAMA, Masayuki
Asst. Prof. SATO, Masahiko (Additional Post)

Project

Large Helical Device Project

Prof. IDA, Katsumi
Prof. OSAKABE, Masaki

Numerical Simulation Reactor Research Project

Prof. SUGAMA, Hideo

Fusion Engineering Research Project

Prof. MURAKAMI, Izumi
Prof. YANAGI, Nagato

Research Enhancement Strategy Office

Prof. YOSHIDA, Zensho (Director)
Specially Appointed Prof. CARR, Stephen
Specially Appointed Prof. MITO, Toshiyuki
Specially Appointed Prof. YAJI Kentaro

Division of Health and Safety Promotion

Prof. SAKAKIBARA, Satoru (Division Director)

Division for Deuterium Experiments Management

Prof. OSAKABE, Masaki (Division Director)

Division of Information and Communication Systems

Prof. SAKAMOTO, Ryuichi (Division Director)

Division of External Affairs

Prof. TAKAHATA, Kazuya (Division Director)

Fusion Science Archives

Prof. MURAKAMI, Izumi (Director)

Library

Prof. MURAKAMI, Izumi (Director)

※ This list was compiled as of March 31, 2023

Visiting Researcher

KRAUS, Werner
SHARAPOV, Sergei
WENZEL, Uwe

Center of Excellence Researcher

FUJITA, Keiji
GUPTA, Shivam
WEI, Shizhao

Research Fellow (Science research)

(None)

Research Fellow (Industrial-Academic coordination)

(None)

JSPS Research Fellow

(None)

Department of Administration

NODA, Takao Department Director

General Affairs Division

ASANO, Masahiro Director
ARAI, Masanori Deputy Director
ICHIOKA, Akihiro Senior Advisor
SHIMIZU, Kazuma Chief/General Affairs Section
UESUGI, Kohtaro Chief/Planning and Evaluation Section
INAGAKI, Tomoko Chief/Employee Section
MURASE, Itaru Chief/Personnel and Payroll Section
MATSUBARA, Tomohisa Chief/Communications and Public Affairs Section

Financial Affairs Division

HIROI, Noriaki Director
OHBA, Ryo Deputy Director
HIBINO, Atsushi Chief/Financial Planning Section
KONDO, Takahiko Chief/Accounts and Properties Administration Section
FUKUOKA, Miwa Chief/Audit Section
IWASHIMA, Itsuki Chief/Procurement Section

Research Support Division

KUMAZAWA, Shuhei Director
OHKAWA, Jun Deputy Director
SUZUKI, Takayuki Chief/Research Support Section
SOGA, Shihoko Chief/International Collaboration Section
KAWAI, Sanae Chief/Graduate Student Affairs Section
OHKAWA, Jun Chief/Academic Information Section
OHKAWA, Jun Leader/Visitor Center (Additional Post)
HAYASHI, Tomomi Chief/Visitor Center

Facilities and Safety Management Division

SHIRAHIGE, Tamio Director
WAKASHIMA, Masahiro Senior Specialist
MIYATA, Kazuaki Chief/Facilities Section
IKEDA, Katsumi Chief/Equipment Section

※ This list was compiled as of March 31, 2023

APPENDIX 5. List of Publications I (NIFS Reports)

NIFS-MEMO-92

Radiation Control Office/Division of Health and Safety Promotion, National Institute for Fusion Science
Report on Administrative Work for Radiation Safety, From April 2021 to March 2022
Feb. 28, 2023

NIFS-MEMO-91

Shinzaburo Matsuda and Kazue Kimura
Shigeru Mori and Kazuhisa Mori, brothers devoted their lives to the new energy developments
Feb. 16, 2023

NIFS-MEMO-90

Department of Engineering and Technical Services, National Institute for Fusion Science
Proceedings of Symposium on Technology in Laboratories, 10–11 March 2022
May 28, 2022

※ This list was compiled as of March 31, 2023

APPENDIX 6. List of Publications II (Journals, etc.)

1. Akiyama Y., Akazawa N., Kunitoku Y., Manabe Y., Sato F., Iwamoto A., Imagawa S., Nishijima S.
Study on irradiation effect of insulating materials for fusion superconducting magnets –interlaminar shear strength at liquid helium temperature–
Radiation Physics and Chemistry 199 110372 -2022
2. Buakham S., Sangaroon S., Ogawa K., Isobe M.
Sensitivity of Gaussian energy broadening function of MCNP pulse height spectra on CLYC7 scintillation detector
Journal of Physics: Conference Series 2431 012070 -2023
3. Chikaraishi H., Ashikawa N., Goto T., Hirano N.
Conceptual Design of Fusion Power Complex with Hydrogen Storage Function in Superconducting Magnet System
Plasma and Fusion Research 18 Regular Issue 1205001 -2023
4. Fujii K., Nunami M.
Relations among Turbulent Fluctuations, Zonal Flows, and Transport Coefficients in Time Series Data of Gyrokinetic Simulations simulations
Plasma and Fusion Research 17 Special Issue 1 2403030 -2022
5. Fujita K., Satake S.
Evaluation of impacts of driving forces on neoclassical transport with weight-splitting method
Plasma and Fusion Research 17 Regular Issue 1403065 -2022
6. Fujita S., Ito A., Miyamoto Y., Kawanishi Y., Torii K., Shimajiri Y., Nishimura A., Tokuda K., Ohnishi T., Kaneko H., Inoue T., Takekawa S., Kohno M., Ueda S., Nishimoto S., Yoneda R., Nishikawa K., Yoshida D.
Distance determination of molecular clouds in the first quadrant of the Galactic plane using deep learning: I. Method and results
Publications of the Astronomical Society of Japan 75 1 279-295 -2023
7. Funaba H., Yamada I., Yasuhara R., Uehara H., Tojo H., Yatsuka E., Lee J., Huang Y.
Fast Signal Modeling for Thomson Scattering Diagnostics and Effects on Electron Temperature Evaluation
Plasma and Fusion Research 17 Special Issue 1 2402032 -2022
8. Funaba H., Yasuhara R., Uehara H., Yamada I., Sakamoto R., Osakabe M., Den hartog D.
Electron temperature and density measurement by Thomson scattering with a high repetition rate laser of 20 kHz on LHD
Scientific Reports 12 15112 -2022
9. Garfias davalos D., Morbey M., Narushima Y., Yanagi N.
Simulation of Non-Uniform Current Distribution in Stacked HTS Tapes
Plasma and Fusion Research 17 Special Issue 1 2405066 -2022
10. Gonzalez-martin J., Du X., Heidbrink W., Zeeland M., Särkimäki K., Snicker A., Wang X., Todo Y.
Modelling the Alfvén eigenmode induced fast-ion flow measured by an imaging neutral particle analyzer
Nuclear Fusion 62 11 112003 -2022
11. Gonzalez-martin J., Garcia-Munoz M., Galdon-Quiroga J., Todo Y., Dominguez-palacios J., Dunne M., Jansen van Vuuren A., Liu Y., Sanchis L., Spong D., Suttrop W., Wang X., Willensdorfer M.
Active Control of Alfvén Eigenmodes by Externally Applied 3D Magnetic Perturbations
Physical Review Letters 130 3 035101 -2023
12. Hayashi Y., Tanaka H., Ohno N., Kajita S., Morgan T., Meiden H., Scholten J., Vernimmen J., Natsume H., Sawada K., Masuda S.
Reduction of pulsed particle load with dynamic pressure induced by transient recycled neutral flux
Plasma Physics and Controlled Fusion 64 10 105013 -2022
13. Hirano N.
Circulation Cooling Technology for Superconducting Coils
Journal of the Cryogenic Society of Japan 57 4 223-229 -2022

14. Huang J., Nakata M., Xu Y., Shimizu A., Isobe M., Okamura S., Liu H., Wang X., Zhang X., Liu H., Cheng J., Tang C.
Identification of electrostatic microinstability maps in quasi-axisymmetric stellarator
Physics of Plasmas 29 5 052505 -2022
15. Ialovega M., Bernard E., Barthe M., Bisson R., Campos A., Cabié M., Neisius T., Sakamoto R., Kreter A., Grisolia C., Angot T., Martin C.
Helium-induced morphology evolution in tungsten under thermal treatment
Nuclear Fusion 62 12 126022 -2022
16. Ida K., Kobayashi T., Yoshinuma M., Nagaoka K., Ogawa K., Tokuzawa T., Nuga H., Katoh Y.
Direct observation of mass-dependent collisionless energy transfer via Landau and transit-time damping
Communications Physics 5 228 -2022
17. Ikeda K., Tsumori K., Nakano H., Nagaoka K., Takeiri Y., Masaki S., Engrhyt R., Osakabe M.
Difference of co-extracted electron current and beam acceleration in a negative ion source with hydrogen-isotope ions
Journal of Physics: Conference Series 2244 012060 -2022
18. Imagawa S., Iwamoto A., Hamaguchi S., Shirai Y., Kawasaki R., Ohya H., Matsumoto F., Shiotsu M., Tsuda M., Nagasaki Y., Yagai T., Kobayashi H.
Design, Fabrication and Soundness Test of A Bi2223 Magnet Designed for Cooling by Liquid Hydrogen
IEEE Transactions on Applied Superconductivity 32 6 4604605 -2022
19. Ishiyama S., Sagara A., Chikaraishi H., Yanagi N.
Design Concept of Supercritical CO₂ Gas Cooled Divertors in FFHR Series Fusion Reactors
Plasma and Fusion Research 17 Regular Issue 1405103 -2022
20. Ishiyama S., Sagara A., Chikaraishi H., Yanagi N.
Up-Grade Bypass Controlled Supercritical CO₂ Gas Turbine for 0.6 GWth FFHR Series Fusion Reactors
Plasma and Fusion Research 17 Special Issue 1 2405054 -2022
21. Ito A.
Simulation for Plasma-Material Interaction on Fusion Science and Nano-technology
Oyo Buturi 92 2 94-97 -2023
22. Iwamoto A., Four A., Baudouy B.
Cryogenic thermal conductivity measurements of Yb:YAG ceramics
Plasma and Fusion Research 17 Special Issue 1 2405033 -2022
23. Kajita S., Ito A., Imano K.
Growth of fiberform nanostructures on metal surfaces by helium plasma irradiation
Journal of Applied Physics 132 18 181101 -2022
24. Kanno R., Kawamura G., Nunami M., Matsuoka S., Satake S.
Monte Carlo Solver for Partly Calculating a Solution to the Poisson Equation in Three-Dimensional Curvilinear Coordinates
Plasma and Fusion Research 17 Regular Issue 1403029 -2022
25. Kawachi Y., Sasaki M., Kosuga Y., Terasaka K., Nishizawa T., Yamada T., Kasuya N., Moon C., Inagaki S.
Spatiotemporal dynamics of high-wavenumber turbulence in a basic laboratory plasma
Scientific Reports 12 19799 -2022
26. Kawamura G., Nakata M., Suzuki Y., Hayashi Y., Sakamoto R.
Divertor leg control of a quasi-symmetry stellarator with external coils and its consequences for transport
Contributions to Plasma Physics 62 6 e202100196 -2022
27. Kawase H., Uehara H., Yasuhara R.
Preliminary Results of H₂O and D₂O Real-Time Measurement Using Mid-IR Lasers with a Wavelength of 2.9 μ m and 3.9 μ m
Plasma and Fusion Research 17 Regular Issue 1205057 -2022

28. Kawate T., Ashikawa N., Goto M., Oishi T., Kawamoto Y., Toyoda H., Shoji M., Kawamura G., Masuzaki S., Nespoli F., Gilson E., Lunsford R., Suzuki C., Nagy A., Gates D.
Experimental study on boron distribution and transport at plasma-facing components during impurity powder dropping in the Large Helical Device
Nuclear Fusion 62 12 126052 -2022
29. Kenmochi N., Ida K., Tokuzawa T., Yasuhara R., Funaba H., Uehara H., Den hartog D., Yamada I., Yoshinuma M., Takemura Y., Igami H.
Preceding propagation of turbulence pulses at avalanche events in a magnetically confined plasma
Scientific Reports 12 6979 -2022
30. Kimura K., Matsuura H., Itoh C., Kawamoto Y., Oishi T., Goto M., Ogawa K., Nishitani T., Isobe M., Osakabe M.
Study on Fast Deuteron Diagnostics Method Using Fast ^3He Visible Spectra in the Large Helical Device Deuterium Plasma
Plasma and Fusion Research 18 Regular Issue 1403002 -2023
31. Kinoshita T., Tanaka K., Takemura Y., Takeshida S., Sakai H.
Development of Two-Color Laser Imaging Interferometer Using CO_2 Laser and Quantum Cascade Laser in the Large Helical Device
Plasma and Fusion Research 17 Regular Issue 1402107 -2022
32. Kitagawa Y., Mori Y., Ishii K., Hanayama R., Okihara S., Arikawa Y., Abe Y., Miura E., Ozaki T., Komeda O., Suto H., Umetani Y., Sunahara A., Johzaki T., Sakagami H., Iwamoto A., Sentoku Y., Nakajima N., Sakata S., Matsuo K., Mirfayzi R., Kawanaka J., Fujiokua S., Tsubakimoto K., Shigemori K., Yamanoi K., Yogo A., Nakao A., Asano M., Shiraga H., Motohiro T., Hioki T., Azuma H.
Direct fast heating efficiency of a counter-imploded core plasma employing a laser for fast ignition experiments (LFEX)
Nuclear Fusion 62 9 096013 -2022
33. Kobayashi M., Ohdachi S., Xu Y., Li W., Shimizu A., Cheng J.
Gas puff imaging system for edge plasma fluctuation measurements in Large Helical Device
Review of Scientific Instruments 93 9 093513 -2022
34. Kobayashi M., Seki R., Hayashi Y., Oishi T., Tanaka K., Takemura Y., Ida K., Kinoshita T., Mukai K., Morita S., Masuzaki S.
Confinement improvement during detached phase with RMP application in deuterium plasmas of LHD
Nuclear Fusion 62 5 056006 -2022
35. Kobayashi M., Yoshihashi S., Yamanishi H., Sangaroon S., Ogawa K., Isobe M., Uritani A., Osakabe M.
Thermal Neutron Measurement Capability of a Single Crystal CVD Diamond Detector near the Reactor Core Region of UTR-KINKI
Plasma and Fusion Research 17 Special Issue 1 2405045 -2022
36. Kobayashi T., Sasaki M., Ido T., Kamiya K., Miura Y., Ida K., Itoh K.
Behavior of geodesic acoustic mode and limit-cycle oscillation approaching L-H transition in JFT-2M tokamak
Plasma Physics and Controlled Fusion 64 11 114002 -2022
37. Kobayashi T., Shimizu A., Nishiura M., Ido T., Tokuzawa T., Tsujimura T., Nagaoka K., Ida K.
Hydrogen isotope effect on self-organized electron internal transport barrier criticality and role of radial electric field in toroidal plasmas
Scientific Reports 12 5507 5507 -2022
38. Kobayashi T., Yan Z., McKee G., Austin M., Grierson B., Gohil P.
Prompt core confinement improvement across the L–H transition in DIII-D: Profile stiffness, turbulence dynamics, and isotope effect
Physics of Plasmas 30 3 032301 -2023
39. Koga M., Uchino S., Maeda E., Yamanoi K., Iwamoto A.
Behavior of Gas Injected Fast Ignition Targets
Plasma and Fusion Research 17 Special Issue 1 2404052 -2022
40. Kotani T., Toida M., Moritaka T., Taguchi S.
Harmonic Structure of Lower Hybrid Waves Driven by Energetic Ions at 4000 km Altitude: PIC Simulation
Geophysical Research Letters 50 5 e20222GL102356 -2023

41. Kovtun Y., Moiseenko V., Lozin A., Pavlichenko O., Shapoval A., Grigor'eva L., Baron D., Kozulya M., Maznichenko S., Korovin V., Kramskoy E., Zamanov M., Siusko Y., Krasiuk A., Romanov V., Garkusha I., Wauters T., Alonso A., Brakel R., Dinklage A., Hartmann D., Kazakov Y., Laqua H., Lazerson S., Ongena J., Thomsen H., Fuchert G., Stange T., Kamio S.
ICRF Plasma Production with the W7-X Like Antenna in the Uragan-2M Stellarator
Plasma and Fusion Research 17 Special Issue 1 2402034 -2022
42. Kuwata H., Akata N., Okada K., Tanaka M., Tazoe H., Kurita N., Otashiro N., Negami R., Suzuki T., Tamakuma Y., Shiroma Y., Hosoda M.
Monthly Precipitation Collected at Hirosaki, Japan: Its Tritium Concentration and Chemical and Stable Isotope Compositions
Atmosphere 13 5 848 -2022
43. Li E., Uehara H., Tokita S., Yao W., Yasuhara R.
A hybrid quantum cascade laser/Fe:ZnSe amplifier system for power scaling of CW lasers at 4.0–4.6 μm
Optics and Laser Technology 157 108783 -2023
44. Li E., Yao W., Uehara H., Yasuhara R.
Cryogenically cooled 2.8 μm Er:YAP laser with watt-level output power
Applied Physics Express 15 9 092003 -2022
45. Li H., Zhang X., Xu Y., Lei G., Tsumori K., Isobe M., Shimizu A., Cui Z., Zhu Y., Hu J., Ni Y., Geng S., Liu H., Wang X., Huang J., Liu H., Cheng J., Tang C.
Theoretical calculation of cesium deposition and co-deposition with electronegative elements on the plasma grid in negative ion sources
Nuclear Materials and Energy 34 101334 -2023
46. Liu H., Zhang J., Xu Y., Shimizu A., Cooper W., Okamura S., Isobe M., Wang X., Huang J., Cheng J.
Effects of bootstrap current on magnetic configuration in Chinese first quasi-axisymmetric stellarator
Nuclear Fusion 63 2 026018 -2023
47. Maekaku K., Yoshida Z.
Hierarchical foliation of one-dimensional Vlasov-Poisson system
Physics of Plasmas 29 8 082303 -2022
48. Maeyama S., Watanabe T., Nakata M., Nunami M., Asahi Y., Ishizawa A.
Multi-scale turbulence simulation suggesting improvement of electron heated plasma confinement
Nature Communications 13 3166 -2022
49. Magee R., Ogawa K., Tajima T., Allfrey I., Gota H., Mccarroll P., Ohdachi S., Isobe M., Kamio S., Klumper V., Nuga H., Shoji M., Ziaei S., Binderbauer M., Osakabe M.
First measurements of p11B fusion in a magnetically confined plasma
Nature Communications 14 955 -2023
50. Matsuura H., Kimura K., Umezaki D., Ogawa K., Isobe M., Kawamoto Y., Oishi T., Goto M., Tamura N., Osakabe M., Nishitani T., Sugiyama S.
Indirect energy transfer channel between fast ions via nuclear elastic scattering observed on the large helical device
Physics of Plasmas 29 9 092502 -2022
51. Minagawa H., Yoshimura S., Terasaka K., Aramaki M.
Analysis of Azimuthal Doppler Shift of Anisotropically Absorbed Laguerre-Gaussian Beam Propagating in Transverse Flow
Plasma and Fusion Research 17 Regular Issue 1401099 -2022
52. Miyazawa T., Saito H., Hishinuma Y., Nagasaka T., Muroga T., Shen J., Okuno Y., Yu H., Kasada R., Hasegawa A.
Effect on impact properties of adding tantalum to V-4Cr-4Ti ternary vanadium alloy
Nuclear Materials and Energy 31 101198 -2022
53. Morace A., Abe Y., Honrubia J., Iwata N., Arikawa Y., Nakata Y., Johzaki T., Yogo A., Sentoku Y., Mima K., Ma T., Mariscal D., Sakagami H., Norimatsu T., Tsubakimoto K., Kawanaka J., Tokita S., Miyanaga N., Shiraga H., Sakawa Y., Nakai M., Azechi H., Fujioka S., Kodama R.
Super-strong magnetic field-dominated ion beam dynamics in focusing plasma devices
Scientific Reports 12 6876 -2022

54. Mori T., Nishiura M., Kenmochi N., Ueda K., Nakazawa T., Yoshida Z.
Absorption Analysis of Electron Cyclotron Waves in the Magnetospheric Plasma Device RT-1
Plasma and Fusion Research 17 Special Issue 1 2405090 -2022
55. Moritaka T., Sugama H., Cole M., Hager R., Ku S., Chang C., Ishiguro S.
Isotope effects under the influence of global radial electric fields in a helical configuration
Nuclear Fusion 62 12 126059 -2022
56. Motojima G.
Commentary: Particle Exhaust in Magnetic Confinement Fusion Plasmas for Particle Control: Past and Future
Journal of Plasma and Fusion Research 98 10 429-438 -2022
57. Mukai K., Kawamura G., Masuzaki S., Hayashi Y., Tanaka H., Peterson B., Oishi T., Suzuki C., Kobayashi M., Munechika K.
Three-dimensional structure of radiative cooling in impurity seeded plasmas in the Large Helical Device
Nuclear Materials and Energy 33 101294 -2022
58. Murase T., Morisaki T., Sogabe T., Shiozaki T.
Bonding of Tungsten and Graphite Using Spark Plasma Sintering for Divertor Component in LHD
Plasma and Fusion Research 18 Regular Issue 1205003 -2023
59. Nagayama Y., Hanashima T., Saito K., Watanabe A., Asai T., Mizuguchi N., Moriyama T., Takenaka T., Tanaka T., Yamaguchi S.
Development of Microwave CT Mammography
IEICE TRANSACTIONS C Electronics J105-C 10 293-301 -2022
60. Nagaoka K., Nakamoto R., Sasaki T., Hamajima T., Nakano H., Ikeda K., Fujiwara Y., Osakabe M., Takeiri Y., Tsumori K.
Beam instability in the vicinity of beam extraction region of negative ion source
Journal of Physics: Conference Series 2244 012043 -2022
61. Nakamura H., Habu S.
Molecular dynamics simulation on fabrication of chiral nanoneedle by optical vortex
Japanese Journal of Applied Physics 62 SA SA1013 -2023
62. Nakamura K., Zhang Y., Onchi T., Idei H., Hasegawa M., Tokunaga K., Hanada K., Chikaraishi H., Mitarai O., Kawasaki S., Higashijima A., Nagata T., Shimabukuro S.
Quaternion Analysis of Transient Phenomena in Matrix Converter Based on Space-Vector Modulation
Plasma and Fusion Research 17 Special Issue 1 2405025 -2022
63. Nakata M.
Microinstability and zonal-flow response in mixture plasmas with medium-Z and nonthermal impurity
Plasma and Fusion Research 17 Regular Issue 1203078 -2022
64. Nakata M., Honda M.
Gyrokinetic turbulent transport simulations on steady burning condition in D-T-He plasmas
Plasma and Fusion Research 17 Regular Issue 1403083 -2022
65. Nakata M., Matsuoka S.
Impact of geodesic curvature on zonal flow generation in magnetically confined plasmas
Plasma and Fusion Research 17 Regular Issue 1203077 -2022
66. Nakayama T., Nakata M., Honda M., Narita E., Nunami M., Matsuoka S.
A simplified model to estimate nonlinear turbulent transport by linear dynamics in plasma turbulence
Scientific Reports 13 2319 -2023
67. Nakayama T., Nakata M., Honda M., Nunami M., Matsuoka S.
Nonlinear functional relation covering near- and far-marginal stability in ion temperature gradient driven turbulence
Plasma Physics and Controlled Fusion 64 7 075007 -2022
68. Nishimura A.
Conceptual Design of Plasma Vacuum Vessel for Fusion DEMO Considering Integration of Core Components
Plasma and Fusion Research 17 Special Issue 1 2405058 -2022

69. Nishitani T., Yoshihashi S., Ogawa K., Miwa M., Matsuyama S., Uritani A.
Neutron yield calculation of thin and thick d-D targets by using PHITS with frag data table
Journal of Nuclear Science and Technology 59 4 534-541 -2022
70. Nishiura M., Adachi S., Tanaka K., Kubo S., Kenmochi N., Shimozuma T., Yanai R., Saito T., Nuga H., Seki R.
Collective Thomson scattering diagnostic with in situ calibration system for velocity space analysis in large helical device
Review of Scientific Instruments 93 5 053501 -2022
71. Nuga H., Seki R., Ogawa K., Kamio S., Fujiwara Y., Yamaguchi H., Osakabe M., Isobe M., Yokoyama M.
Estimation of the Tritium Yields in Deuterium Fusion Plasmas Considering the Fast-Ion Velocity Distribution Function
Plasma and Fusion Research 17 Special Issue 1 2402023 -2022
72. Nunami M., Toda S., Nakata M., Sugama H.
Improved prediction scheme for ion heat turbulent transport
Physics of Plasmas 29 10 102505 -2022
73. Obana T.
Electromagnetic-structural analysis of a superconducting magnet with active shielding for a rotating gantry
IEEE Transactions on Applied Superconductivity 32 6 4400304 -2022
74. Obana T., Kawagoe A.
Numerical analysis of hysteresis loss in stacked REBCO tapes for large current-carrying conductors
Plasma and Fusion Research 18 Special Issue 1 2405013 -2023
75. Ogawa K., Isobe M., Kamio S., Nuga H., Seki R., Sangaroon S., Yamaguchi H., Fujiwara Y., Takada E., Murakami S., Jo J., Takemura Y., Sakai H., Tanaka K., Tokuzawa T., Yasuhara R., Osakabe M.
Studies of Energetic Particle Transport induced by Multiple Alfvén Eigenmodes using Neutron and Escaping Energetic Particle Diagnostics in Large Helical Device Deuterium Plasmas
Nuclear Fusion 62 11 112001 -2022
76. Ogawa K., Isobe M., Weiss C., Griesmayer E., Sangaroon S., Takada E., Masuzaki S., Ohtani H., Liao L., Tamaki S., Murata I., Osakabe M.
Fusion product diagnostics based on commercially available chemical vapor deposition diamond detector in large helical device
Journal of Instrumentation 18 P01022 -2023
77. Ohtani H., Masuzaki S., Ogawa K., Ishiguro S.
Virtual-Reality Visualization of loss points of 1 MeV tritons in the Large Helical Device, LHD
Journal of Visualization 25 2 281-292 -2022
78. Oishi T., Kobayashi M., Takahashi H., Hayashi Y., Mukai K., Morita S., Goto M., Kawamoto Y., Kawate T., Masuzaki S., Suzuki C., Kawamura G., Motojima G., Seki R.
Spatial Profiles of NeVI-NeX Emission in ECR-Heated Discharges of the Large Helical Device with Divertor Detachment Induced by RMP Application and Ne Impurity Seeding
Plasma and Fusion Research 17 Special Issue 1 2402022 -2022
79. Oishi T., Morita S., Murakami I., Kato D., Sakaue H., Kawamoto Y., Kawate T., Goto M.
EUV spectral shape variation of tungsten unresolved transition arrays in electron temperature range of 2–4 keV observed in the Large Helical Device
Journal of Physics: Conference Series 2439 012005 -2023
80. Osakabe M., Takahashi H., Yamada H., Tanaka K., Kobayashi T., Ida K., Ohdachi S., Varela J., Ogawa K., Kobayashi M., Tsumori K., Ikeda K., Masuzaki S., Tanaka M., Nakata M., Murakami S., Inagaki S., Mukai K., Sakamoto M., Nagasaki K., Suzuki Y., Isobe M., Morisaki T., The LHD Experimental Group .
Recent results from deuterium experiments on the large helical device and their contribution to fusion reactor development
Nuclear Fusion 62 4 042019 -2022
81. Ozaki T., Abe Y., Arikawa Y., Sentoku Y., Kawanaka J., Tokita S., Miyanaga N., Jitsuno T., Nakata Y., Tsubakimoto K., Sunahara A., Johzaki T., Miura E., Komeda O., Iwamoto A., Sakagami H., Okihara S., Ishii K., Hanayama R., Mori Y., Kitagawa Y.
Hot electron and ion spectra on blow-off plasma free target in GXII-LFEX direct fast ignition experiment
Nuclear Fusion 63 3 036009 -2023

82. Ozaki T., Miura E., Kojima S., Arikawa Y., Abe Y., Yamanoi K., Ikeda T., Ishii K., Sunahara A., Johzaki T., Sawada H., Fujioka S., Sakagami H., Kitagawa Y., Mori Y.
Estimation of a Plasma Mirror Reflectivity of LFEX Laser and Relevant Results Using Electron Energy Spectrometers
Plasma and Fusion Research 17 Special Issue 1 2404084 -2022
83. Paenthong W., Wisitsorasak A., Sangaroon S., Promping J., Ogawa K., Isobe M.
Fast-Ion Orbit Analysis in Thailand Tokamak-1
Fusion Engineering and Design 183 113254 -2022
84. Peterson B., Nishitani T., Reichle R., Munechika K., O'mullane M., Mukai K.
Estimates of foil thickness, signal, noise, and nuclear heating of imaging bolometers for ITER
Journal of Instrumentation 17 6 P06034 -2022
85. Saitoh H., Nishiura M., Nakazawa T., Morikawa J., Yoshida Z., Osawa R.
Electro-optic Bdot probe measurement of magnetic fluctuations in plasma
Review of Scientific Instruments 93 10 103540 -2022
86. Sakaue H., Kato D., Yamamoto N., Murakami I., Hara H., Nakamura N.
Energy Dependence of the Line Ratio $I(233.9 \text{ \AA})/I(243.8 \text{ \AA})$ in Fe xv Observed with an Electron Beam Ion Trap
The Astrophysical Journal 943 1 14 -2023
87. Sangaroon S., Ogawa K., Isobe M.
Initial operation of perpendicular line-of-sight compact neutron emission spectrometer in the large helical device
Review of Scientific Instruments 93 9 093504 -2022
88. Sangaroon S., Ogawa K., Isobe M., Wisitsorasak A., Paenthong W., Promping J., Poolyarat N., Tamman A., Ploykrachang K., Dangtip S., Onjun T.
Feasibility study of neutral beam injection in Thailand Tokamak-1
Fusion Engineering and Design 188 113419 -2023
89. Seki R., Ogawa K., Isobe M., Murakami S., Nuga H., Shimizu A., Okamura S., Takahashi H., Oishi T., Kinoshita S., Murase T., Nakagawa S., Tanoue H., Osakabe M., Liu H., Xu Y.
Prediction of Neutron Emission Rate in Deuterium Neutral Beam heated CFQS plasmas using FIT3D-DD code
Plasma and Fusion Research 17 Special Issue 1 2403063 -2022
90. Sharad Y., Miura H., Rahul P.
Statistical Properties of Three-Dimensional Hall Magnetohydrodynamics Turbulence
Physics of Fluids 34 9 095135 -2022
91. Shen J., Nagasaka T., Tokitani M., Muroga T., Kasada R., Sakurai S.
Effects of titanium concentration on microstructure and mechanical properties of high-purity vanadium alloys
Materials and Design 224 111390 -2022
92. Shi Q., Fujiwara H., Kajita S., Yasuhara R., Tanaka H., Ohno N., Uehara H.
Structural Correlation of Random Lasing Performance in Plasma-Induced Surface-Modified Gallium Nitride
ACS Applied Optical Materials 1 1 412-420 -2023
93. Shimizu A., Isobe M., Okamura S., Kinoshita S., Ogawa K., Takahashi H., Oishi T., Yoshimura Y., Murase T., Nakagawa S., Tanoue H., Takubo H., Osakabe M., Hayashi H., Kobayashi S., Liu H., Xu Y.
Feasibility study of heavy ion beam probe in CFQS quasi-axisymmetric stellarator
Journal of Instrumentation 17 C06004 -2022
94. Shoji M., Kawamura G., Romazanov J., Kirschner A., Masuzaki S., Tokitani M., Brezinsek S.
Validation of the plasma-wall interaction simulation code ERO2.0 by the analysis of tungsten migration in the open divertor region in the Large Helical Device
Nuclear Materials and Energy 33 101257 -2022
95. Someya H., Asai T., Kobayashi D., Seki T., Yamanaka T., Watanabe T., Takahashi T., Mizuguchi N.
Effect of Collision Axes Offset of the Plasmoid in the Collisional Merging Process of FRC Plasma
Plasma and Fusion Research 17 Special Issue 1 2402068 -2022
96. Sugama H., Matsuoka S., Nunami M.
Polarization and magnetization in collisional and turbulent transport processes
Physics of Plasmas 29 5 052509 -2022

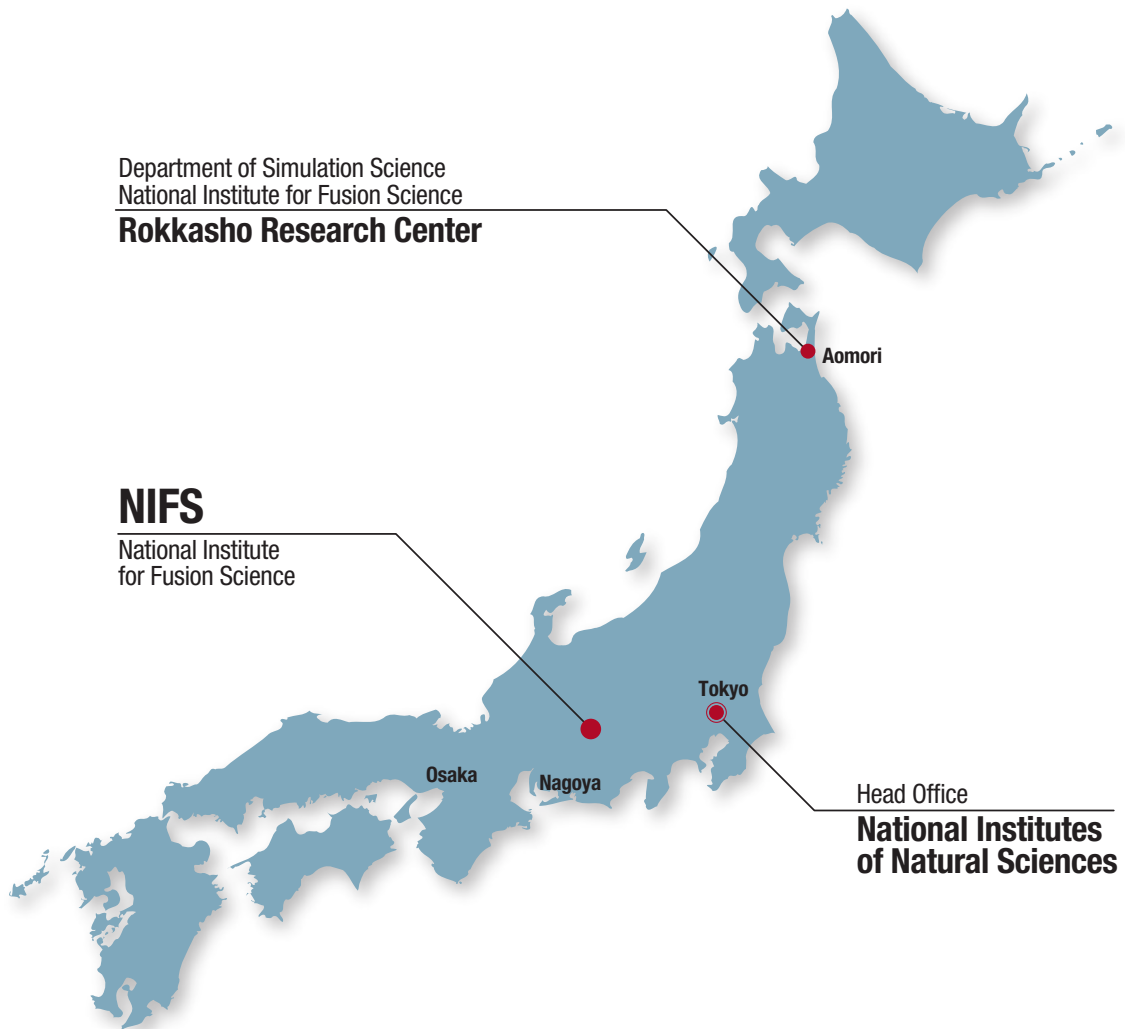
97. Tachibana Y., Kalak T., Tanaka M.
Chromatographic Purification of Lithium, Vanadium, and Uranium from Seawater Using Organic Composite Adsorbents Composed of Benzo-18-Crown-6 and Benzo-15-Crown-5 Embedded in Highly Porous Silica Beads
ACS Omega 7 31 27410-27421 -2022
98. Takase Y., Ejiri A., Fujita T., Hanada K., Idei H., Nagata M., Onchi T., Ono Y., Tanaka H., Tsujii N., Uchida M., Yasuda K., Kasahara H., Murakami S., Takeiri Y., Todo Y., Tsuji-Iio S., Kamada Y.
Overview of coordinated spherical tokamak research in Japan
Nuclear Fusion 62 4 042011 -2022
99. Takemura Y., Watanabe K., Sakakibara S., Ohdachi S., Narushima Y., Tanaka K., Tokuzawa T.
Onset of instability with collapse observed in relatively high density and medium beta regions of LHD
Physics of Plasmas 29 9 092505 -2022
100. Takenaka K., Hashida M., Sakagami H., Masuno S., Kusaba M., Yamaguchi S., Iwamori S., Sato Y., Tsukamoto M.
Uniformity evaluation of laser-induced periodic surface structures formed by two-color double-pulse femtosecond laser irradiation
Review of Scientific Instruments 93 9 093001 -2022
101. Tamaru Y., Fuchimukai A., Uehara H., Miura T., Yasuhara R.
Verdet constant dispersion of magnesium fluoride for deep-ultraviolet and vacuum-ultraviolet Faraday rotators
Optics Express 31 5 7807-7812 -2023
102. Tamaru Y., Hikaru K., Fuchimukai A., Uehara H., Miura T., Yasuhara R.
Effect of erbium concentration on the Verdet constant dispersion of LiY1.0-xErxF4 single crystal
Optical Materials Express 12 4 1427-1432 -2022
103. Tanaka M., Yoshimura Y., Ito S., Wang J., Hirayama H., Uda T., Fujiwara O.
Measurement of Leakage Electromagnetic Field Around Megawatt Millimeter Wave Band Gyrotron Oscillator in a Large Fusion Test Facility
IEICE TRANSACTIONS B Communications J105-B 8 629-636 -2022
104. Tamura H., Goto T., Miyazawa J., Tanaka T., Yanagi N.
Seismic analysis of magnet systems in helical fusion reactors designed with topology optimization
IEEE Transactions on Applied Superconductivity 32 6 4900504 -2022
105. Tanaka H., Masuzaki S., Kawamura G., Hayashi Y., Kobayashi M., Suzuki Y., Mukai K., Kajita S., Ohno N.
Correlation of the orthogonal basis of the core plasma distribution to the divertor footprint distribution in LHD
Plasma and Fusion Research 18 Special Issue 1 2402021 -2023
106. Tanaka M., Iwata C., Nakada M., Kato A., Akata N.
LEVELS OF ATMOSPHERIC TRITIUM IN THE SITE OF FUSION TEST FACILITY
Radiation Protection Dosimetry 198 13-15 1084-1089 -2022
107. Tanaka T., Chikada T., Hinoki T., Muroga T.
Electrical insulation performances of ceramic materials developed for advanced blanket systems under intense radiations
Journal of Nuclear Materials 569 153917 -2022
108. Toda S., Nunami M., Sugama H.
Prediction of temperature profiles in helical plasmas by integrated code coupled with gyrokinetic transport models
Plasma Physics and Controlled Fusion 64 8 085001 -2022
109. Todo Y.
Information: The 31st International Toki Conference (ITC31)
Journal of Plasma and Fusion Research 99 3 103 -2023
110. Toida M., Ohsawa Y.
Theory and simulations of field strengths in magnetosonic shock waves in finite beta plasmas
Physics of Plasmas 29 4 042302 -2022
111. Tokitani M., Hamaji Y., Hiraoka Y., Masuzaki S., Tamura H., Noto H., Tanaka T., Muroga T., Sagara A., Group F.
Deformation and fracture behaviour, and thermal stability of ODS-Cu/ODS-Cu and SUS/ODS-Cu joints fabricated by advanced brazing technique
Fusion Engineering and Design 184 113312 -2022

112. Tokunaga S., Nakanishi H., Yamanaka K., Ozeki T., Homma Y., Ishii Y.
Investigation of Required Network-Storage System toward Fusion Information Science Center in Rokkasho
Plasma and Fusion Research 17 Special Issue 1 2405091 -2022
113. Tokuzawa T., Goto Y., Kuwahara D., Nishiura M., Shimizu T.
New Q and V-band ECE radiometer for low magnetic field operation on LHD
EPJ Web of Conferences 277 03008 -2023
114. Tokuzawa T., Inagaki S., Inomoto M., Ejiri A., Nasu T., Tsujimura T., Ida K.
Application of Dual Frequency Comb Method as an Approach to Improve the Performance of Multi-frequency
Simultaneous Radiation Doppler Radar for High Temperature Plasma Diagnostics
Applied Sciences 12 9 4744 -2022
115. Tokuzawa T., Nasu T., Inagaki S., Moon C., Ido T., Idei H., Ejiri A., Imazawa R., Yoshida M., Oyama N.,
Tanaka K., Ida K.
3D Metal Powder Additive Manufacturing Phased Array Antenna for Multichannel Doppler Reflectometer
Review of Scientific Instruments 93 11 113535 -2022
116. Tran N., Hochin T., Nomiya H., Nakanishi H., Shoji M.
Generation of Unusual Plasma Discharge Video by Generative Adversarial Network
International Journal of Software Innovation 10 1-24 -2022
117. Tsubasa S., Kitazawa S., Nunami M., Katagiri T., Ohshima S., Nagai T.
A Novel Approach for Data Analysis Based on Visualization of Phase Space Distribution Function in Plasma Turbulence
Simulations
Plasma and Fusion Research 17 Special Issue 1 2403079 -2022
118. Tsubasa S., Nunami M., Katagiri T., Ohshima S., Nagai T.
Image-based Analysis for Turbulence Simulation Data of Magnetic Confined Plasmas
Journal of the Japan Society for Simulation Technology 41 4 228-233 -2022
119. Tsujimura T., Goto Y., Okada K., Kobayashi S., Kubo S.
Development of off-axis spiral phase mirrors for generating optical vortices in a range of millimeter waves
Review of Scientific Instruments 93 4 043507 -2022
120. Tsumori K., Ikeda K., Kisaki M., Nakano H., Nagaoka K., Fujiwara Y., Kamio S., Osakabe M.
Challenges toward improvement of deuterium-injection power in the Large Helical Device negative-ion-based NBIs
Nuclear Fusion 62 5 056016 -2022
121. Varela J., Spong D., Todo Y., Garcia L., Ghai Y., Ortiz J., Seki R.
Simulation of the TAEs' saturation phase in the Large Helical Device: MHD burst
Nuclear Fusion 62 12 126020 (18pp) -2022
122. Wang H., Todo Y., Huang J., Suzuki Y., Shimizu A., Ogawa K., Wang X., Adulsiriswad P.
Simulations of energetic particle driven instabilities in CFQS
Nuclear Fusion 62 10 106010 -2022
123. Xiong G., Xu Y., Isobe M., Shimizu A., Ogawa K., Kinoshita S., Liu H., Wang X., Cheng J., Liu H., Huang J.,
Zhang X., Zhang Y., Yin D., Wang A., Okamura S., Tang C.
Effect of discreteness and misalignment on magnetic field and charged particle confinement in CFQS quasi-axisymmetric
stellarator
Plasma Physics and Controlled Fusion 65 3 035020 -2023
124. Yamada I., Funaba H., Lee J., Huang Y., Liu C.
Neural Network Data Analysis in the Large Helical Device Thomson Scattering System
Plasma and Fusion Research 17 Special Issue 1 2402061 -2022
125. Yamagishi O.
An alternative expression for ad hoc field collision model
Physics of Plasmas 29 10 102507 -2022
126. Yamaguchi T., Ohtani H., Satake S., Yanagi N., Onodera Y.
Numerical Investigation on Applicability of jC-Measurement Method to Multiple High-Temperature Superconducting
Tape
Plasma and Fusion Research 17 Special Issue 1 2405035 -2022

127. Yamamoto T., Inoue N., Takayama A.
Investigation and response to SMSs falsifying authentication code notification for multi-factor authentication
Journal for Academic Computing and Networking 26 1 131-134 -2022
128. Yanagi N., Terazaki Y., Narushima Y., Onodera Y., Hirano N., Hamaguchi S., Chikaraishi H., Takada S., Ito S., Takahata K.
Progress of HTS STARS Conductor Development for the Next-Generation Helical Fusion Experimental Device
Plasma and Fusion Research 17 Special Issue 1 2405076 -2022
129. Yang H., Yasuhara R., Noto H., Suzuki C., Miyagawa R., Uehara H.
A Study on Laser Processing of Tungsten-Rhenium Alloys for Divertor Development
Plasma and Fusion Research 18 Regular Issue 1205017 -2023
130. Yang H., Yasuhara R., Noto H., Suzuki C., Miyagawa R., Uehara H.
Crack-free nanosecond laser processing of mechanically enhanced tungsten-rhenium alloys
Journal of Laser Micro/Nanoengineering 17 3 162-167 -2022
131. Yokoyama M.
Front Runner: "Statistical-mathematics" fusion research ~Fusion research from the viewpoints of statistical mathematics~
Journal of Plasma and Fusion Research 99 1 3-8 -2023
132. Yoshida K., Miura H., Tsuji Y.
Energy Transfer of the Gross-Pitaevskii Turbulence in Weak-Wave-Turbulence and Strong-Turbulence Ranges
Journal of Low Temperature Physics 210 103-112 -2023
133. Yoshida Z.
Nambu mechanics viewed as a Clebsch parameterized Poisson algebra: Toward canonicalization and quantization
Progress of Theoretical and Experimental Physics 2022 7 ptac096 -2022
134. Yoshida Z.
Saloon: Towards a New Era of NIFS
Journal of Plasma and Fusion Research 98 8 368-374 -2022
135. Yoshimura Y., Kanda M., Yanai R., Shimizu A., Kinoshita S., Isobe M., Okamura S., Ogawa K., Takahashi H., Murase T., Nakagawa S., Tanoue H., Liu H., Xu Y.
Investigation of Capability of Current Control by Electron Cyclotron Waves in the Quasiasymmetric Stellarator CFQS
Plasma and Fusion Research 17 Special Issue 1 2402039 -2022
136. Zhang Y., Liu H., Huang J., Xu Y., Zhang J., Shimizu A., Satake S., Isobe M., Wang X., Cheng J., Liu H., Zhang X., Tang C.
Suppression of non-axisymmetric field-induced α -particle loss channels in a quasi-axisymmetric stellarator
AIP Advances 12 5 055214 -2022
137. Zhang Y., Zhang J., Cheng S., Zhu J., Isobe M., Zhang P., Yuan G., Zhan X., Zhu Y., Liu Y., Shi Z., Zhong W., Xu M.
A gamma ray spectrometer with Compton suppression on the HL-2A tokamak
Review of Scientific Instruments 93 12 123509 -2022
138. Zhao M., Masuzaki S., Motojima G., Tokitani M., Yajima M., Gao Y., Jakubowski M., Sitjes A., Pisano F., Dhard C., Naujoks D., Romazanov J., Brezinsek S.
Distributions of deposits and hydrogen on the upper and lower TDUs3 target elements of Wendelstein 7-X
Nuclear Fusion 62 10 106023 -2022
139. Zheng L., Kotschenreuther M., Waelbroeck F., Todo Y.
ATEQ: Adaptive toroidal equilibrium code
Physics of Plasmas 29 7 072503 -2022

※ This list was compiled as of March 31, 2023

National Institute for Fusion Science



**National Institute for Fusion Science
National Institutes of Natural Sciences**
(TOKI Area)

322-6 Oroshi-cho
Toki-city, GIFU
509-5292

TEL: 0572-58-2222 FAX: 0572-58-2601

**Rokkasho Research Center
Department of Helical Plasma Research
Located in the Aomori Research and
Development Center
Japan Atomic Energy Agency**

2-166 Oaza-Obuchi-Aza-Omotodate,
Rokkasho-mura, Kamikita-gun,
AOMORI
039-3212

TEL/FAX: 0175-73-2151

How to Reach National Institute for Fusion Science



ACCESS

When you use the public transportation facility

- ◇ **from Centrair** (Central Japan International Airport)
Centrair – (μ-sky) – **Meitetsu Kanayama Sta.** (36km)
 about 25min
JR Kanayama Sta. – (JR Chuo Line) – **JR Tajimi Sta.** (33km)
 about 33min (express)
JR Tajimi Sta. – (Totetsu Bus) – **Kenkyuugakuentoshi** (7km)
 about 15min
- ◇ **from JR Nagoya Sta.**
JR Nagoya Sta. – (JR Chuo Line) – **JR Tajimi Sta.** (36km)
 about 22min (limited express) / about 30min (lapid) / about 40min (local)
JR Tajimi Sta. – (Totetsu Bus) – **Kenkyuugakuentoshi** (7km)
 about 15min

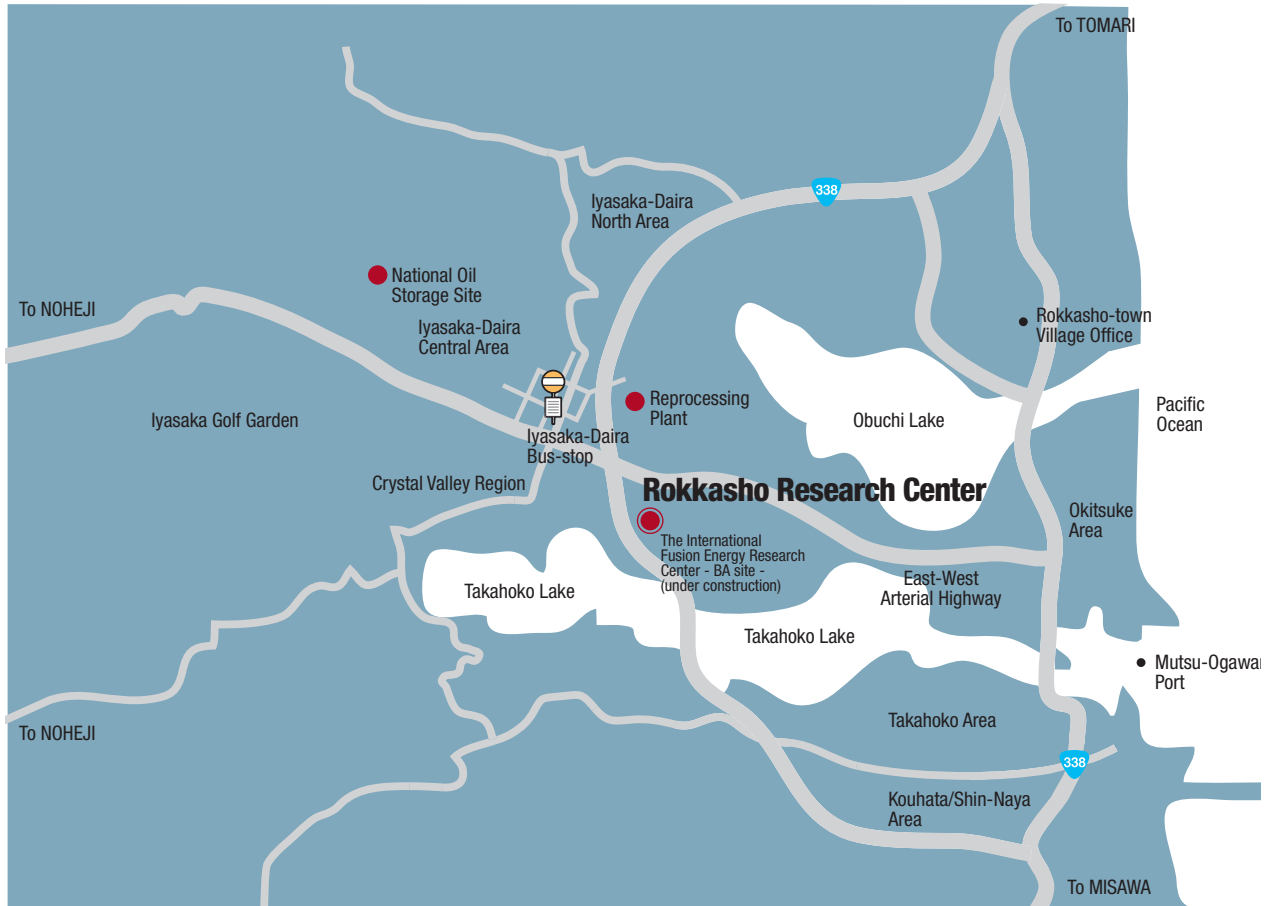
◇ from Nagoya Airport

- (Obihiro•Akita•Yamagata•Niigata•Kouchi•Matsuyama•Fukuoka•Kumamoto•Nagasaki)
- Nagoya Airport** – (Taxi) – **JR Kachigawa Sta.** (4km)
 about 10min
 - Nagoya Airport** – (Meitetsu Bus) – **JR Kachigawa Sta.** (4km)
 about 19min
 - JR Kachigawa Sta.** – (JR Chuo Line) – **JR Tajimi Sta.** (21km)
 about 20min
 - JR Tajimi Sta.** – (Totetsu Bus) – **Kenkyuugakuentoshi** (7km)
 about 15min

When you use a car

- from Chuo Expressway Toki I.C. or Tajimi I.C.** (8km)
 about 20min
- from Tokai-Kanjo Expressway Tokiminami Tajimi I.C.** (2km)
 about 5min

How to Reach Rokkasho Research Center



ACCESS

When you use the public transportation facility

◇ from Tokyo

Tokyo – (Tohoku-Shinkansen) – **Hachinohe Sta.** (630km)
about 3hr

Hachinohe Sta. – (JR Tohoku Limited Express) – **Noheji** (51km)
about 30min

Noheji – (Shimokita Koutsu Bus) – **Iiyasa-Daira** (10km)
about 40min

Iiyasa-Dairaon foot..... **Rokkasho Research Center** (0.7km)
about 8min

◇ from Misawa Airport

Misawa Airport – (Bus) – **Misawa** (2km)
about 13min

Misawa – (JR Tohoku Limited Express) – **Noheji** (30km)
about 20min

Noheji – (Shimokita Koutsu Bus) – **Iiyasa-Daira** (10km)
about 40min

Iiyasa-Dairaon foot..... **Rokkasho Research Center** (0.7km)
about 8min

◇ from Aomori Airport

Aomori Airport – (Bus) – **Aomori** (12km)
about 40min

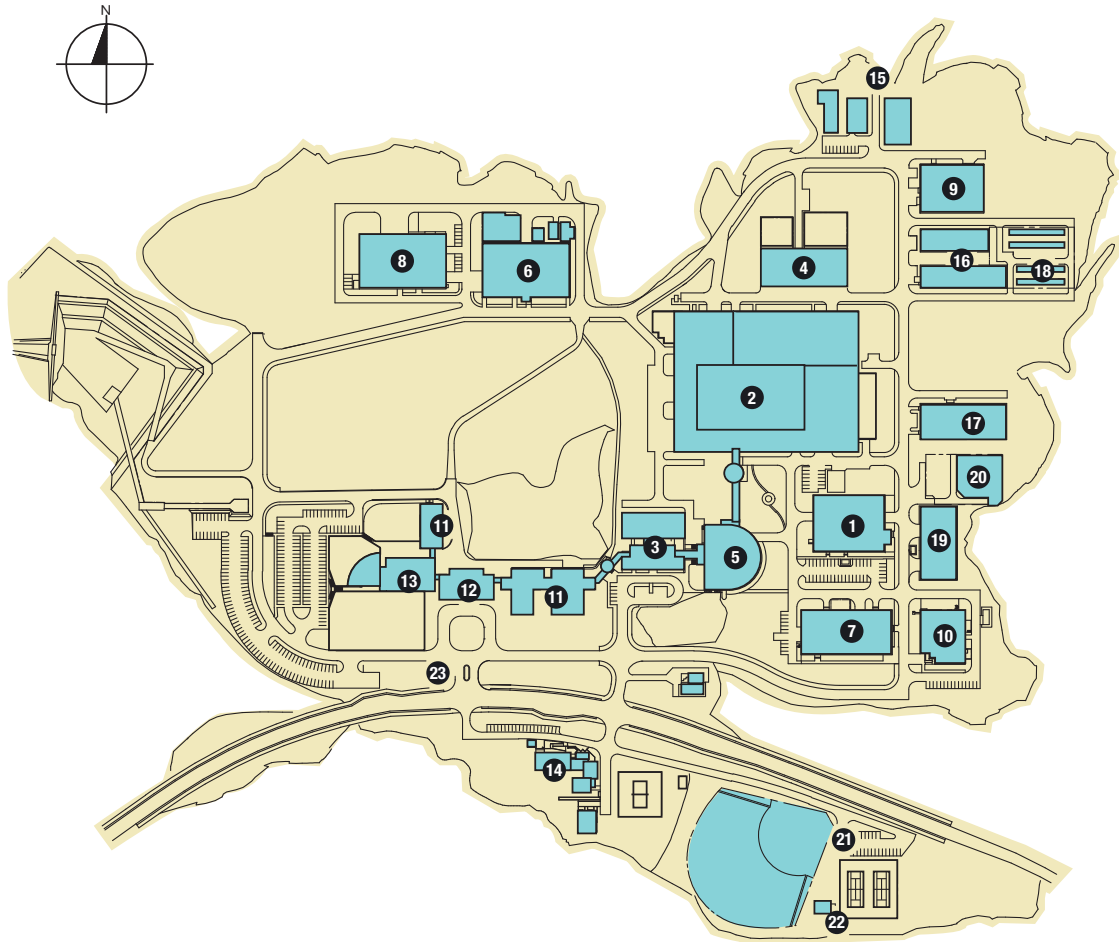
Aomori – (JR Tohoku Limited Express) – **Noheji** (45km)
about 30min

Noheji – (Shimokita Koutsu Bus) – **Iiyasa-Daira** (10km)
about 40min

Iiyasa-Dairaon foot..... **Rokkasho Research Center** (0.7km)
about 8min

National Institute for Fusion Science

Building Arrangement



NIFS plot plan

- ① Superconducting Magnet System Laboratory
- ② Large Helical Device Building
- ③ Simulation Science Research Laboratory
- ④ Heating and Power Supply Building
- ⑤ LHD Control Building
- ⑥ Fusion Engineering Research Laboratory
- ⑦ Plasma Diagnostics Laboratories
- ⑧ R & D Laboratories
- ⑨ Motor-Generator Building
- ⑩ Central Workshops
- ⑪ Research Staff Building
- ⑫ Library Building
- ⑬ Administration Building
- ⑭ Helicon Club (Guest Housing)
- ⑮ High-Voltage Transformer Station
- ⑯ Cooling Water Pump Building
- ⑰ Helium Compressor Building
- ⑱ Cooling Tower
- ⑲ Equipments Room
- ⑳ Helium Tank Yard
- ㉑ Recreation Facilities
- ㉒ Club House
- ㉓ Guard Office

